DairyMod and the SGS Pasture Model

A mathematical description of the biophysical model structure

Ian R Johnson

Published by IMJ Consultants
PO Box 182
Dorrigo
NSW 2453
Australia
www.imj.com.au

Originally published November 2005

This version published 30 September, 2013

Updated 17 November, 2013

Citation:

Johnson IR (2013). *DairyMod and the SGS Pasture Model: a mathematical description of the biophysical model structure*. IMJ Consultants, Dorrigo, NSW, Australia.

DairyMod and the SGS Pasture Model

1 Background to biophysical modelling

1.1 Introduction

The SGS Pasture Model and DairyMod are biophysical pasture simulation models, with a common underlying structure. There are modules for pasture growth and utilization by grazing animals, animal physiology including animal production, water and nutrient dynamics, as well as a range of options for pasture management, irrigation and fertilizer application. The principal features of the individual modules are:

- The pasture growth module includes calculations of light interception and photosynthesis; growth and maintenance respiration, nutrient uptake and nitrogen fixation, partitioning of new growth into the various plant parts, development, tissue turnover and senescence, and the influence of atmospheric CO_2 on growth. The model allows up to five pasture species in any simulation, which can be annual or perennial, C_3 or C_4, as well as legumes.
- The water module accounts for rainfall and irrigation inputs that can be intercepted by the canopy, surface litter or soil. The required hydraulic soil parameters are saturated hydraulic conductivity, bulk density, field capacity or drained upper limit, wilting point and air-dry water content. (Saturated water content is calculated from bulk density.)
- Different soil physical properties can be defined through the soil profile. The nutrient module incorporates the dynamics of inorganic nitrogen (including leaching) and soil organic matter. The soil organic matter module gives a complete description of soil carbon in the system and its response to factors such as climate variation and management. In addition, gaseous losses of nitrogen through volatilization and denitrification are included.
- The animal module has a sound treatment of animal intake and metabolism including growth, maintenance, pregnancy and lactation. There are options to select sheep (wethers or ewes with lambs), cattle (steers or beef cows with calves), and dairy cows. Wool growth is included for sheep.
- The farm management module describes the movement of stock around paddocks as well as strategies for conserving forage, and incorporates a wide range of rotational grazing management strategies that are used in practice. There are options for single- and multi-paddock simulations that can each be defined independently to represent spatial variation in soil types, nutrient status, pasture species, fertilizer and irrigation management.

The model has been applied to a range of research questions, which include comparisons with experimental data from several disparate geographical locations for a range of pasture species, as well as addressing important questions such as climate variability, drought, business risk, and the impacts of climate change and carbon mitigation strategies. The biophysical structure of the model means it is well suited to be developed to explore issues such as new management strategies or plant characteristics, as well as the environmental impacts of likely future climate change scenarios.

This book provides a complete mathematical description of the model. Before embarking on the model description, this first chapter provides a detailed background to the mathematical methods that are used in the model, as well as some general topics of importance. For a further discussion of modelling techniques see Thornley and Johnson (2000) and Thornley and France (2007).

1.2 Plant, crop and pasture modelling

In recent years, models have become an integral component of the plant, crop and pasture sciences. They have a wide variety of uses in many aspects of agricultural management, such as irrigation scheduling and pasture management. Equally so, they play an important role in plant and crop research: for example, models have helped identify the growth and maintenance components of plant respiration. This interest in modelling has had many benefits and has provided a means of integrating concepts from many different branches of science.

When constructing models it is important that model design meets the objectives of the project. It is therefore important to consider the different types of model and how these relate to each other. The main types used in this model are *mechanistic* and *empirical*, as discussed in Section 1.2.2 below. Before proceeding, it is worth noting that it is unlikely that one model of a particular process will suit all likely modelling objectives.

1.2.1 Hierarchical systems

Plant biology, and biology in general, has many organizational levels. In physics and chemistry there is a clear distinction between moving from atomic and molecular behaviour to that of liquids and solids, in biology there are several levels that can be considered. This range of different levels gives rise to the great diversity of the biological world. A typical hierarchical scheme for the plant sciences is:

…	…
…	landscape
$i+1$	crop or pasture
i	plant
$i-1$	organs
…	tissues
…	cells
…	organelles
…	macromolecules
…	molecules and atoms

The model described here focuses on processes primarily at levels $i+1$, i, $i-1$.

The principal features of this hierarchical system are:

1. Each level has its own language. For example, crop yield has little meaning at the cell level.
2. Each level is an integration of items at lower levels, so that the response of the system at one level can be related to responses at lower levels. For example, canopy photosynthesis is calculated in terms of the sum of the photosynthesis of the leaves in the plants that make up the canopy.

Other features of this system are discussed in Thornley and Johnson (2000) and Thornley and France (2007).

1.2.2 Types of models

Models can be divided into several categories, with perhaps the most widely used being mechanistic and empirical, deterministic and stochastic. The difference between deterministic and stochastic models is that deterministic models predict a precise value for a variable of the system, whereas stochastic models involve statistical variation. Both have their value, but in the present model the statistical features of the behaviour of the system are not considered.

Empirical models

Empirical models are curves that are used to describe patterns of behaviour or to summarize sets of data but do not involve details of the underlying scientific basis of the system. An example of empirical modelling is the use of growth functions to describe animal weight during growth. Generally, an empirical model describes the response of the system at a single level in the hierarchical structure mentioned in the previous section.

Although empirical models are usually curves that can be fitted to experimental data, and that display the general expected characteristics of the response, they are much more useful if the curves have readily interpreted parameters. For example, the temperature response functions discussed in Section 1.3.5 below are used to describe the influence of temperature on various processes in the model. These response functions are empirical but are formulated with minimum, optimum and maximum temperature parameters for the processes, which makes them simple to apply.

Mechanistic models

Mechanistic models are constructed from descriptions of the underlying processes involved in the system being studied, and these descriptions are quite often empirical (or semi-empirical). They generally operate between two or three levels in the hierarchical structure discussed in the previous section. For example, canopy gross photosynthesis can be defined in terms of an equation describing single leaf photosynthesis in response to light and another equation describing light attenuation through the canopy. Ideally, each of these sub-models will have parameters that have some biophysical interpretation, but they may not be founded on detailed mechanisms.

The complexity of mechanistic models will increase as the range of processes used to build that model increases, or if greater detail is used to describe these processes. The complexity at which a model is developed is therefore subject to some degree of choice. The greater the detail, the more complex the model. It is important that the complexity of the model suits the objectives of the system being investigated and this means that there is generally no single model of a biological process that suits all purposes.

The distinction between mechanistic and empirical models is not always clear. For example, the equation used to describe single leaf gross photosynthesis in the model, the *non-rectangular hyperbola* which is discussed in detail later, can be derived from a very simple model of leaf photosynthesis. However, the underlying model contains such broad assumptions that it does not really encapsulate the biochemical details of leaf photosynthesis. In this case, we can regard the equation as semi-empirical, recognising that it has the desired behaviour but with a limited biophysical basis.

1.3 Background mathematical functions

Some background calculations are now presented. These are used in the later model descriptions.

1.3.1 Rectangular hyperbola

The simple rectangular hyperbola (RH) can be derived from basic concepts of enzyme kinetics. It is generally presented in one of two forms:

$$y = \frac{\alpha x y_m}{\alpha x + y_m} \tag{1.1}$$

or

$$y = y_m \frac{x}{x+K} \tag{1.2}$$

although the symbol v for the speed of the reaction, and S for substrate concentration are often used instead of x and y. In both equations, y_m is the asymptotic value of y as $x \to \infty$; with eqn (1.1), α is the initial slope of the curve, while for eqn (1.2) y takes half its maximum value when $x = K$, that is $y(x = K) = y_m/2$. These two forms of the RH are mathematically equivalent and it is readily shown that

$$K = \frac{y_m}{\alpha} \tag{1.3}$$

The rectangular hyperbola of the form (1.2) is often referred to as the Michaelis-Menten equation due to their early application of this equation to enzyme kinetics in 1913.

The form of the equation that is used depends on the particular application – sometimes it is convenient to prescribe the initial slope of the response, α, while in other cases the value of x for half-maximal response, K, is more convenient.

The equation is referred to as a *rectangular hyperbola* since it has two asymptotes that are at right angles to each other. These are:

$$y = y_m \tag{1.4}$$

and

$$x = \frac{-y_m}{\alpha} \quad \text{or} \quad x = -K \tag{1.5}$$

In practice, only positive values of x are used. The RH is illustrated in Fig. 1.1.

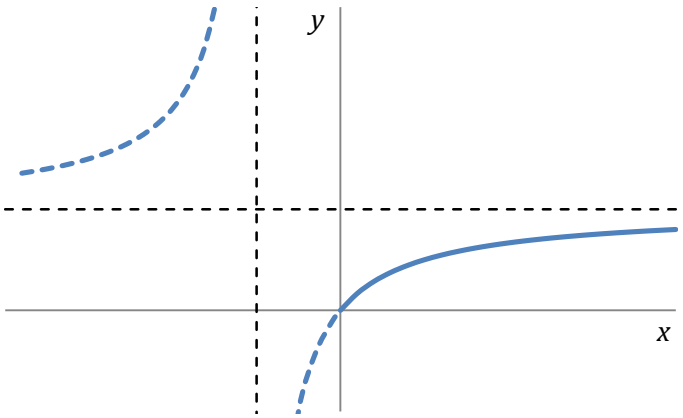

Figure 1.1: Rectangular hyperbola (blue lines), eqn (1.1) or (1.2), and the asymptotes given by eqns (1.4) and (1.5) (black dashed lines). The solid blue line is the part of the equation that is generally used in biological models.

The RH is also shown in Fig. 1.2 where now only the part of the curve that is biologically meaningful is shown, along with the key equation parameters. While the RH is a simple curve to work with, and the parameters have biological meaning, it is limited in that it generally approaches the asymptote quite slowly. The more general non-rectangular hyperbola that is discussed in the next section overcomes this limitation.

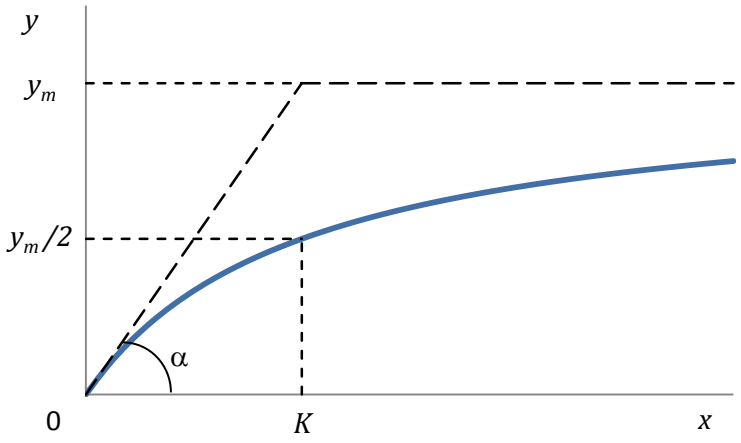

Figure 1.2: Rectangular hyperbola (blue line) with the key parameters as indicated. See text for details.

1.3.2 Non-rectangular hyperbola

The non-rectangular hyperbola (NRH) is a useful generic equation that is widely used to describe the leaf photosynthetic response to irradiance (see Chapter 3). It will also be used here for the CO_2 response. Mathematically, it is a modification of the rectangular hyperbola (RH) discussed in the previous section that has an extra parameter and where the asymptotes are now not perpendicular to each other. An overview of the equation is given here and for more detail, see Thornley and Johnson (2000) or Thornley and France (2007). Adding a quadratic equation to the RH, the NRH equation can be written

$$\xi y^2 - (\alpha x + y_m) y + \alpha x y_m = 0 \tag{1.6}$$

For $\xi = 0$ it reduces to the RH, eqn (1.1).

The solutions to eqn (1.6) are

$$y = \frac{1}{2\xi}\left[\alpha x + y_m \pm \left\{(\alpha x + y_m)^2 - 4\alpha\xi y_m x\right\}^{1/2}\right] \tag{1.7}$$

Note that for this equation to have two real solutions, it is necessary that

$$4\alpha\xi y_m x \le (\alpha x + y_m)^2 \tag{1.8}$$

for all values of x. For $x \ge 0$ this requires

$$\xi \le \frac{(\alpha x + y_m)^2}{4\alpha y_m x} \tag{1.9}$$

It is easy to show that the right-hand side of this equation takes its minimum value of 1 when $\alpha x = y_m$, so that the required constraint is

$$\xi \le 1 \tag{1.10}$$

Before looking at these solutions given by (1.7), note that eqn (1.6) can be factorized to give

$$(y - y_m)\left[\xi y - \left\{\alpha x + y_m(1-\xi)\right\}\right] = y_m^2(1-\xi) \tag{1.11}$$

from which it can be seen that there are two asymptotes at

$$y = y_m \quad \text{and} \quad y = \frac{\alpha x + y_m(1-\xi)}{\xi} \tag{1.12}$$

The solutions to eqn (1.6) as given by (1.7), along with the asymptotes (1.11) are illustrated in Fig. 1.3.

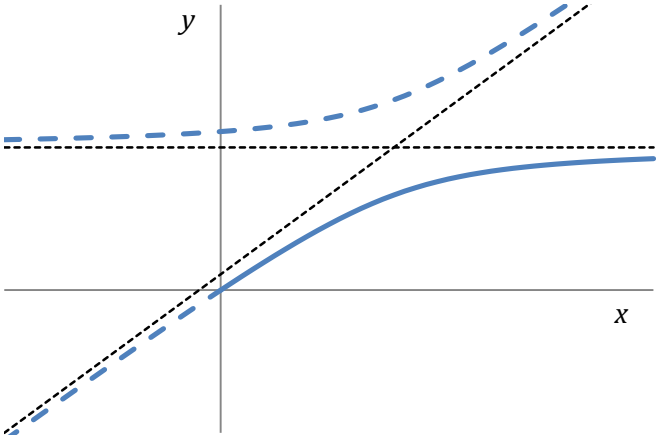

Figure 1.3: Non-rectangular hyperbola (blue lines), eqns (1.6) and (1.7), and the asymptotes given by eqns (1.12) (black dashed lines). The solid blue line is the part of the equation that is generally used in biological models.

In biological models, and all the present applications, the lower solution in (1.7) is used, with $x \geq 0$, that is

$$y = \frac{1}{2\xi}\left[\alpha x + y_m - \left\{(\alpha x + y_m)^2 - 4\alpha\xi y_m x\right\}^{1/2}\right], \quad x \geq 0 \tag{1.13}$$

This is illustrated with the solid line in Fig. 1.3 and for a range of ξ values in Fig. 1.4. This is a powerful, versatile equation that is easy to work with. The three parameters each control the key aspects of the response: the initial slope, curvature and asymptote. This is the form of the equation that is used to describe the light response for leaf gross photosynthesis. It is also used in the CO_2 response function.

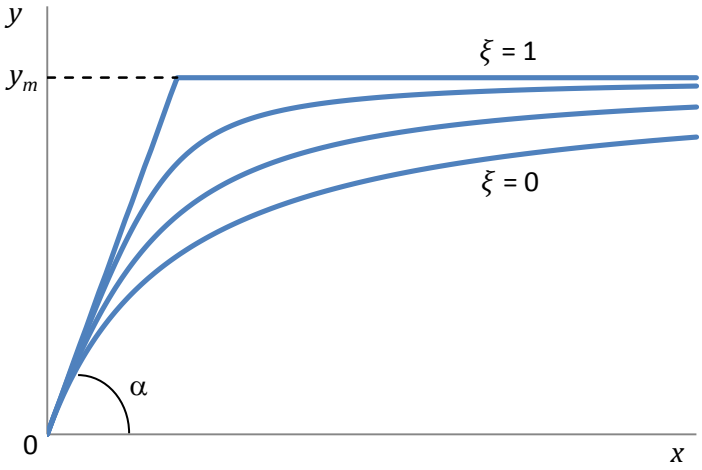

Figure 1.4: Non-rectangular hyperbola, eqn (1.13) for ξ increasing from 0 (lower line,) to 1 (upper line). The initial slope is α and the asymptote is y_m.

1.3.3 Switch functions

It is sometimes useful to have expressions to define 'switch-on' or 'switch-off' behaviour. Simple equations for this are

$$y_{on} = y_m \frac{x^n}{x^n + K^n} \tag{1.14}$$

which is quite similar to the rectangular hyperbola, and

$$y_{off} = y_m \frac{K^n}{x^n + K^n} \tag{1.15}$$

Both of these equations, which are illustrated in Fig. 1.5, take the value $y_m/2$ when $x = K$.

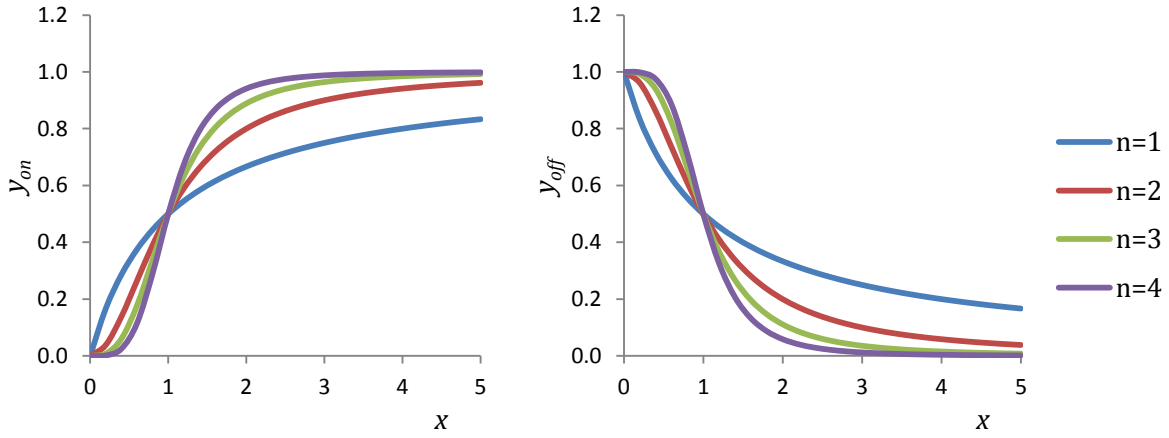

Figure 1.5: 'Switch-on' (left) and 'switch-off' (right) functions given by eqns (1.14) and (1.15), with $y_m = 1$, $K = 1$ and n as indicated

These functions are not actually used in the present model, but are presented here as simple extensions of the rectangular hyperbola that may be of use in other modelling exercises.

1.3.4 CO_2 response function

The NRH will be used in the treatment of the photosynthetic response to CO_2. However, it is convenient to re-cast the equation. First consider the general equation given by

$$f_C(C) = \frac{1}{2\phi}\left[\beta C + f_{C,m} - \left\{\left(\beta C + f_{C,m}\right)^2 - 4\phi\beta f_{C,m} C\right\}^{1/2}\right] \tag{1.16}$$

which is of the form eqn (1.13), where C is atmospheric CO_2 concentration, β is the initial slope, ϕ $(0 \le \phi \le 1)$ the curvature and $f_{C,m}$ the asymptote.

In order to assist with parameterization, the function is constrained to take the value unity at ambient CO_2 and λ at double ambient, so that

$$\left.\begin{aligned} f_C(C = C_{amb}) &= 1 \\ f_C(C = 2C_{amb}) &= \lambda \end{aligned}\right\} \tag{1.17}$$

which are the values at ambient and double ambient CO_2 concentration, where C_{amb} is the ambient atmospheric CO_2 concentration, taken to be $C_{amb} = 380\ \mu\text{mol mol}^{-1}$, eqn (1.91) below.

For example, consider this equation as used for leaf gross photosynthesis at saturating irradiance. If $\lambda = 1.5$ and $f_{C,m} = 2$ then the photosynthetic rate increases by 50% when CO_2 is double ambient, and is increased by 100% at saturating CO_2. It is now necessary to calculate the appropriate values of β and ϕ in eqn (1.16) in order to satisfy (1.17). After some algebra, it can be shown that

$$\phi = \frac{f_{C,m}\left[\lambda\left(f_{C,m}-1\right)-2\left(f_{C,m}-\lambda\right)\right]}{\lambda^2\left(f_{C,m}-1\right)-2\left(f_{C,m}-\lambda\right)} \tag{1.18}$$

and

$$\beta = \frac{\lambda\left(f_{C,m}-\phi\lambda\right)}{2C_{amb}\left(f_{C,m}-\lambda\right)} \tag{1.19}$$

so that β and ϕ are evaluated in terms of λ and $f_{C,m}$. Care must be taken to ensure that values for λ and $f_{C,m}$ are selected such that $0 \le \phi \le 1$ and $\beta > 0$. To do so, note that

$$\phi = 1 \text{ when } f_{C,m} = \lambda; \text{ and } \phi = 0 \text{ when } f_{C,m} = \lambda/(2-\lambda) \tag{1.20}$$

Since $\lambda > 1$, it then follows that the required constraint is

$$f_{C,m} \le \frac{\lambda}{2-\lambda} \tag{1.21}$$

This is checked in the program. Note that with the default values

$$\lambda = 1.5, \quad f_{C,m} = 2 \tag{1.22}$$

it follows that

$$\beta = 0.0032, \quad \phi = 0.8 \tag{1.23}$$

The function is illustrated in Fig. 1.6 where ambient, double ambient, and the asymptote are also shown.

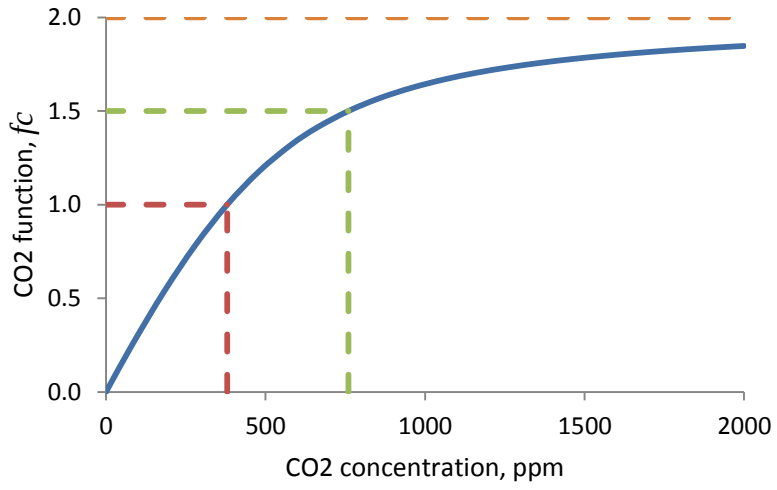

Figure 1.6: Generic CO_2 response function f_C, eqn (1.16), subject to (1.17), (1.18), (1.19)with C_{amb} = 380ppm, $f_C(C = C_{amb})$ = 1, $f_C(C = 2C_{amb})$ = 1.5, $f_C(C \to \infty)$ = 2.

1.3.5 Temperature response functions

Two forms of temperature response are used in the model – either with or without a temperature optimum. For more details see Johnson and Thornley (1985), Thornley and Johnson (2000), Thornley and France (2007).

Temperature response without an optimum

The simplest equation to use is the so-called Q_{10}, which is given by

$$k = k_r Q_{10}^{(T-T_r)/10} \tag{1.24}$$

where k is the reaction rate, T is temperature, T_r is a reference temperature, taken to be

$$T_r = 20°\text{C} \tag{1.25}$$

k_r is the value of k at the reference temperature T_r, and Q_{10} is the temperature coefficient. According to this equation,

$$\frac{k(T+10)}{k(T)} = Q_{10} \tag{1.26}$$

for all values of T, so that the reaction rate increases by a factor Q_{10} for every 10°C increase in temperature. Q_{10} is typically of order 1.5 to 2 for most practical applications.

An alternative equation that is sometimes used is the Arrhenius equation, which is defined by

$$k = Ae^{-E_a/RT} \tag{1.27}$$

where A is a rate parameter with the same dimensions as k, E_a (J mol^{-1}) is the *activation energy*, T (K) is the absolute temperature, and $R = 8.3145$ J K^{-1} mol^{-1} is the gas constant. A derivation of eqn (1.27) can be found in Johnson and Thornley (1985) or Thornley and Johnson (2000).

It is convenient to normalize (1.27) so that it takes a reference value at the reference temperature T_r, which requires

$$A = k_r e^{E_a/293.15R} \tag{1.28}$$

where the factor 293.15 is 20°C converted to absolute degrees (K). Equation (1.27) is now written

$$k = k_r \exp\left[\frac{E_a}{R}\left(\frac{1}{T_r} - \frac{1}{T}\right)\right] \tag{1.29}$$

so that

$$k = k_r \left(T = T_r\right) \tag{1.30}$$

In practice, the activation energy, E_a is treated as an empirical parameter to fit to data. This can be compared to the Q_{10} equation, eqn (1.24), by using the fact that they both take the value k_r at the reference temperature, T_r, and then equating them at 30°C to give

$$E_a = 8.3145 \times \frac{293.15 \times 303.15}{10} \ln(Q_{10}) = 74{,}130 \ln(Q_{10}) \tag{1.31}$$

With typical values of 1.5 and 2 for Q_{10}, the corresponding E_a values are

$$Q_{10}=1.5; \quad E_a=29{,}960 \text{ J mol}^{-1}$$
$$Q_{10}=2; \quad E_a=51{,}216 \text{ J mol}^{-1} \tag{1.32}$$

The Q_{10} and Arrhenius equations are illustrated in Fig. 1.7 for these parameter values. It can be seen that the responses are virtually identical over a practical temperature range.

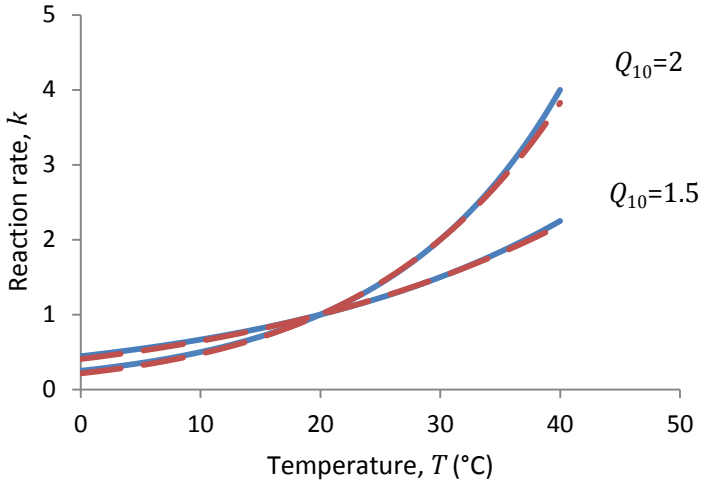

Figure 1.7. Q_{10} equation, blue lines, and Arrhenius equation, dashed red lines, for the Q_{10} values as indicated and activation energies given by eqn (1.32). The two equations give virtually identical responses.

Given the close similarity between the two equations, the choice here is to use the Q_{10} approach since the Q_{10} parameter is intuitive to work with and is simple to relate to data. Furthermore, the Arrhenius equation is based on a single chemical reaction, whereas processes such as plant respiration involve sequences of many reactions which may have different individual energy characteristics.

Temperature response with an optimum

Temperature responses with a temperature optimum are more complex to deal with than those without that were considered above. The scheme for the Arrhenius equation can be generalized to generate a response function that has a maximum, and the resulting equation is

$$k=\frac{A\exp\left(-E_a/RT\right)}{1+\exp\left(\Delta S/R-\Delta H/RT\right)} \tag{1.33}$$

where, again, A is a rate constant, E_a (J mol^{-1}) is the activation energy, T (K) is the absolute temperature, and R is the gas constant. The additional parameters are ΔS (J K^{-1} mol^{-1}) which is an entropy term, and ΔH (J mol^{-1}) which is an enthalpy term. A derivation of eqn (1.33) is given in Johnson and Thornley (1985) or Thornley and Johnson (2000). Equation (1.33) is illustrated in Fig. 1.8.

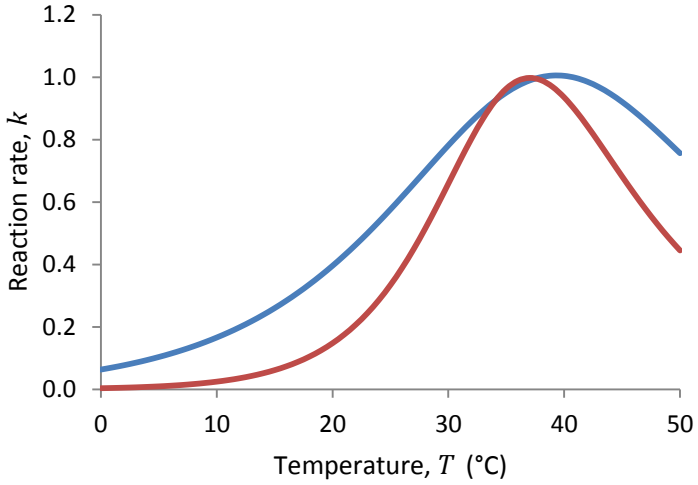

Figure 1.8: Temperature response function, eqn (1.33).
Blue line: $A = 5.33 \times 10^{10}$, $E_a/R = 7.5 \times 10^3$ K, $\Delta S/R = 48$, $\Delta H/R = 1.5 \times 10^4$ K.
Red line: $A = 2.5 \times 10^{10}$, $E_a/R = 1.5 \times 10^3$ K, $\Delta S/R = 81$, $\Delta H/R = 2.5 \times 10^4$ K

While parameter values can be selected in eqn (1.33) to describe temperature responses, it is quite complex to vary the parameters routinely to adjust the details of the curve. As for the Arrhenius equation discussed above, eqn (1.27), the underlying scheme that leads to eqn (1.33) involves an idealized single enzyme-substrate reaction where the enzyme can exist in either an active or inactive state. There is little theoretical justification in using this scheme for the sequence of reactions that occur in photosynthesis. It should be noted that variations to eqn (1.33) can be derived.

For the present purposes, a simpler empirical temperature response function is used. Following Thornley (1998), Thornley and France (2007), consider the temperature response function given by

$$f_T(T) = \left(\frac{T - T_{mn}}{T_r - T_{mn}}\right)^q \left(\frac{T_{mx} - T}{T_{mx} - T_r}\right) \tag{1.34}$$

where T_{mn} and T_{mx} are the minimum and maximum temperatures such that

$$f_T(T_{mn}) = f_T(T_{mx}) = 0 \tag{1.35}$$

$q \geq 1$ is a curvature parameter, and T_r is a reference temperature with

$$f_T(T_r) = 1 \tag{1.36}$$

This equation has a maximum value at

$$T_{opt} = \frac{T_{mn} + qT_{mx}}{1+q} \tag{1.37}$$

from which

$$T_{mx} = \frac{(1+q)T_{opt} - T_{mn}}{q} \tag{1.38}$$

Equation (1.38) can be used in (1.34) to eliminate T_{mx}, giving

$$f_T(T)=\begin{cases}0, & T\le T_{mn}\\ \left(\dfrac{T-T_{mn}}{T_r-T_{mn}}\right)^q\left(\dfrac{(1+q)T_{opt}-T_{mn}-qT}{(1+q)T_{opt}-T_{mn}-qT_r}\right), & T_{mn}<T<T_{mx}\\ 0 & T\ge T_{mx}\end{cases} \quad (1.39)$$

where T_{mx} is given by eqn (1.38). This T_{mn}, T_{opt} equation describes the temperature response in terms of the minimum and optimum temperatures, as well as the curvature coefficient q. Alternatively, if it was more convenient, q could be derived from eqn (1.37) to give an equation in terms of the minimum, optimum and maximum temperatures. This is not presented here, and eqn (1.39) will be used.

In applying this function, the constraint

$$T_r \le T_{opt} \quad (1.40)$$

should be applied. While this is not absolutely necessary, it does ensure sensible behaviour of eqn (1.39).

The function is illustrated in Fig. 1.9.

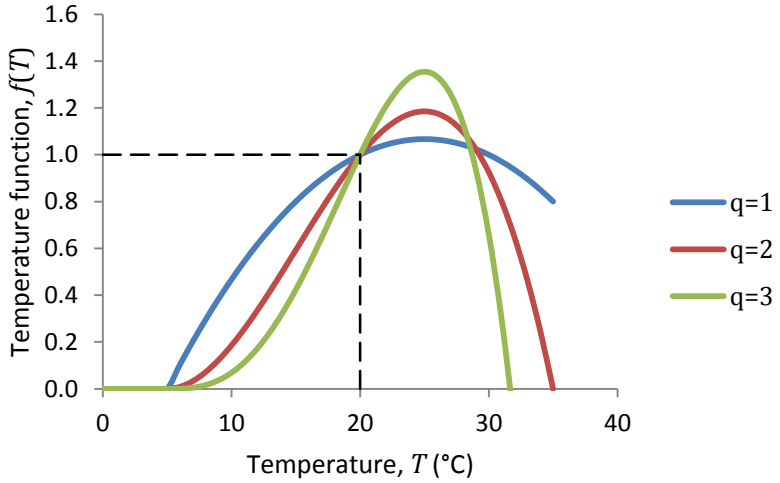

Figure 1.9. Generic temperature function, eqn (1.39). Parameters are: $T_r = 20$°C, $T_{mn} = 5$°C, $T_{opt} = 25$°C, q as indicated. Note that $f(T = T_r) = 1$.

This equation is versatile and simple to use, having easily interpreted parameter values, and will be used for temperature responses that have an optimum. It should be noted that when $q = 1$ the temperature response is symmetric around the optimum temperature. This rarely happens in biological processes and values of q in the range 2 to 3 are generally more appropriate.

For situations where a temperature function without an optimum is required, eqn (1.39) is modified to be

$$f_T(T)=\begin{cases}0, & T\le T_{mn}\\ \left(\dfrac{T-T_{mn}}{T_r-T_{mn}}\right)^q\left(\dfrac{(1+q)T_{opt}-T_{mn}-qT}{(1+q)T_{opt}-T_{mn}-qT_r}\right), & T_{mn}<T<T_{opt}\\ \left(\dfrac{T_{opt}-T_{mn}}{T_r-T_{mn}}\right)^q\left(\dfrac{T_{opt}-T_{mn}}{(1+q)T_{opt}-T_{mn}-qT_r}\right) & T\ge T_{opt}\end{cases} \quad (1.41)$$

This equation is illustrated in Fig. 1.10 for the same parameter values as used in Fig. 1.9.

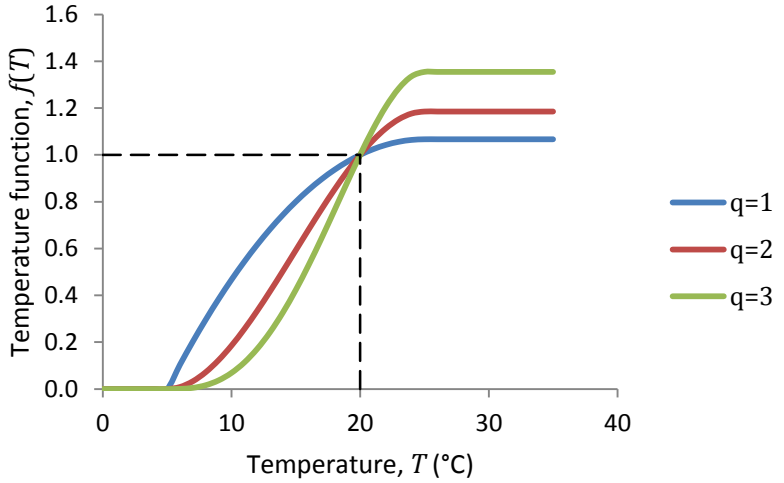

Figure 1.10. Generic temperature function with an asymptoted, eqn (1.41). Parameters are: $T_r = 20$°C, $T_{mn} = 5$°C, $T_{opt} = 25$°C, q as indicated. Note that $f(T = T_r) = 1$.

1.3.6 Gompertz growth equation

Growth functions are widely applied in many branches of the biological sciences, generally in the analysis of the time course of experimental data in plant and animal studies, although they can be adapted to respond dynamically to changes in driving variables – in the present model the Gompertz growth equation (described in detail in this section) is used in the dynamic animal growth model in response to available energy intake. The term growth function generally denotes an analytical function which can be written as a single equation. Thus, a growth function for the time course of mass or weight W is

$$W = f(t) \tag{1.42}$$

where t is time.

While a wide range of growth functions are used in agricultural modelling, there are two characteristics which, as discussed by Thornley and Johnson (2000), they should satisfy if they are to be of significant use. First, it should be derived from a differential equation for $\mathrm{d}W/\mathrm{d}t$, so that there is an explicit equation for the growth rate. Second, the parameters in the model should have some meaningful biophysical interpretation so that variation in these parameters can be interpreted biologically. Thus,

$$\frac{dW}{dt} = g(W,t) \tag{1.43}$$

which defines the growth rate in terms of the current weight and time. This choice of formulation implies that the growth rate at any particular time also depends on the actual value of W. A further desirable characteristic is that time can be eliminated from eqn (1.43) so that the growth rate can be written as a 'rate-state' equation – that is, the growth rate is a function of the current state of the system which, in this case, is W, so that eqn (1.43) can be written

$$\frac{dW}{dt} = h(W) \tag{1.44}$$

Once the growth rate has been defined by either eqn (1.43) or (1.44), the differential equation is solved for $W(t)$. However, if the equation is being applied with varying inputs, such as for animal growth, the

equation must be solved numerically. (Numerical techniques are discussed in Section 1.4). Growth functions are discussed in detail in Thornley and Johnson (2000) and Thornley and France (2007).

The Gompertz equation is derived from two equations. First, it is assumed that growth rate is directly proportional to weight, so that

$$\frac{\mathrm{d}W}{\mathrm{d}t} = \mu W \tag{1.45}$$

where μ d^{-1} is the specific growth rate and also is derived from a differential equation which is

$$\frac{\mathrm{d}\mu}{\mathrm{d}t} = -D\mu \tag{1.46}$$

where D is a parameter describing the decay of the specific growth rate. Integrating eqn (1.46) gives

$$\mu = \mu_0 \mathrm{e}^{-Dt} \tag{1.47}$$

with μ_0 being the initial value of μ (that is, the value at $t = 0$). Using eqn (1.47) in (1.45) gives

$$\frac{\mathrm{d}W}{\mathrm{d}t} = \mu_0 W \mathrm{e}^{-Dt} \tag{1.48}$$

which is the general formulation for the Gompertz differential equation.

To integrate eqn (1.48), it is written as

$$\int_{W_0}^{W} \frac{\mathrm{d}W'}{\mathrm{d}t} = \mu_0 \int_0^t e^{-Dt'} \mathrm{d}t' \tag{1.49}$$

where $W(t = 0) = W_0$ is the initial weight and the primes denote dummy variables of integration. This equation is now easily solved to give

$$\ln\left(\frac{W}{W_0}\right) = \frac{\mu_0}{D}\left(1 - \mathrm{e}^{-Dt}\right) \tag{1.50}$$

and hence

$$W = W_0 \exp\left[\frac{\mu_0}{D}\left(1 - \mathrm{e}^{-Dt}\right)\right] \tag{1.51}$$

which is the Gompertz equation.

There are some useful characteristics of this equation. When t is small, using the series expansion of e^{-Dt},

$$1 - \mathrm{e}^{-Dt} \approx Dt \tag{1.52}$$

so that eqn (1.51) reduces to

$$W \approx W_0 \exp(\mu_0 t) \tag{1.53}$$

This means that growth is approximately exponential during the early growth phase with specific growth rate μ. As $t \to \infty$, W approaches an asymptote given by

$$W_f = W_0 \exp\left(\frac{\mu_0}{D}\right) \tag{1.54}$$

Differentiating eqn (1.51) gives

$$\frac{1}{\mu_0}\frac{\mathrm{d}^2W}{\mathrm{d}t^2}=\frac{\mathrm{d}W}{\mathrm{d}t}\mathrm{e}^{-Dt}-DW\mathrm{e}^{-Dt} \tag{1.55}$$

Equating this to zero and substituting for $\mathrm{d}W/\mathrm{d}t$ from eqn (1.48), there is a point of inflexion at t^*, where

$$t^*=\frac{1}{D}\ln\left(\frac{\mu_0}{D}\right) \qquad \text{and} \qquad W\left(t=t^*\right)=\frac{W_f}{\mathrm{e}} \tag{1.56}$$

Thus, the point of inflexion occurs at about 37% of the final weight.

It was mentioned earlier that there are benefits in prescribing the growth rate equation independently of time. This can be done by substituting for $\exp(-Dt)$ from (1.51) in (1.48) to give

$$\frac{\mathrm{d}W}{\mathrm{d}t}=\mu_0 W\left[1-\frac{D}{\mu_0}\ln\left(\frac{W}{W_0}\right)\right] \tag{1.57}$$

In turn, either D or μ_0 can be eliminated using eqn (1.54) so that the Gompertz equation can be written as

$$\frac{\mathrm{d}W}{\mathrm{d}t}=\mu_0 W\left[\frac{\ln\left(W_f/W\right)}{\ln\left(W_f/W_0\right)}\right] \tag{1.58}$$

or

$$\frac{\mathrm{d}W}{\mathrm{d}t}=DW\ln\left(\frac{W_f}{W}\right) \tag{1.59}$$

In practice, the parameter μ_0 is probably easier to prescribe from an intuitive understanding of the system being modelled – that is, the specific growth rate during early growth – so that eqn (1.58) may be preferable to eqn (1.59). Note that the maximum growth rate, which occurs at the inflexion point, can be derived from eqns (1.56) and (1.58) as

$$\left.\frac{\mathrm{d}W}{\mathrm{d}t}\right|_{mx}=\frac{\mu_0 W_f}{\mathrm{e}\,\ln\left(W_f/W_0\right)} \tag{1.60}$$

The Gompertz equation is illustrated in Fig. 1.11 using parameters that represent typical cattle growth, where both the weight and growth rate are shown. The point of inflexion, which is the point where the growth rate is maximum and as given by (1.56), is indicated. The equation has the typical sigmoidal growth pattern that is generally observed for animals and that is also characteristic of plant growth. The Gompertz equation is used in AgMod in the formulation of the animal growth model, but is adapted to allow for fluctuating energy intake by the animals, as discussed in Chapter 6.

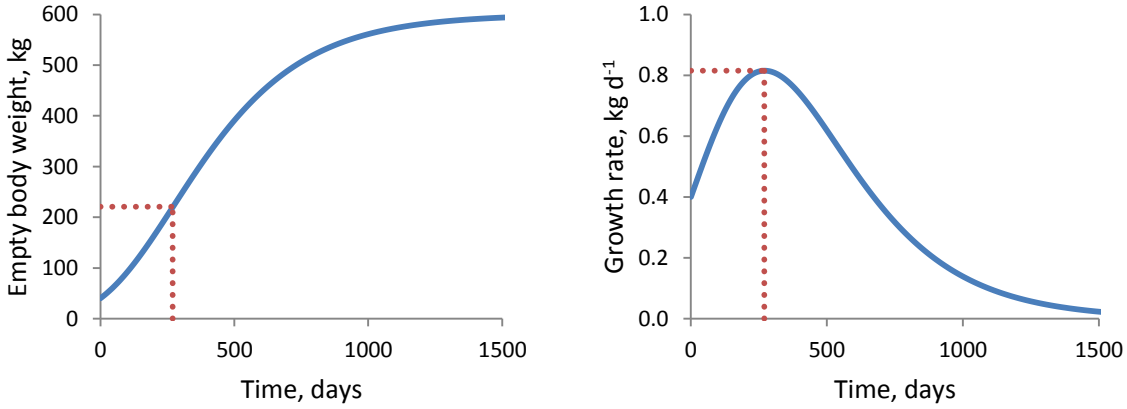

Figure 1.11. The Gompertz equation, eqn (1.51), illustrated with parameters that are typical for cattle growth. The parameters are W_0 = 40 kg, W_f = 600 kg, μ_0 = 0.01 d^{-1}, with D derived from eqn (1.54). The red dotted lines indicate the point of inflexion, along with the weight and growth rate at this point, as given by eqns (1.56) and (1.60).

1.4 Euler's method for solving differential equations

The dynamic models in the SGS Pasture Model and DairyMod are characterized by generally being written as first order differential equations, that is, rate-state equations as discussed in the previous section for the Gompertz equation. These equations generally cannot be solved analytically due to their complexity as well as the fact that inputs are generally varying – for example, climate for plant growth, available pasture for animal growth, and so on. Consequently, the equations must be solved using numerical techniques. Numerical methods for solving differential and other forms of equations is a large field in mathematics known as *numerical analysis*. It is not my intention to discuss this in any great detail here, but an introductory discussion is given in Thornley and Johnson (2000).

Most of the dynamic equations that have to be solved numerically in the present model have the form

$$\frac{\mathrm{d}x}{\mathrm{d}t} = f(x,t) \tag{1.61}$$

where x is the state variable, t is time, and f denotes a function that defines the rate of change of x with t. This is referred to as a *rate-state* equation. In practice, the function f will also include model parameters and environmental inputs, but these are not included here explicitly.

The simplest method for solving eqn (1.61) numerically is Euler's method. By definition,

$$\frac{\mathrm{d}x}{\mathrm{d}t} = \lim_{\Delta t \to 0}\left[\frac{x(t+\Delta t)-x(t)}{\Delta t}\right] \tag{1.62}$$

Substituting eqn (1.61) into (1.62) gives

$$f\left[x(t),t\right] = \lim_{\Delta t \to 0}\left[\frac{x(t+\Delta t)-x(t)}{\Delta t}\right] \tag{1.63}$$

For small values of Δt it is approximately true that

$$f\left[x(t),t\right] = \frac{x(t+\Delta t)-x(t)}{\Delta t} \tag{1.64}$$

Rearranging this equation gives Euler's formula as

$$x(t+\Delta t)=x(t)+\Delta t\, f\left[x(t),t\right] \tag{1.65}$$

Thus, the state variable x at time $t+\Delta t$ is given as a function of its derivative at t and the time increment Δt. Equation (1.65) is also referred to as a *forward difference equation*.

As with any numerical technique, it is important to assess the accuracy of the method. This is not discussed here, but the interested reader can read section 1.6 in Thornley and Johnson (2000). However, it can be noted that for biophysical simulation models, Euler's method generally works well for pasture and animal growth using a daily time-step, and is applied widely in the model.

1.5 Plant composition components

The theory presented here involves plant dry weight (d.wt) as well as photosynthetic rates. While the mole is the preferred unit for photosynthesis, in most plant growth experiments the units of plant dry weight are usually kg d.wt. To reconcile these units, it is assumed that the plant comprises sugars, which are mono and disaccharides, protein, and cell wall material which is primarily cellulose and hemicelluloses. Other components such as lipids are not considered here, although the analysis could be extended to include them in a straightforward way. Taking the sugars to be primarily disaccharides (sucrose, fructose), the following carbon compositions by mass are used:

$$\left.\begin{aligned}&\text{Cell wall:}\quad 0.44\ \text{kg carbon}\ (\text{kg cell wall})^{-1}\\&\text{Protein:}\quad 0.53\ \text{kg carbon}\ (\text{kg protein})^{-1}\\&\text{Sugars:}\quad 0.42\ \text{kg carbon}\ (\text{kg sugar})^{-1}\end{aligned}\right\} \tag{1.66}$$

Denote the molar and dry weight fractions of plant material by

	mole	dry weight
Cell wall fraction:	f_w	F_w
Protein fraction:	f_p	F_p
Sugar fraction:	f_s	F_s

It follows that the fraction of carbon in total plant dry weight is

$$F_C = 0.44F_w + 0.53F_p + 0.42F_s \tag{1.67}$$

The conversions between mole and dry weight fractions of the individual components are:

$$\left.\begin{aligned}f_w &= F_w \times 0.44/F_C\\f_p &= F_p \times 0.53/F_C\\f_s &= F_s \times 0.42/F_C\end{aligned}\right\} \tag{1.68}$$

As an example, consider the plant dry weight composition to be 60% cell wall, 20% protein and 20% sugars by weight, so that

$$F_w = 0.6,\quad F_p = 0.2,\quad F_s = 0.2, \tag{1.69}$$

which gives (working to 2 significant figures)

$$F_C = 0.45, \tag{1.70}$$

and

$$f_w = 0.58,\ f_p = 0.23,\ f_s = 0.09 \tag{1.71}$$

Thus, while the mole and dry weight fractions of plant material do not vary greatly, they are, nevertheless, not identical and appropriate care should be taken.

F_C can be seen to be relatively insensitive to moderate changes in plant composition, although the carbon content of the plant components will affect the calculation of F_C.

For whole plant material,

$$1 \text{ mol C} = \frac{0.012}{F_C} \text{ kg d.wt} \tag{1.72}$$

and, using eqn (1.70), this gives

(1.73)

or

$$1 \text{ kg d.wt} = 37 \text{ mol C} \tag{1.74}$$

This is the conversion used here, although alternative values for F_C could readily be used. The parameter

$$\gamma = 37 \text{ mol C (kg d.wt)}^{-1} \tag{1.75}$$

will be used to convert from dry weight to mole units.

1.6 Atmospheric composition

Photosynthesis is influenced by atmospheric CO_2 concentration, while transpiration and evaporation depend on the water vapour concentration in the atmosphere. Methods for defining atmospheric gas components are now considered.

Density is defined as kg m^{-3} and concentration as mol m^{-3}. From the gas laws, the mole concentration of any gas, φ (mol m^{-3}), is given by

$$\varphi = \frac{P}{RT_K} \tag{1.76}$$

where P (Pa) is the atmospheric pressure, T_K (K) is temperature and $R = 8.314$ J K^{-1} mol^{-1} is the gas constant. Note that, while C is often used to define concentration in analysis of this type, φ is used here to allow C to be used in the treatment for CO_2. Also, the notation T_K is used to avoid confusion with T °C. The atmosphere is taken to comprise the dry air components plus water vapour, with the principal constituents of dry air (working to 2 percentage decimal places) being nitrogen (78.08%), oxygen (20.95%), argon (0.93%), and carbon dioxide (0.04%). When water vapour is included, it can account for up to around 4% of the atmosphere (although this is subject to considerable variation) and in this case the proportions of the main atmospheric constituents will decline slightly.

It is convenient to use either normal temperature and pressure (NTP) or standard temperature and pressure (STP). NTP is usually taken to be 20°C and 101.325 kPa. STP is 0°C and 101.325 kPa. Note that 101.325 kPa is the SI definition of pressure and is equivalent to 1 atmosphere (atm) which, in turn, is equivalent to 760 mm Hg and is a traditional value for atmospheric pressure at sea level. In all of the analysis here, NTP will be used, since 20°C is generally a more appropriate temperature for biological processes than 0°C, and is defined as:

$$\text{NTP: } 20°\text{C},\ 101.325 \text{ kPa}. \tag{1.77}$$

Thus, at NTP

$$\varphi_{NTP} = 41.574 \text{ mol m}^{-3} \tag{1.78}$$

which is the molar concentration of any gas.

The density ρ, kg m^{-3}, is given by

$$\rho = M\varphi \tag{1.79}$$

where M (kg mol^{-1}) is the molar mass, for example 44.01×10^{-3} kg mol^{-1} for CO_2.

In practice, the components of the atmosphere, such as CO_2, O_2, or water vapour are required. Denoting the concentration of the atmosphere as φ_{atm}, eqn (1.76) can be rewritten as

$$\varphi_{atm} = \frac{P}{RT_K} \tag{1.80}$$

The partial concentration of any component of the atmosphere, φ_i (mol m^{-3}), such as CO_2 or water vapour, has concentration

$$\varphi_i = \frac{e_i}{RT_K} \tag{1.81}$$

where e_i (Pa) is the partial pressure of the gas.

The fractional concentration of gas i, c_i mol gas i (mol atmosphere)$^{-1}$, is simply

$$c_i = \frac{\varphi_i}{\varphi_{atm}} \tag{1.82}$$

so that, using (1.80)

$$\varphi_i = c_i \frac{P}{RT_K} \tag{1.83}$$

which defines the molar concentration in terms of the fractional concentration, atmospheric pressure, the gas constant and temperature. As an example, consider CO_2 at NTP, eqn (1.77), and with $c_i = 380$ μmol mol^{-1} (equivalent to 380 ppm), so that the true concentration of CO_2 is

$$\varphi_{CO_2} = 0.01580 \text{ } \mu\text{mol m}^{-3} \tag{1.84}$$

Similarly, the partial pressure of constituent i, using (1.81) and (1.83), is

$$e_i = c_i P \tag{1.85}$$

so that the sum of the partial pressures of all the constituent gas components is equal to the atmospheric pressure.

In general, fractional concentration is independent of temperature and pressure so that, for example, the proportion of oxygen in the air at the top of Mount Everest is the same as at sea level, but the actual mole concentration will decline. Thus, if c_i is constant then eqn (1.83) implies that

$$\varphi_i \propto \frac{P}{T_K} \tag{1.86}$$

and (1.85) that

$$e_i \propto P \tag{1.87}$$

Although fractional molar concentration is generally used in models and analysis, the true mole concentration, φ_i, is arguably more appropriate for describing physiological processes as it defines the absolute number of molecules per unit volume. As an example consider humans breathing oxygen. It is common knowledge that we struggle at high altitudes. In this case, the fractional oxygen concentration is the same as at sea level but the true concentration declines substantially. Clearly, our physiology is responding to the true concentration. One possible reason why fractional concentrations are used in plant physiology relates to the physiology of leaf photosynthesis, which is discussed in Chapter 3.

Now consider the air. Equation (1.79) gives

$$\rho_a = M_a \varphi_a \tag{1.88}$$

and for the constituent gases

$$\rho_i = M_i \varphi_i \tag{1.89}$$

For eqn (1.88) to be applied, it is necessary to derive an expression for the molar mass of air, M_a. This is generally evaluated for dry air and the standard values for the molar mass and fractional concentration are given in Table 1.1. Denoting the molar mass of dry air as $M_{a,dry}$, this is given by

$$M_{a,dry} = M_{N_2} c_{N_2} + M_{O_2} c_{N_2} + M_{Ar} c_{ar} + M_{CO_2} c_{CO_2} = 0.02895 \text{ kg mol}^{-1} \tag{1.90}$$

If water vapour is present, as is usually the case, then M_a will be slightly lower than $M_{a,dry}$, although the difference is small (around 1%).

Table 1.1: Composition of dry air. M is the molar mass and c the fractional concentration. These values are taken from Monteith and Unsworth (2008), but adjusted so that the CO_2 fractional concentration is closer to current ambient.

Gas	Nitrogen	Oxygen	Argon	CO_2
M (kg mol^{-1})	0.02801	0.03200	0.03898	0.04401
c (%)	78.08	20.95	0.93	0.04

1.6.1 CO_2 concentration

As mentioned above, atmospheric CO_2 concentration is often defined in *parts per million,* or ppm, which refers to volume parts per million, and is equivalent to μmol mol^{-1}, which is *fractional molar concentration*, or *mole fraction.* Following convention, C will be used to define CO_2 concentration in units μmol CO_2 mol air, or ppm, and the current ambient CO_2 is taken to be

$$C_{amb} = 380 \ \mu\text{mol mol}^{-1} \tag{1.91}$$

Equation (1.83) can be applied to the fractional molar concentration of CO_2, C μmol mol, to give

$$\varphi_{CO_2} = \frac{C}{10^6} \frac{P}{RT_K} \tag{1.92}$$

so that, for example, at normal temperature and pressure, eqn (1.77)

$$\varphi_{CO_2,NTP}\left(C = C_{amb}\right) = 0.01580 \text{ mol } CO_2 \text{ m}^{-3} \tag{1.93}$$

and, taking the molar mass of CO_2 to be 0.04401 kg mol^{-1} in eqn (1.89), the density is

$$\rho_{CO_2,NTP}\left(C = C_{amb}\right) 0.0006953 \text{ kg } CO_2 \text{ m}^{-3} = 0.6953 \text{ g } CO_2 \text{ m}^{-3} \tag{1.94}$$

1.6.2 Water vapour

Atmospheric water vapour content can be defined using the same approach as for CO_2 above. However, the two most common methods are to use vapour density, ρ_v kg H_2O m^{-3}, or vapour pressure, e_v Pa. Using eqns (1.88) and (1.89) with (1.80) and (1.81) gives

$$\rho_v = \rho_a \frac{M_v}{M_a} \frac{e_v}{P} \tag{1.95}$$

where subscript v refers to water vapour. Assuming M_a can be represented by $M_{a,dry}$, eqn (1.90), and taking $M_v = 0.01802$, this becomes

$$\rho_v = 0.622 \rho_a \frac{e_v}{P} \tag{1.96}$$

It should be noted that in some texts the analysis leading to eqns (1.95) and (1.96) uses the density and pressure for dry air and then combines that with the water vapour, rather than the present approach which considers the total air composition including water vapour. This leads to a similar expression, but with the term $P - e_v$ in the denominator which is subsequently approximated to P (see, for example, Thornley and Johnson (2000) pp 423 and 633). With the present approach, it is necessary to assume that the molar mass of air can be represented by the value for dry air. In practice, any errors are small and eqns (1.95) and (1.96) can be used with confidence.

As the amount of water vapour in the air increases it eventually reaches saturation. The *saturation vapour pressure*, e'_v, is related to temperature and is given by Tetens formula (Campbell and Norman, 1998)

$$e'_v = 611 \exp\left(\frac{17.5T}{T + 241}\right) \text{ Pa} \tag{1.97}$$

which defines e'_v in units of Pa, with T in °C. The coefficients in (1.97) differ slightly from those given by Allen *et al.* (1998), although the effect on e'_v is negligible. Equation (1.97) is illustrated in Fig. 1.12, with units kPa rather than Pa.

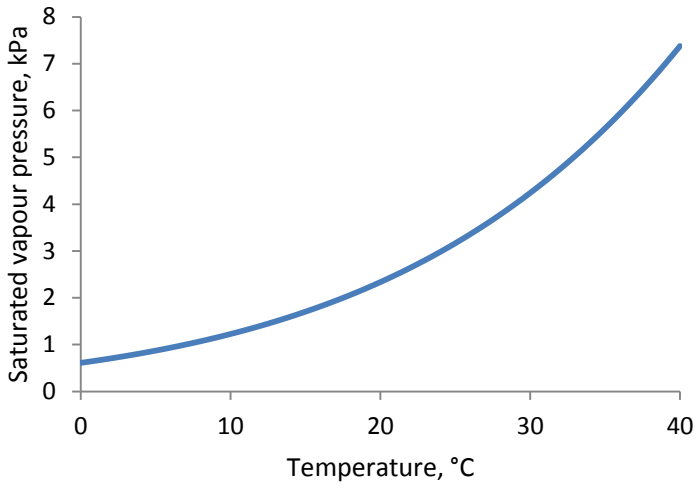

Figure 1.12: Saturated vapour pressure, e'_v (kPa), as a function of temperature.

The vapour density, ρ_v, is often referred to as the *absolute humidity*, and the ratio of the actual vapour density to saturated vapour density is the *relative humidity*, h_r, that is

$$h_r = \frac{\rho_v}{\rho_v'} = \frac{e_v}{e_v'} \tag{1.98}$$

where the prime denotes saturation and eqn (1.95) has been used to convert between pressure and density. Relative humidity cannot exceed unity and is often expressed as a percentage.

Vapour pressure deficit is widely used and is the difference between the saturated and actual vapour pressure, that is

$$\Delta e_v = e_v' - e_v \tag{1.99}$$

which, using eqn (1.98), may be written

$$\Delta e_v = e_v'\left(1 - h_r\right) \tag{1.100}$$

Relative humidity is a simple unit to work with and has appeal. However, it has limitations in terms of defining plant and canopy processes since for a given amount of water in the atmosphere it will vary substantially in response to temperature. To illustrate this point, Fig. 1.13 (left) shows the relative humidity as a function of temperature with $e_v = 0.6e_v'(T = 20°\text{C})$ so that the relative humidity at 20°C is 60%. It is quite clear that the relative humidity will vary substantially for a fixed amount of atmospheric water vapour. The corresponding vapour pressure deficit, in units kPa, is shown in Fig. 1.13 (right) which demonstrates that the driving force for transpiration and evaporation, the vapour pressure deficit, will vary in response to temperature for a fixed vapour pressure. Equation (1.100) should be used with caution and (1.99) is preferable.

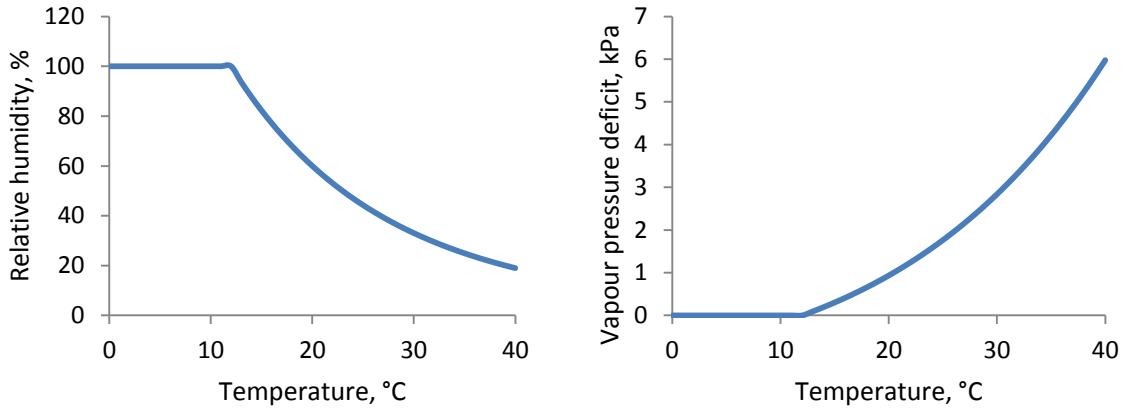

Figure 1.13: Left: relative humidity, h_r (%), as a function of temperature for vapour pressure corresponding to 60% saturation at 20°C. Thus, h_r = 60% at 20°C in this illustration.
Right: the corresponding vapour pressure deficit.

1.7 Final comments

The theory described in this Chapter covers the mathematical concepts of the background topics that are required for the various modules in the SGS Pasture Model and DairyMod. It is intended that this Chapter provides all of the necessary background for the full model description in the remainder of this book. However, many of the topics presented in this Chapter are also discussed in Thornley and Johnson (2000) and Thornley and France (2007). These texts also cover a wide range of models and modelling approaches in plant and crop physiology, and agricultural simulation modelling in general.

1.8 References

Allen RG, Pereira LS, Raes D and Smith M (1998). FAO irrigation and drainage paper no. 56: crop evapotranspiration. www.kimberly.uidaho.edu/ref-et/fao56.pdf.

Ball JT, Woodrow IE & Berry JA (1987). A model predicting stomatal conductance and its contribution to the control of photosynthesis under different environmental conditions. In: *Progress in Photosynthesis Research*, vol IV, ed J Biggens. Martinus Nijhoff / American Society of Agronomy, Dordrecht, the Netherlands / Madison, WI, USA, 221-224.

Blonquist Jr JM, Norman JM & Bugbee B (2009). Automated measurement of canopy stomatal conductance based on infrared temperature. *Agricultural and Forest Meteorology,* **149,** 1931-1945.

Bunce JA (2000). Responses of stomatal conductance to light, humidity and temperature in winter wheat and barley grown at three concentrations of carbon dioxide in the field. *Global Change Biology,* **6,** 371-382.

Campbell GS and Norman JM (1998). *An Introduction to environmental biophysics*, second edition. Springer, New York, USA.

Gale, J (2004). Plants and altitude – revisited. *Annals of Botany*, **92(4)**, 199.

Johnson and Thornley (1985). Temperature dependence of plant and crop processes. *Annals of Botany,* **55,** 1-24.

Jones HG (1992). *Plants and microclimate*. Cambridge University Press, Cambridge, UK.

Mackowiak CL, Wheeler RM & Yorio NC (1992). Increased leaf stomatal conductance at very high carbon dioxide concentrations. *HortScience*, **27,** 683-684.

Monteith JL & Unsworth MH (2008). *Principles of environmental physics*, third edition. Elsevier, Oxford, UK.

Thornley JHM (1998). *Grassland dynamics: an ecosystem simulation model*. CAB International, Wallingford, UK.

Thornley JHM and France J (2007). *Mathematical models in agriculture*. CAB International, Wallingford, UK.

Thornley JHM & Johnson IR (2000). *Plant and crop modelling*. Blackburn Press, Caldwell, New Jersey, USA.

2 Climate

2.1 Introduction

Plant growth responds directly to climatic conditions, in particular light (irradiance), temperature, rainfall, atmospheric CO_2 concentration, vapour pressure deficit and windspeed. The model underlying the SGS Pasture Model and DairyMod has been developed to use SILO climate data files (Jeffrey, 2001), which is a tremendous resource available for pasture and crop modelling in Australia. SILO files provide daily data for locations on a 0.05^o longitude and latitude grid across Australia, which is a grid of approximately 5.5km, from the late 1800s until yesterday. Daily data that are used in AgMod are rainfall, maximum and minimum temperature, total solar (or global) radiation, and vapour pressure. Windspeed data are not routinely available and so it is necessary to assume a fixed value for windspeed in the model. Atmospheric CO_2 is prescribed by the user and it is quite straightforward to work with variable CO_2 concentration. SILO also provides an estimate of the FAO56 (Allen *et al.*, 1998) estimate of reference evapotranspiration and this is used in the model interface to analyse long-term trends in rainfall surplus, that is rainfall in excess of potential evapotranspiration demand, for the location being studied. This reference evapotranspiration is also used in the irrigation strategy based on rainfall deficit (which is just the negative value of rainfall surplus), but it is not used in any of the evapotranspiration calculations in the model.

The key biophysical responses to climate are photosynthesis and transpiration. Photosynthesis responds to the photosynthetically active component of solar radiation, as discussed in Chapter 1, as well as temperature and CO_2 concentration. Transpiration is dependent on the longwave radiation balance of the canopy, and also temperature and vapour deficit, as well as leaf stomatal conductance and the canopy architecture through their influence on the transfer of water vapour from the canopy to the bulk air stream. Atmospheric CO_2 concentration and vapour pressure deficit were discussed in Chapter 1. The climate inputs required for the model are discussed in turn.

2.2 Rainfall

Rainfall inputs are applied from above the canopy so that they are first intercepted by the canopy and then the litter and ground, as illustrated in Fig. 2.1.

Rainfall intensity can be important in water dynamics, in particular with relation to runoff. Since the model is designed to work with daily rainfall data, it is necessary to estimate rainfall intensity. This is done by allowing the user to specify the daily rainfall duration in hours, either as a constant for all months, or for individual months of the year. Thus, for example, it is possible to characterise regions that may have a high incidence of summer storms but where winter rainfall is generally light. Using the daily rainfall duration, the model then randomly selects a start time for the rain for each day of the simulation. This uses the in-built random number generator in the development programming language, Delphi (Embarcadero), although it should be noted that the random number generator is 'seeded' to ensure the same sequence of random numbers is generated each time a specific climate file is loaded.

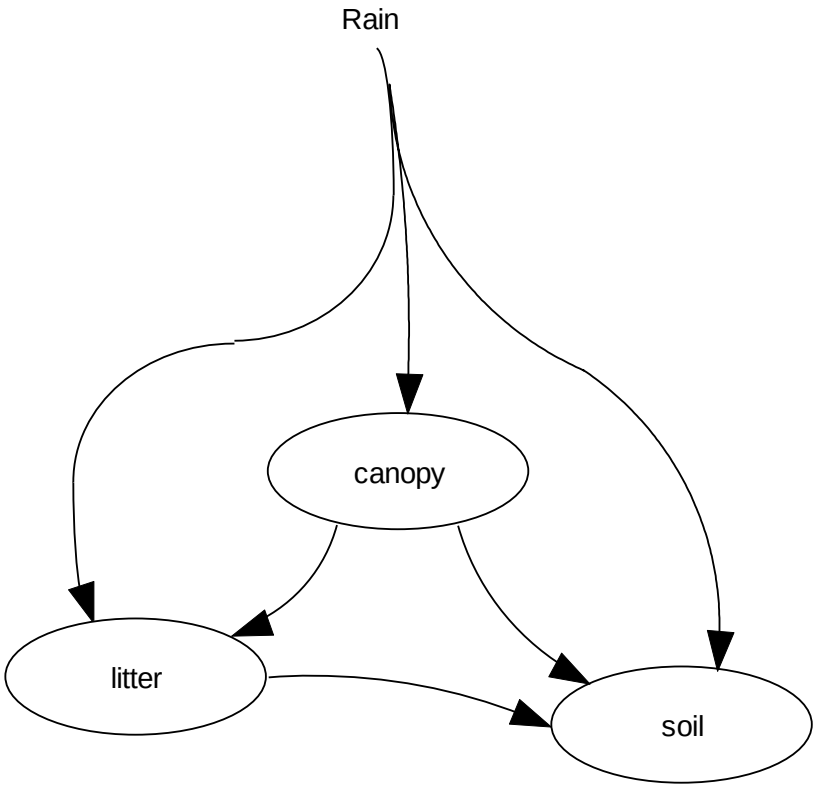

Figure 2.1: Schematic representation of rainfall inputs

2.3 Temperature

The model is designed to work with maximum and minimum daily temperature data, T_{mx} and T_{mn} respectively, with the mean daily temperature, T_{mean}, defined simply as the average of these values:

$$T_{mean} = 0.5\left(T_{mx} + T_{mn}\right) \tag{2.1}$$

For some processes, such as plant maintenance respiration, it is sufficient to work with T_{mean}, although for others the day or night temperature may be required, for example in the calculations for day and night soil evaporation (although most evaporation will generally occur during the day). Representative day and night temperatures are taken to be

$$\begin{aligned} T_{day} &= \left(T_{mx} + T_{mean}\right)/2 = \left(3T_{mx} + T_{mn}\right)/4 \\ T_{night} &= \left(T_{mn} + T_{mean}\right)/2 = \left(T_{mx} + 3T_{mn}\right)/4 \end{aligned} \tag{2.2}$$

2.4 Radiation

Radiation plays a crucial role in plant, crop and pasture physiological processes. The visible component of solar, or shortwave, radiation is the fundamental energy source for photosynthesis. The longwave radiation that is emitted by terrestrial bodies as well as the atmosphere, combined with solar radiation, is the key energy driver for the evaporation of water. A background to the basic principles relating to radiation components is now presented, but for a more complete discussion see, for example, Jones (1992), Campbell and Norman (1998), Monteith and Unsworth (2008).

A background to the basic physics of radiation is presented, followed by the analysis required for canopy photosynthesis and energy balance, which includes the calculations of evaporation and transpiration in response to environmental conditions. The radiation analysis forms the bulk of this Chapter. Some of the symbols in the early sections are used with different definitions later for canopy calculations.

The models presented in this Chapter can be explored in detail in the software package PlantMod (Johnson, 2013), and some of the illustrations presented here are taken directly from that program.

2.4.1 Black body radiation

The energy level distribution from a body is a function of its temperature, its wavelength and surface properties. If the surface properties are such that there is no reduction in energy emitted due to those surface properties, then that body is referred to as a *black body*. Planck's law, published in 1900, is derived from quantum mechanics, and states that

$$I(\lambda, T_K) = \frac{2hc^2}{\lambda^5}\left(\frac{1}{e^{hc/\lambda k T_K} - 1}\right) \tag{2.3}$$

where $I(\lambda, T_K)$ is the *spectral emittance*, W m^{-2} (m wavelength)$^{-1}$ (sometimes written as W m^{-3}), which is the energy per unit surface area per unit wavelength of the emitting body as a function of its temperature T_K (K) (the subscript K is used to differentiate from °C), and wavelength λ (m) of the emitted radiation. $h = 6.626 \times 10^{-34}$ J s is Planck's constant; $c = 2.998 \times 10^8$ m s^{-1} is the speed of light; and $k = 1.3807 \times 10^{-23}$ J K^{-1} is the Boltzmann constant. $I(\lambda, T)$ is illustrated in Fig. 2.2 for $T_K = 6000$ K, which approximates to the external surface of the sun, and $T_K = 300$ K (equivalent to 27°C) which is representative of temperatures on earth. The scales of these graphs are different since the energy emitted by the sun is much greater than that from the surface of the earth. The ultraviolet, photosynthetically active (see below) and infrared components of solar radiation are also indicated. It can be seen that $I(\lambda, T_K)$ peaks at a shorter wavelength for the higher temperature, and Wein's law can be derived which states that the peak wavelength is

$$\lambda_m = \frac{2897}{T_K} \times 10^{-6} \text{ m} \tag{2.4}$$

so that $\lambda_m(T_K = 6000) = 0.480$ μm and $\lambda_m(T_K = 300) = 9.597$ μm, which means that the peak energy emitted by terrestrial bodies has a much longer wavelength than for the sun – hence the terms shortwave and longwave. Longwave radiation is sometimes referred to as terrestrial or far-infrared radiation.

The total energy emitted at a particular temperature is the integral of $I(\lambda, T_K)$ for all wavelengths, which is the area under the curve shown in Fig. 2.2. This can be derived from eqn (2.3) and is known as the Stefan-Boltzmann equation, which (for a black body) is

$$E = \sigma T_K^4 \tag{2.5}$$

with units W m^{-2}, where $\sigma = 5.670 \times 10^{-8}$ W m^{-2} K^{-4} is the Stefan-Boltzmann constant. Thus, $E(T_K = 6000) = 7.35 \times 10^7$ W m^{-2} $\equiv 73.5$ MW m^{-2} and $E(T_K = 300) = 459$ W m^{-2}, demonstrating the greater energy emitted per unit area of the sun compared with the earth.

Of the radiation emitted by the sun about half of it is visible and this is the middle part of the frequency distribution, ranging from around 0.4 μm (blue light) to 0.7 μm (red light). Ultraviolet (UV) radiation is the component from below 0.4 μm, while the infrared (IR) component is the range 0.7 to 3 μm. These values, which are indicated in Fig. 2.2, are not exact since there is no sharp transition between the different components. The visible component of radiation is also known as *photosynthetically active radiation* (PAR) as this is the component of radiation that provides the energy for photosynthesis – this is discussed below. The wavelength of the radiation emitted by terrestrial bodies covers the range from about 3 to 100 μm, which is much greater than that for the sun, and hence is referred to as longwave, or far-IR, radiation.

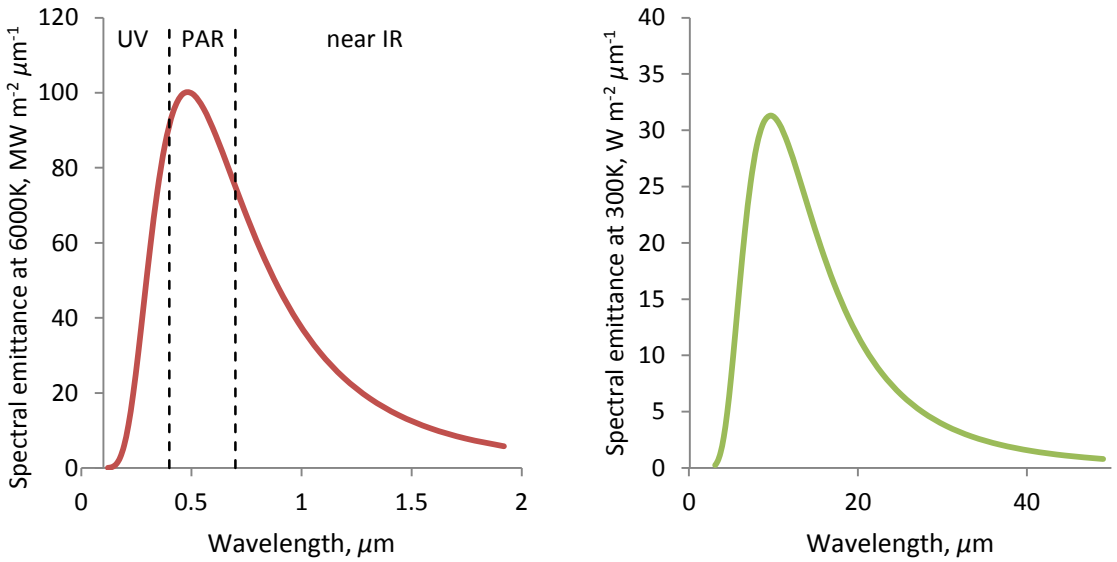

Figure 2.2: Spectral distribution of radiation emitted from black bodies for $T_K = 6000$ K (left) and $T_K = 300$ K (right), which correspond roughly to the surface of the sun and earth respectively, as a function of wavelength. The red line is shortwave, or solar, radiation, and the green line is longwave, or terrestrial, radiation. Also indicated for the shortwave radiation are the ultraviolet (UV), photosynthetically active radiation (PAR) and near-infrared (IR). The longwave radiation is also known as far-infrared. The components of radiation are discussed in the text. Note the scale for the shortwave radiation axis (left) is 10^6 times that on the right, which highlights the much greater energy emission by the sun.

2.4.2 Non-black body and grey body radiation

In practice, most terrestrial bodies do not behave like perfect black bodies and eqn (2.5) is modified to give

$$E = \varepsilon \sigma T_K^4 \tag{2.6}$$

where $\varepsilon, 0 < \varepsilon \leq 1$, (dimensionless) is the *emissivity*. Equation (2.6) applies to bodies where the emissivity is independent of wavelength. Black bodies therefore have an emissivity of 1 and bodies with $\varepsilon < 1$ are referred to as *grey bodies*. For most natural surfaces (including snow) ε lies between 0.95 and 1. Although it is reasonable to use the value 1, it is assumed that

$$\varepsilon = 0.97 \tag{2.7}$$

for calculation in the model.

2.4.3 Radiation energy for photosynthesis: PAR and PPF

As mentioned earlier, the visible component of the radiation emitted by the sun, which is in the range 0.4 to 0.7 μm (or 400 to 700 nm), provides the energy for photosynthesis. This is referred to as *photosynthetically active radiation*, or PAR, and is commonly assumed to be around half the total solar radiation. However, the precise fraction depends on climatic factors such as cloud cover and solar elevation. From the Clear Sky Calculator (www.clearskycalculator.com), it can be seen that a more accurate conversion is for PAR to be 45% of the total solar radiation. This fraction is not fixed, but increases when humidity increases and can reach close to 50%. The units for describing PAR are W $m^{-2} \equiv$ J m^{-2} s^{-1}.

For photosynthesis studies, the energy is generally expressed as the molar flux of photons between 0.4 to 0.7 μm, and is referred to as *photosynthetic photon flux*, or PPF. The term PPF will be used throughout this discussion for the definition of the energy source for photosynthesis.

There is no precise conversion between PAR and PPF that can be applied for all atmospheric conditions since, as discussed above, the energy of the radiation depends on the wavelength and so depends on the spectral composition of the light. A reasonable value, using the Clear Sky Calculator and based on summer conditions at Logan, Ut, (Bruce Bugbee, *pers. comm.,* www.clearskycalculator.com) is

1 μmol photons PAR $\cong$ 0.218 J PAR. (2.8)

Finally, note that the term *photon flux density*, or PFD, is sometimes used, but this is now discouraged in the literature. I'm grateful to Professor Bruce Bugbee for clarifying these definitions.

2.4.4 Radiation units and terminology

In the theory presented above, both J m^{-2} s^{-1} (equivalent to W m^{-2}) and μmol photons m^{-2} s^{-1} have been used for radiation energy. In the physics literature, J m^{-2} s^{-1} (W m^{-2}) is almost universally used, while in photosynthesis studies the recent trend has been towards μmol photons m^{-2} s^{-1}. In the present theory, both sets of units will be used, although this should not cause confusion. For discussions of photosynthesis, the convention for using μmol photons m^{-2} s^{-1} (PPF) is followed, but for energy dynamics and evaporation, J m^{-2} s^{-1} units are preferred, and this is referred to as irradiance which is the *total* solar radiation and not just the photosynthetically active component. The choice of J m^{-2} s^{-1} rather than W m^{-2}, which are equivalent, is because daily radiation values are also used which have units J m^{-2} d^{-1}.

2.4.5 Canopy light interception and attenuation

In order to model canopy photosynthesis in response to environmental factors, it is necessary to develop models of light interception and attenuation through the depth of the canopy. The canopy photosynthetic rate is then calculated in terms of the photosynthetic response to PPF of the leaves within the canopy and the variation of PPF through the depth of the canopy. The approach taken here is to look at the mean PPF through the canopy as well as the components of direct and diffuse sunlight. In doing so, the PPF components within the canopy and those that are actually incident on the leaf surfaces are considered. This component of the theory deals with the PPF with units μmol photons m^{-2}, where the area unit can refer either to ground or the leaf. The model for light interception and attenuation can be explored in PlantMod and so only a few illustrations are presented here.

Mean PPF

First consider the mean PPF within the canopy. In overcast conditions, there will be little variation in PPF in the horizontal plane and so this approach is applicable without modification. However, for clear skies with strong sunflecks in the canopy, there will be considerable horizontal variation in the PPF. The following theory still applies to these situations but it has to be extended to identify the direct and diffuse components of PPF.

As light is intercepted and absorbed by leaves within the canopy, the PPF declines, as described by Beer's law:

$$I(\ell) = I_0 e^{-k\ell} \quad (2.9)$$

where I_0 is the PPF incident on the canopy and k is the canopy extinction coefficient. A derivation of this equation is given in Thornley and Johnson (2000, Chapter 8). Note that since ℓ has dimensions (m^2leaf) (m^{-2} ground) it follows that k has dimensions (m^2 ground) (m^{-2} leaf), and hence eqn (2.2) is dimensionally

consistent. However, for most purposes it is sufficient to regard k as dimensionless. The PPF through the canopy as described by eqn (2.9) is illustrated in Fig. 2.3 for $k = 0.5$ which is typical of cereals and grasses, and $k = 0.8$ which is appropriate for canopies with more horizontally inclined leaves.

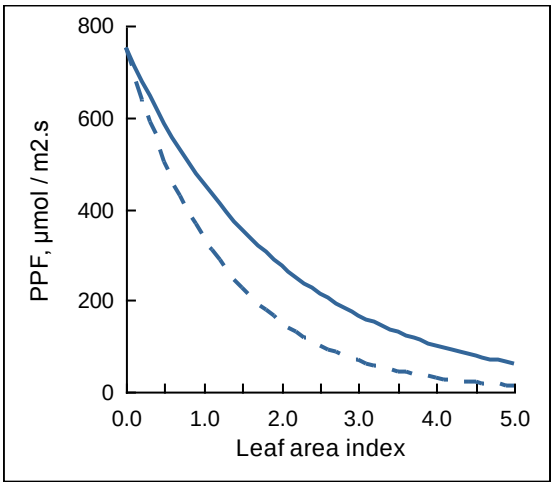

Figure 2.3: Mean PPF as a function of cumulative leaf area index through the canopy, as given by eqn (2.9) for $k = 0.5$ (solid) and $k = 0.8$ (dash), and with the PPF incident on the canopy given by $I_0 = 1000$ μmol m^{-2} s^{-1}. From PlantMod.

A simple interpretation of the extinction coefficient, k, is the cosine of the angle between the leaves and the horizontal plane. Thus, for perfectly horizontal leaves $k = \cos(0) = 1$.

Equation (2.9) defines the PPF per unit horizontal (or ground) area, but the PPF per unit leaf area is required in order to calculate the rate of photosynthesis of the leaves in the canopy. This is given by

$$I_\ell(\ell) = kI(\ell) \tag{2.10}$$

where the factor k projects the leaf area index onto the horizontal plane – for a derivation, see Thornley and Johnson (2000, p. 203)

Direct and diffuse PPF

The theory is now developed to identify the direct and diffuse components of PPF within the canopy. This approach is based on the early work of Norman (1980, 1982) as well as that by Campbell (1977) and Stockle and Campbell (1985). This treatment of direct and diffuse PPF is widely used and the analysis presented here closely follows Johnson *et al.* (1995) and has been applied, for example, by Thornley (2002).

Using subscripts s and d to denote the direct solar beam and diffuse PPF respectively, above the canopy, the PPF is

$$I_0 = I_{0,s} + I_{0,d} \tag{2.11}$$

Within the canopy at leaf area index ℓ it is

$$I = I_s + I_d \tag{2.12}$$

and the corresponding PPF incident on the leaf surfaces is

$$I_\ell = I_{\ell,s} + I_{\ell,d} \tag{2.13}$$

It is assumed that the direct and diffuse components of I_0 decline through the depth of the canopy according to eqn (2.9). Defining f_s as the fraction of total radiation that is direct, so that

$$I_{0,s} = f_s I_0 \tag{2.14}$$

it therefore follows that

$$I_s = f_s I_0 \mathrm{e}^{-k\ell} \tag{2.15}$$

and

$$I_d = \left(1 - f_s\right) I_0 \mathrm{e}^{-k\ell} \tag{2.16}$$

To calculate the incident PPF on the leaves, it is necessary to evaluate the components of leaf area index which are in direct sunlight and diffuse PPF, denoted by ℓ_s and ℓ_d respectively. ℓ_s is obtained by noting that the reduction in the direct beam is intercepted by ℓ_s , so that

$$k\ell_s I_{0,s} = I_{0,s}\left(1 - \mathrm{e}^{-k\ell}\right) \tag{2.17}$$

from which

$$\ell_s = \frac{1 - \mathrm{e}^{-k\ell}}{k} \tag{2.18}$$

The factor k on the left hand side of eqn (2.17) is required as this projects the leaf area index, ℓ_s, onto the horizontal plane. The remainder of the leaves are in diffuse PPF and have leaf area index

$$\ell_d = \ell - \ell_s \tag{2.19}$$

The incident PPF on ℓ_d is, applying eqns (2.10) and (2.16)

$$\begin{aligned} I_{\ell,d} &= kI_d \\ &= kI_0\left(1 - f_s\right)\mathrm{e}^{-k\ell} \end{aligned} \tag{2.20}$$

The PPF incident on ℓ_s is the combination of the diffuse component and the direct solar beam, as given by

$$\begin{aligned} I_{\ell,s} &= kI_{0,s} + I_{\ell,d} \\ &= kI_0\left[f_s + \left(1 - f_s\right)\mathrm{e}^{-k\ell}\right] \end{aligned} \tag{2.21}$$

Note that Norman (1982) relates the extinction coefficient, k to solar elevation. While this is a good objective for detailed study of light interception in canopies, difficulties arise when looking at mean values over the day (for further discussion, see Johnson *et al.*, 1995). One value for the extinction coefficient for both direct and diffuse PPF is used and it is assumed to be constant.

The mean PPF, I, direct and diffuse components, I_s, I_d, and PPF incident on leaves in direct and diffuse light, $I_{l,s}$, $I_{l,d}$, are shown in Fig. 2.4.

The theory presented here provides a complete description of the attenuation and interception of the direct and diffuse PPF components through the canopy. It is necessary to define the canopy light extinction coefficient, k, the PPF on the canopy, I_0, and the fraction of I_0 that is from the direct solar beam, f_s. In practice, the extinction coefficient may vary from around 0.5 for cereals and grasses to 0.8 for species with more horizontally inclined leaves such as clover. For skies where the sun is not obscured by cloud, f_s may be typically around 0.7, although this can depend on atmospheric composition.

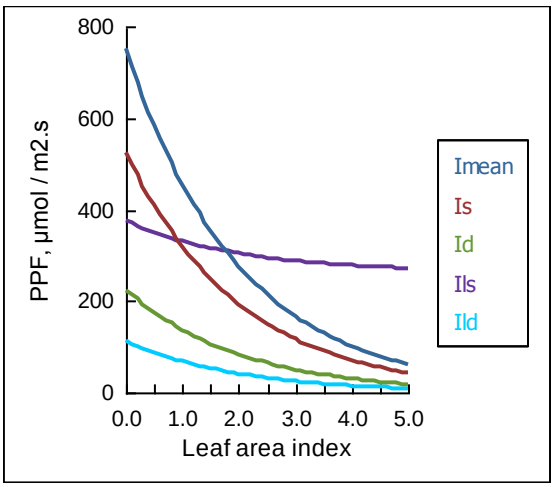

Figure 2.4: The mean PPF, I, direct and diffuse components, I_s, I_d, and PPF incident on leaves in direct and diffuse light, $I_{l,s}$, $I_{l,d}$, with $k = 0.5$. From PlantMod.

There are some simplifying assumptions in this approach, as discussed by Thornley and France (2007). The main simplifications are that the leaves are assumed to be randomly distributed (see Thornley and Johnson, 2000, for a discussion on leaf distribution), and variation in the direction of the direct solar beam throughout the day is not included. Also, light reflection and transmission through the leaves has not been incorporated directly, although in photosynthesis studies, the rate of leaf photosynthesis is generally calculated in terms of incident light and not absorbed light. By working with eqn (2.9) directly (Beer's law), it is reasonable to assume that the reflected and transmitted components are incorporated implicitly. While the analysis is relatively simple, this level of complexity is widely used in crop and pasture studies for the calculation of canopy photosynthesis, which is considered in Chapter 3.

Ground cover

In the analysis for the canopy energy balance the fractional ground cover is required. According to eqn (2.9), the solar radiation that is transmitted through the canopy is

$$I_t = I_0 e^{-kL} \tag{2.22}$$

Defining the fractional ground cover, f_g, as the proportion of solar radiation that is not transmitted, it follows that

$$f_g = 1 - e^{-kL} \tag{2.23}$$

This simple expression will be used in the analysis for the canopy radiation balance.

2.4.6 Clear-sky solar radiation and daylength

In the treatment of canopy transpiration, temperature and energy balance, it is necessary to estimate the clear-sky daily solar radiation, $R_{S,0}$, MJ m^{-2} day. The theory presented here follows Campbell (1977) and Thornley and France (2007).

Three standard equations relating to the geometry of the earth's rotation and its orbit around the sun are first presented without derivation. These are the solar declination angle, δ (rad), which is the angle between the earth's equatorial plane and the line from the earth to the sun, and accounts for the tilt of the earth's axis relative to the sun; the solar elevation angle at local noon, ϕ (rad); and the daylength, f_d, as a fraction of the 24 hour period. If t is the day of year from 1 January, λ (rad) the latitude, then

$$\delta = \frac{\pi}{180} 23.45 \sin\left(2\pi \frac{t-81}{365} \right) \tag{2.24}$$

$$\phi = \sin^{-1}\left(\sin\lambda \sin\delta + \cos\lambda \cos\delta \right) \tag{2.25}$$

$$f_{day} = \frac{1}{\pi} \cos^{-1}\left(-\tan\lambda \tan\delta \right) \tag{2.26}$$

and the number of daylight hours per day is

$$h_{day} = 24 \times f_{day} \tag{2.27}$$

If λ is prescribed in degrees then, using obvious notation,

$$\lambda = \frac{\pi}{180} \lambda_{deg} \tag{2.28}$$

To convert δ and ϕ to degrees, multiply by $180/\pi$. Also note that latitudes in the northern hemisphere are positive while they are negative in the southern hemisphere.

δ, ϕ and h_{day} are illustrated in Fig. 2.5 for elevations of 0 (the equator), 20, 40, 60°. It can be seen that the solar declination is positive in summer, negative in winter and zero at the spring and autumn equinoxes (which are around 21 March and 22 Sept). For latitudes outside locations between the tropic of Cancer and Capricorn, which are $\pm$ 23.4° respectively, the solar elevation angle at local noon, ϕ, is maximum in the middle of summer. However, at the equator, ϕ is maximum at the spring and autumn equinoxes and, moving towards the tropics, the two maxima converge. Finally, the daylength follows a familiar pattern and is seen to be fixed at 12 hours for the equator while, for other locations it is, of course, greater in summer, with longer days and shorter nights as the latitude increases.

Turning to irradiance, three sets of variables are used with appropriate subscripts (R_S has already been defined above). These are:

J, instantaneous irradiance outside the earth's atmosphere: W m^{-2} or J m^{-2} s^{-1};

I, instantaneous irradiance at the earth's surface: W m^{-2} or J m^{-2} s^{-1};

In all cases, irradiance is measured parallel to the horizontal plane at the surface of the earth.

The irradiance outside the earth's surface at solar noon, J_{noon}, is

$$J_{noon} = \gamma \sin\phi \tag{2.29}$$

where

$$\gamma = 1367 \text{ W m}^{-2} \text{ s}^{-1} \tag{2.30}$$

is the solar constant, and is the irradiance perpendicular to the sun at the edge of the earth's atmosphere. It is now assumed that the potential, or clear-sky, irradiance at the earth's surface, $I_{p,noon}$, is given by

$$I_{p,noon} = \tau J_{noon} \tag{2.31}$$

where τ is an atmospheric diffusivity coefficient. While more complex equations have been used this approach works well for a range of locations in Australia, as will be seen shortly, and there is no obvious reason to suggest other locations will behave much differently. Comparisons with experimental data suggest

$$\tau = 0.73 \tag{2.32}$$

is a good default value, although it may be necessary to adjust this parameter for different sites. However, this is relatively easy to estimate, as discussed below. It should be noted that a slightly different approach than a fixed constant in eqn (2.31) is used by Allen *et al*, (1998) although, as will be seen below, the present approach works well. $I_{p,noon}$ is illustrated in Fig. 2.6 for the latitudes used in Fig. 2.5. It can be seen that the variation in $I_{p,noon}$ is most apparent as the latitude moves further from the equator. It peaks at the equinoxes at the equator and, outside the tropics, it peaks in mid-summer, with the range between summer and winter increasing as the distance from the equator increases.

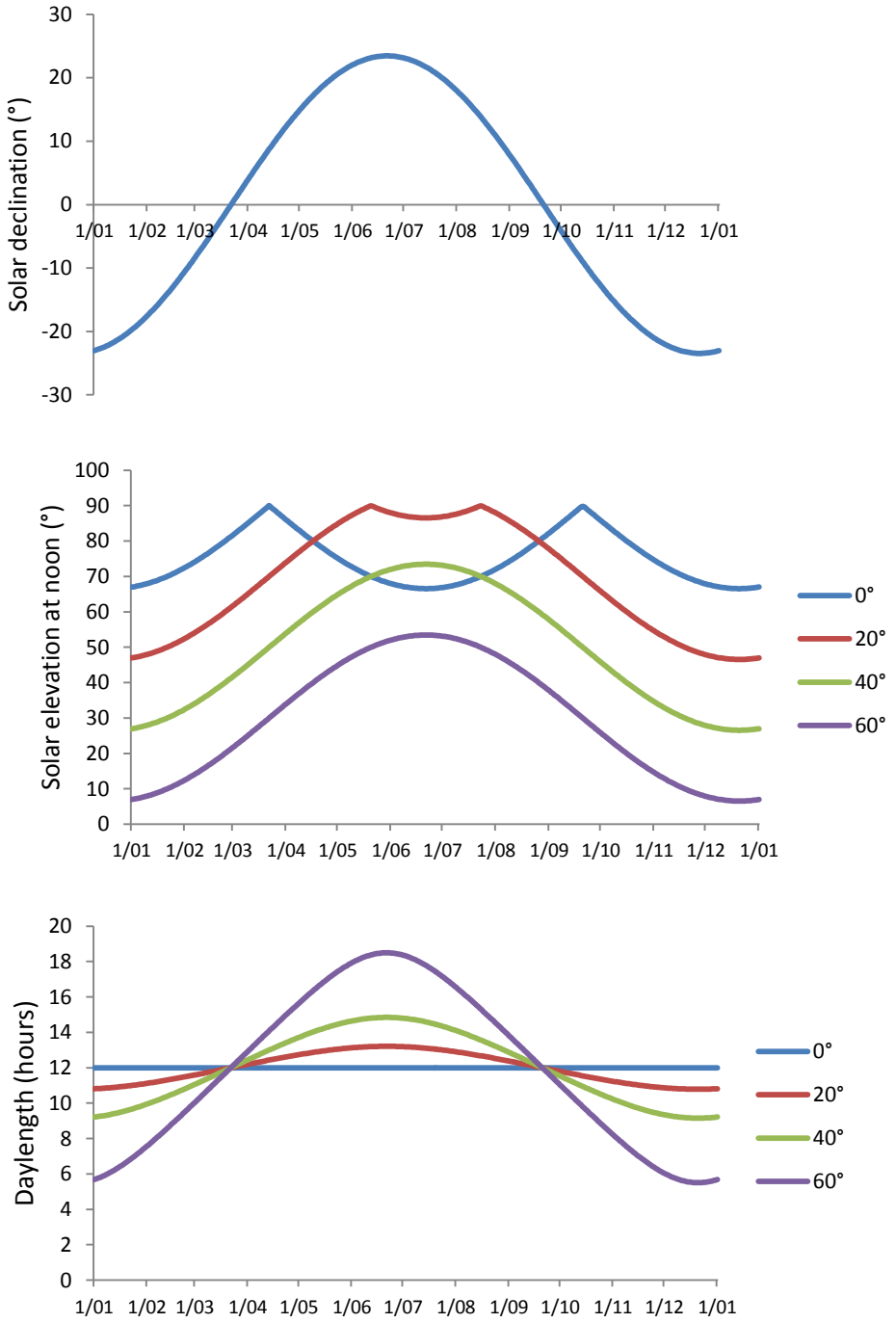

Figure 2.5: Solar declination angle, δ (°), solar elevation angle at local noon, ϕ (°), and the daylength, h_{day} (hours), as given by eqns (2.24) to (2.27). The latitude is as indicated (δ is independent of latitude). Note that in the theory δ and ϕ are prescribed in radians.

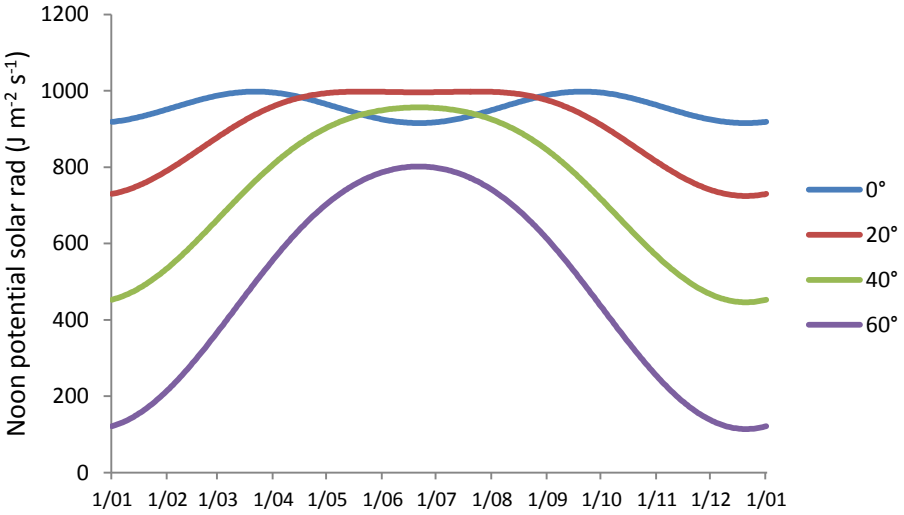

Figure 2.6: Noon potential solar radiation, $I_{p,noon}$, as given by eqn (2.31).

To calculate the potential daily solar radiation, it is assumed that the potential solar radiation throughout the day, I_p, varies sinusoidally, and can be written

$$I_p = I_{p,noon} \sin(\pi d),\ d = 0\text{–}1 \text{ over the daylight period} \tag{2.33}$$

so that the mean daily potential, or clear-sky, irradiance is

$$R_{S,p} = 86,400\, f_{day} \frac{2}{\pi} I_{p,noon} \tag{2.34}$$

where 86,400 is the number of seconds in a day. Thus,

$$R_{S,p} = 86,400\, f_{day} \frac{2}{\pi} \tau\gamma \sin\phi \tag{2.35}$$

This is a simple equation for the clear-sky irradiance in terms of latitude and day of year, and is illustrated in Fig. 2.7 for the latitudes used in Figs 2.5 and 2.6. The general trend for $R_{S,p}$ is similar to that for $I_{p,noon}$, although the maximum value for $R_{S,p}$ is greater as latitudes increase, whereas this is not the case for $I_{p,noon}$. This difference is due to the fact that the maximum daylength increases at higher latitudes and the total potential daily solar radiation ($R_{S,p}$) is the combination of the potential instantaneous solar radiation (I_p) and daylength.

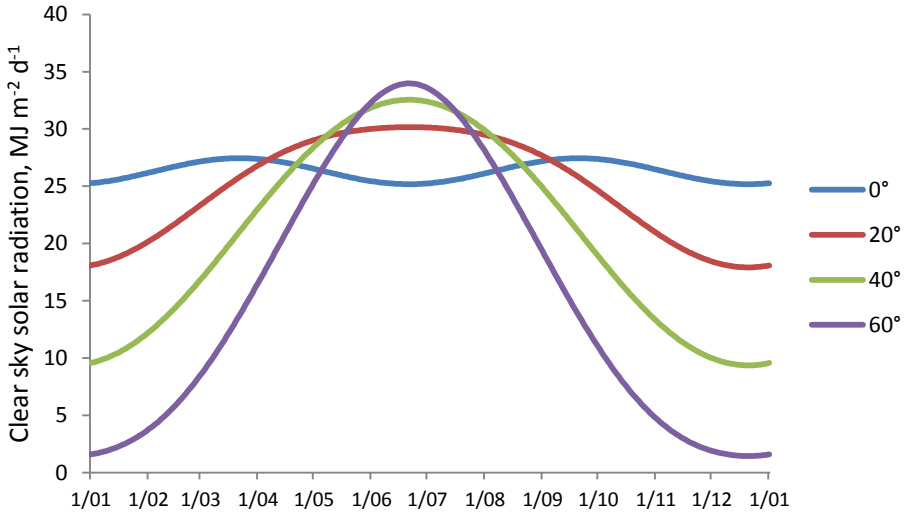

Figure 2.7: Clear-sky potential solar radiation, $R_{S,p}$ (MJ m^{-2} d^{-1}), as given by eqn (2.35) for the latitudes as indicated.

In order to test the approach, data from two sites in Australia from 1901 to 2008 are used from the SILO data set (Jeffrey, 2001). These sites are Barraba, NSW, at latitude -30.5°, and Albany, WA, at latitude -35°. Potential irradiance for each day of the year is estimated as the maximum observed for each day in the climate file. This assumes, therefore, that for each day of the year there was at least one occasion in the 108 years where the sky was clear. Figure 2.8 shows the observed and predicted clear-sky irradiance. Also shown are the mean and minimum irradiance, to illustrate the range of values that occur. There are occasional 'blips' in the data for maximum and minimum irradiance, but these may well be due to fluctuations in the accuracy of the measurement equipment. The data and model for clear-sky irradiance are virtually identical which gives confidence in the theoretical approach.

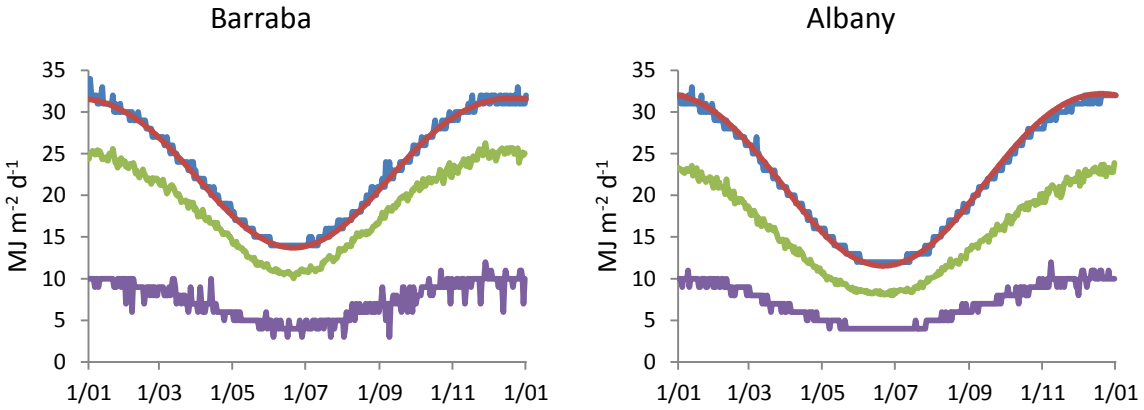

Figure 2.8: Observed maximum daily irradiance (blue) and predicted values (red) using eqn (2.35). Note that the blue lines are obscured for much of the data due to the close similarity of the values. Also shown are the mean (green) and minimum (purple) daily irradiance values.

Equation (2.35) has been tested for several other sites around Australia with similar close agreement with the data. The key parameter defining potential solar radiation is the atmospheric diffusivity, τ, which may vary for different locations, although the value 0.73 has been found to be appropriate in many cases. This equation will be used in Chapter 4 which considers canopy transpiration, temperature and energy budget.

2.4.7 Net radiation

The net radiation balance, which accounts for both shortwave and longwave radiation components, is central to the treatment of canopy transpiration, temperature and energy budget. Radiation is generally described for instantaneous (s) or daily (d) time scales and detailed discussions of the underlying physics relevant to plant canopies can be found, for example, in Thornley and France (2007) and Johnson (2013). The present discussion describes the net radiation balance of a canopy as required for the description of canopy transpiration.

The radiation balance of the canopy is shown in Fig. 2.. Solar radiation is incident on the canopy, which is either reflected and absorbed by the canopy or transmitted through the canopy. Longwave radiation transmitted from the atmosphere is intercepted and absorbed by the canopy with a small component that is reflected (and often ignored). Longwave radiation is also emitted by the canopy as a function of its temperature. Both shortwave and longwave radiation components that are not intercepted by the canopy will be transmitted through the canopy.

The theory for the radiation balance of canopies is presented with the assumption of full ground cover. In Chapter 4 canopy transpiration is calculated for ground cover and then adjusted for partial cover. The theory with partial ground cover is discussed by Johnson (2013).

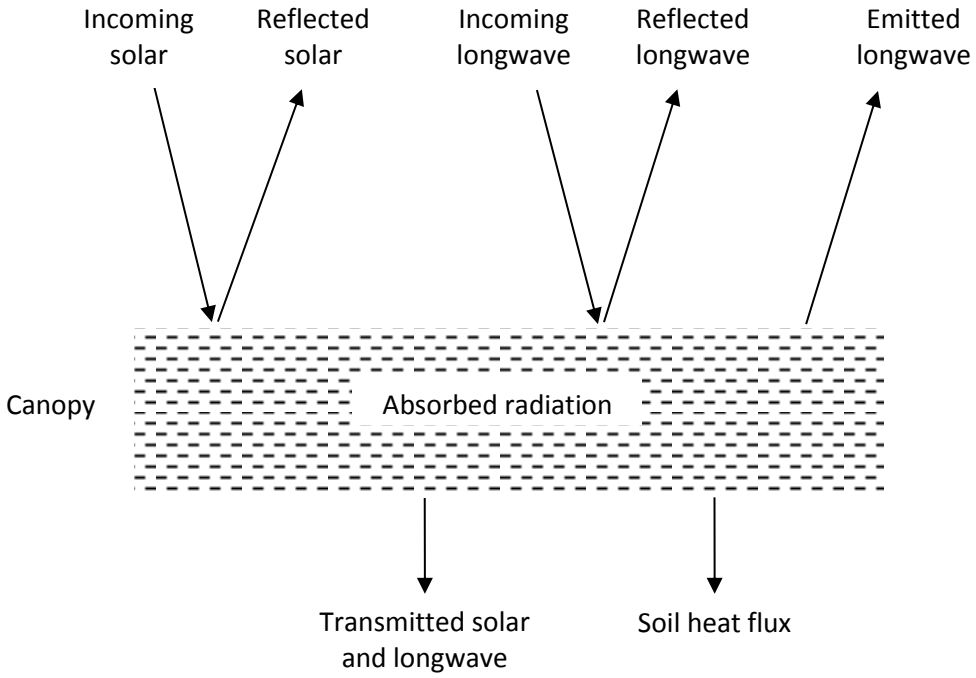

Figure 2.9: Schematic representation of the radiation balance of the canopy.

Denoting the incoming shortwave radiation by R_S J m^{-2} d^{-1}, the absorbed solar radiation as $R_{S,a}$ J m^{-2} d^{-1}is

$$R_{S,a} = (1-\alpha) R_S \tag{2.36}$$

where the reflection coefficient, or albedo, α, has default value

$$\alpha = 0.23 \tag{2.37}$$

Longwave, or terrestrial radiation, is the radiation emitted by a body as a function of its temperature. Incoming longwave radiation from the atmosphere depends primarily on atmospheric properties and temperature, generally increasing in response to vapour density and cloud cover. Note that in the analysis presented here, the net longwave radiation term is defined as outgoing rather than incoming. In some

texts, it is defined as incoming to be consistent with incoming solar radiation. The choice to use outgoing here is because this term is generally positive.

The present approach uses the empirical equation of Allen *et al.* (1998, eqn (39)) to define the daily net outgoing longwave radiation as

$$R_{L,n} = 86,400\sigma T_{K,day}^4 \left(0.34 - 0.14\sqrt{e_{v,a}/1000}\right)\left(1.35\frac{R_S}{R_{S,p}} - 0.35\right) \tag{2.38}$$

where T_K (K) is the mean daily temperature in Kelvin units, σ is the Stefan-Boltzmann constant, where $\sigma = 5.6704 \times 10^{-8}$ J m^{-2} s^{-1}K^{-4}, $e_{v,a}$ (Pa) is vapour pressure with the factor 1000 converting this to kPa, R_S (J m^2 d^{-1}) as defined above is daily solar radiation, and $R_{S,p}$ (J m^2 d^{-1}) is the potential, or clear-sky, solar radiation with $R_S \le R_{S,p}$. Clear-sky solar radiation was derived in terms of the latitude and day of year in section 2.6 above. The factor 86,400 is the number of seconds per day and converts the radiation components in the Stefan-Boltzmann equation to daily values. According to Allen *et al.* (1998), the $\left(0.34 - 0.14\sqrt{e_{v,a}/1000}\right)$ term corrects for air humidity and declines as humidity increases. The $\left(1.35\, R_S/R_{S,p} - 0.35\right)$ term incorporates the influence of cloud cover and decreases as cloud cover increases, since this will result in a reduction in R_S. The approach of eqn (2.38) is widely used – for example the SILO dataset (Jeffrey, 2001) available in Australia, which gives access to daily climate data from the late 1800s to the present day for any location in Australia, uses this approach for the calculation of the net radiation balance. Note that Allen *et al.* (1998) incorporated the daily maximum and minimum temperatures, although using a single mean daily temperature gives very similar results.

Combining eqns (2.36) and (2.38), the daily net radiation during the daylight period is

$$R_{n,day} = R_{s,a} - f_{day}R_{L,n} \tag{2.39}$$

where f_{day} is the daylight fraction and $R_{n,day}$ applies to the daylight period only.

2.5 Final comments

This Chapter starts with the basic physics of radiation and then deals with the theory of radiation as it is required to model canopy photosynthesis and energy balance, including evaporation and transpiration, which are considered in the following Chapters and are central to the growth of plants. The distinction between shortwave and longwave radiation is crucial in the study of photosynthesis and energy dynamics. The visible component of shortwave radiation is the source of energy for photosynthesis, and is known as photosynthetic photon flux (PPF). The direct and diffuse components of PPF have been considered, and are used in the description of canopy photosynthesis. The overall canopy energy balance includes both shortwave and longwave radiation, and care must be taken to ensure that these components are described appropriately. Direct measurements of longwave radiation are often not available and a simple approach for estimating longwave radiation has been described, along with the overall canopy energy balance, in relation to incoming shortwave radiation, air temperature and relative humidity.

2.6 References

Allen RG, Pereira LS, Raes D and Smith M (1998). FAO irrigation and drainage paper no. 56: crop evapotranspiration. www.kimberly.uidaho.edu/ref-et/fao56.pdf.

Campbell GS (1977). *An introduction to environmental biophysics*. Springer-Verlag, New York, USA.

Campbell GS and Norman JM (1998). *An Introduction to environmental biophysics*, second edition. Springer, New York, USA.

Jeffrey SG, Carter JO, Moodie KB and Beswick AR (2001) Using spatial interpolation to construct a comprehensive archive of Australian climate data. *Environmental Modelling & Software* **16,** 309–330.

Johnson IR (2013). *PlantMod: exploring the physiology of plant canopies.* IMJ Software, Dorrigo, NSW 2453, Australia. www.imj.com.au/software/plantmod.

Johnson IR, Riha SG and Wilks DS (1995). Modelling daily net canopy photosynthesis and its adaptation to irradiance and atmospheric CO_2 concentration. *Agricultural Systems* **50,** 1-35.

Jones HG (1992). *Plants and microclimate*. Cambridge University Press, Cambridge, UK.

Monteith JL & Unsworth MH (2008). *Principles of environmental physics,* third edition. Elsevier, Oxford, UK.

Norman JM (1980). Interfacing leaf and canopy light interception models. In: *Predicting photosynthesis for ecosystem models,* (Eds JD Hesketh and JW Jones), CRC Press, Boca Raton, Fl, USA.

Norman JM (1982). Simulation of microclimates. In *Biometeorology in integrated pest management.* Academic Press, New York, USA.

Stockle CO & Campbell GS (1985). A simulation model for predicting effect of water stress on yield: an example using corn. *Advances in Irrigation,* **3,** 283-323.

Thornley JHM (2002). Instantaneous canopy photosynthesis: analytical expressions for sun and shade leaves based on exponential light decay down the canopy and an acclimatized non-rectangular hyperbola for leaf photosynthesis. *Annals of Botany,* **89,** 451-458.

Thornley JHM and France J (2007). *Mathematical models in agriculture*. CAB International, Wallingford, UK.

Thornley JHM & Johnson IR (2000). *Plant and crop modelling*. Blackburn Press, Caldwell, New Jersey, USA.

3 Pasture Growth

3.1 Introduction

The pasture growth module of the SGS Pasture Model and DairyMod originates from the general structure of the models described by Johnson and Thornley (1983, 1985); Johnson and Parsons (1985); and Parsons, Johnson and Harvey (1988), although a number of modifications have been made. More recent discussions of physiological pasture growth models can be found in Thornley and Johnson (2000) and Thornley and France (2007). In addition, the approach has been developed in order to incorporate water and nutrient effects.

The following key points apply:

- The model is constructed for generic pasture species so that particular species are defined through the basic model parameters.
- The model includes carbon assimilation through photosynthesis and respiration followed by tissue growth, turnover and senescence.
- Pasture growth and tissue dynamics are influenced by environmental conditions (light, temperature and atmospheric CO_2 concentration) as well as soil water and nutrient status.
- Nitrogen dynamics and influence on pasture growth are incorporated.
- For annual species, vegetative (emergence to anthesis) and reproductive (anthesis to maturity) growth phases are included.
- Multiple species can be included, which may be perennial, annual, legume, C_3 or C_4.
- Pasture utilisation by grazing animals is considered in Chapter 6.
- Plant digestibility and metabolic energy content is calculated in terms of the plant nutrient status, although this is described in Chapter 6.
- Throughout the discussion, the area of ground that is used is m^2 although frequently in the interface the hectare, ha, is used. The choice is generally to give the user access to familiar units and should not cause any difficulty.
- Photosynthesis calculations use moles CO_2, which is converted to carbon units.
- Carbon is the internal unit of plant mass used in the model and this can be converted to dry weight, with conversion factor 0.45 kg C (kg d.wt)$^{-1}$ as discussed in section 1.5 in Chapter 1.

Unlike the original models referenced above, the model described here does not include specific substrate pools for labile carbon and nitrogen. Instead, in order to simplify the model, the daily carbon assimilation and respiratory costs are calculated and the net carbon balance is then directly available for growth on that day. In addition, the effect of available water and nutrients, as well as the influence of actual plant nutrient status on growth are included.

Growth is calculated as follows:

- The daily transpiration rate and the effect of water stress are calculated;
- Daily photosynthesis is calculated in response to light, temperature, atmospheric CO_2 concentration, canopy architecture, available water, and leaf nitrogen status;
- Potential nutrient uptake is calculated in relation to root distribution and soil nutrient status;
- Plant mass flux is calculated, incorporating tissue turnover, senescence, shoot and root growth;

Other processes, such as species interaction, nitrogen fixation (in legumes) and the growth of annual species are also included and a more detailed description follows.

3.2 Transpiration and the influence of water stress

Potential transpiration, $E_{T,pot}$, is the transpiration rate that occurs when there is no limitation due to available soil water content, and is calculated according to the Penman-Monteith equation as discussed in detail in Chapter 4. Potential transpiration is derived for full ground cover, so the actual transpiration demand is given by

$$E_{T,demand} = f_g E_{T,pot} \tag{3.1}$$

where f_g is the live ground cover and is given by eqn (2.24) in Chapter 2.

Once transpiration demand is known it is then necessary to calculate the impact of soil water status and so the actual transpiration. First, the growth limiting factor for water, g_{water}, is defined in relation to the available soil water as a function of wilting point (θ_w), recharge point (θ_r), field capacity (θ_{fc}), and saturated water content (θ_{sat}), as shown in Fig. 3.1. If g_{water} is 1 then there is no limitation to growth; if it is zero then there is total limitation. θ_r is the soil water content below which transpiration is reduced as a result of limited available soil water. Field capacity and saturated water content are discussed in more detail in Chapter 4.

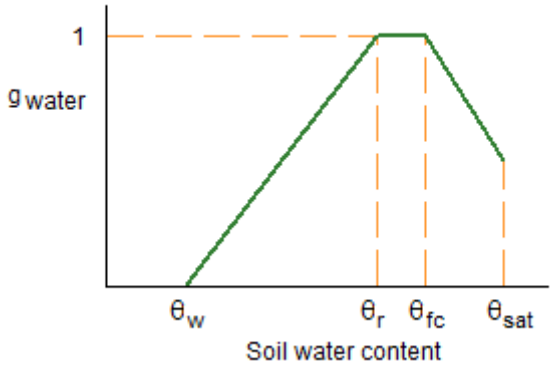

Figure 3.1: Schematic representation of the influence of limiting soil water content on transpiration.

For water contents below the wilting point, plants cannot extract water from the soil. Between the wilting point and recharge point, g_{water} increases from 0 to 1. Between recharge point and field capacity, g_{water} is 1. Between field capacity and saturation, g_{water} may decline, although this can be defined by the user. The reason the g_{water} can decline at soil water contents greater than field capacity is that plants may be susceptible to water logging. Note that wilting point, field capacity and saturation are defined in the soil water module of the interface, while the recharge point and any decline in the g_{water} at saturation are defined in the pasture module. The term *recharge point* is used as this is the point at which irrigation would have to be applied in order to prevent any water stress.

The strategy for calculating transpiration is to calculate g_{water} for each soil layer, $g_{water,\ell}$ according to the scheme illustrated in Fig. 3.1. The water uptake from each layer is then given by

$$E_{T,\ell} = f_{r,\ell} g_{water,\ell} E_{T,demand} \tag{3.2}$$

where $f_{r,\ell}$ is the root fraction in each layer, so that the total transpiration is

$$E_T = \sum_{\ell=1}^{L_{tot}} E_{T,\ell} \tag{3.3}$$

where L_{Tot} is the total number of soil layers.

If there is no limitation to water uptake from any layer due to available soil water then water uptake through the profile is taken out according to the relative root distribution. As water becomes unavailable from layers, uptake from those layers is reduced according to $g_{water,\ell}$.

According to eqn (3.3) there is no compensation for water limitation in dry layers by other layers that might have abundant water. To allow this situation, the transpiration routines are run three times, or until demand is satisfied. As long as the routines are run more than once, the results are relatively insensitive to how many times they are repeated. Thus, eqn (3.3) with (3.2) becomes

$$E_T = \sum_{i=1}^{3} \sum_{\ell=1}^{L_{tot}} f_{r,\ell} g_{water,\ell,i} E_{T,demand,i} \tag{3.4}$$

$g_{water,\ell,i}$ is evaluated for each calculation loop, and $E_{T,demand,i}$ is reset for each loop to allow for cumulative transpiration. The choice of three has been selected as giving appropriate responses for pasture production for a wide range of locations.

Once the transpiration is known, the overall water growth limiting factor is defined as

$$\Omega_{water} = \frac{E_T}{E_{T,demand}} \tag{3.5}$$

This is a useful indicator of water stress, and is also used in the calculations for partitioning growth between shoots and roots.

3.3 Canopy photosynthesis

The calculations for daily canopy photosynthetic rate lie at the heart of this model as this is the source of carbon for the whole system (apart from any imported supplementary feed). The canopy photosynthesis component of the model is based directly on Johnson *et al.* (2010) and so the details are kept fairly brief here. The source of energy for photosynthesis is the visible component of solar radiation, which was discussed in Chapter 2 (section 2.4), and is referred to as *photosynthetically active radiation* (PAR) with units J m^{-2} s^{-1}, or *photosynthetic photon flux* (PPF) with units μmol photons: PPF is the standard terminology in the plant physiology literature, and will be used here.

The strategy for calculating daily canopy photosynthesis is:

- Define the instantaneous rate of leaf gross photosynthesis in response to PPF, temperature, atmospheric CO_2, leaf N;
- Define light interception and attenuation through the canopy, which includes direct and diffuse PPF components;
- Integrate through the canopy to get canopy instantaneous gross photosynthesis;
- Integrate through the day to get daily canopy gross photosynthesis;
- Calculate the daily growth and maintenance
- Combine gross photosynthesis and respiration to get daily net photosynthesis, which is the net carbon assimilation by the canopy.

3.3.1 Units

The conventional units for leaf photosynthetic rate are μmol CO_2 $(m^2$ leaf$)^{-1}$ s^{-1} whereas, for crop or pasture growth rates, these are usually prescribed as kg d.wt. ha^{-1} d^{-1}. Accordingly, in this model the leaf and canopy photosynthetic rates use μmol CO_2 for instantaneous or mol CO_2 for per second or per day rates

respectively, and the daily canopy photosynthetic rate is then converted to carbon units, using eqn (1.69) as discussed in Chapter 1, Section 1.5, which is then readily converted to d.wt units using eqn (1.73).

3.3.2 Leaf gross photosynthesis

The rate of single leaf photosynthesis, P_ℓ μmol CO_2 (m^2 leaf)$^{-1}$ s^{-1}, in response to incident PPF, μmol photons (m^2 leaf)$^{-1}$ s^{-1} is described by the non-rectangular hyperbola. This equation is discussed in detail in Chapter 1 (Section 1.3.2) and the equation for P_ℓ can be written as

$$\xi P_\ell^2 - (\alpha I_\ell + P_m) P_\ell + \alpha I_\ell P_m = 0 \qquad (3.6)$$

where the parameters are:

P_m	rate of single leaf gross photosynthesis at saturating PPF	μmol CO_2 (m^2 leaf)$^{-1}$ s^{-1}
α	leaf photosynthetic efficiency	mol CO_2 (mol photons)$^{-1}$
ξ	curvature parameter	(dimensionless)

P_ℓ is given by the lower root of eqn (3.6), which is

$$P_\ell = \frac{1}{2\xi}\left[\alpha I_\ell + P_m - \left\{(\alpha I_\ell + P_m)^2 - 4\xi\alpha I_\ell P_m\right\}^{1/2}\right] \qquad (3.7)$$

Equation (3.7) is shown in Fig. 3.2

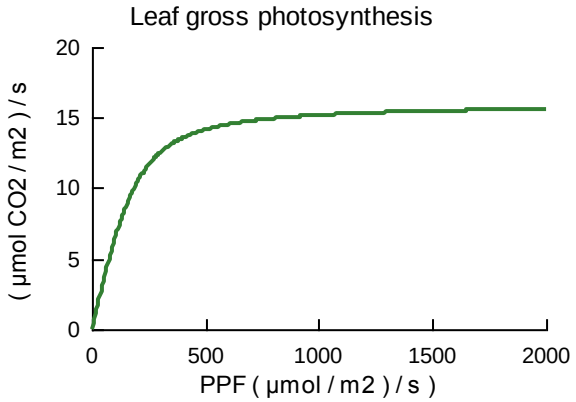

Figure 3.2: Leaf gross photosynthesis for P_m =16 μmol CO_2 (m^2 leaf)$^{-1}$ s^{-1}, α = 80 m mol CO_2 (mol photons)$^{-1}$, ξ= 0.8.

The influence of temperature, CO_2 and nitrogen level on leaf gross photosynthesis is dominated by the effect on the parameter P_m in eqn (3.7). The quantum efficiency α also depends on temperature and CO_2, although to a lesser extent than P_m. There is less evidence that the curvature parameter ξ responds to these factors (Sands, 1995; Cannell and Thornley, 1998) and so this parameter is treated as constant. The methods used here follow, or are adapted from, Cannell and Thornley (1998), Thornley (1998), and Thornley and France (2007). The overall leaf photosynthetic response to the interaction between PPF, temperature and CO_2 is consistent with general observations in the literature: for more discussion, see Johnson *et al.* (2010).

Light saturated photosynthesis, P_m

The general characteristics of the response of P_m to temperature, CO_2 concentration, and protein concentration are:

- P_m increases from zero as temperature increases from some low value;
- There is an optimum temperature above which there is no further increase;
- The temperature optimum increases in response to atmospheric CO_2 concentration, C, which is due to the fall in photorespiration;
- As temperature continues to rise there is a decline in P_m for C_3 species, also due to the increase in photorespiration;
- For C_4 species, P_m may remain stable or may decline slightly as temperature increases past the optimum.
- For C_3 species, P_m increases in response to increasing C in an asymptotic manner, approaching a maximum value at saturating C.
- C_4 species show little photosynthetic response to increasing C above ambient, C_{amb},
- P_m increases as the photosynthetic enzyme concentration increases, and it is assumed that this enzyme concentration is proportional to the nitrogen content.
- N content is expressed on a mass basis, kg N (kg C)$^{-1}$

These factors are incorporated by defining

$$P_m = P_{m,ref}\, f_C(C)\, f_{Pm,TC}(T,C)\, f_{Pm,\mathrm{N}}(f_N) \tag{3.8}$$

where $f_C(C)$ is a CO_2 response function, $f_{Pm,TC}$ (*T,C*) is a combined response to temperature and CO_2, $f_{Pm,N}$ is the response to protein concentration as related to N, f_N kg N (kg C)$^{-1}$, and $P_{m,ref}$ is a reference value for P_m, and is the value of P_m at a reference temperature, T_{ref}, ambient CO_2 concentration, C_{amb}, and reference N concentration, as discussed below. The functions are constrained by

$$f_C(C = C_{amb}) = f_{Pm,TC}(T = T_{ref}, C = C_{amb}) = f_{Pm,\mathrm{N}}(f_N = f_{N,ref}) = 1 \tag{3.9}$$

Default values for $P_{m,ref}$ are

$$\begin{aligned} &\mathrm{C_3}: \quad P_{m,ref} = 16\ \mu\mathrm{mol\ mol}^{-1} \\ &\mathrm{C_4}: \quad P_{m,ref} = 22\ \mu\mathrm{mol\ mol}^{-1} \end{aligned} \tag{3.10}$$

which are taken to be representative of photosynthetic capacity within the canopy. However, it must be noted that leaf photosynthetic potential is subject to considerable variation.

The CO_2 response function, $f_C(C)$, is described in detail in Chapter 1 and is not discussed further here, other than to note that

$$f_C(C = C_{amb}) = 1 \tag{3.11}$$

and that the response is parameterised by defining the parameters λ and $f_{C,m}$ where

$$\left.\begin{aligned} f_C(C = 2C_{amb}) &= \lambda \\ f_C(C \to \infty) &= f_{C,m} \end{aligned}\right\} \tag{3.12}$$

Default values are

$$\begin{aligned} &\mathrm{C}_3: \quad \lambda = 1.2; \quad f_{C,m} = 1.5 \\ &\mathrm{C}_4: \quad \lambda = 1.05; \quad f_{C,m} = 1.1 \end{aligned} \tag{3.13}$$

According to these values, $f_C(C)$ increases by 20% and 50% when CO_2 is double ambient and saturating respectively, while for C_4 plants the corresponding increases are 5% and 10%, which are lower than for C_3 due to the lack of photorespiration and subsequent limited impact of increasing CO_2 on the photosynthetic capacity of C_4 plants.

The N response function is the same for both C_3 and C_4 species and is defined as a simple ramp function, so that

$$f_{Pm,\mathrm{N}}\left(f_N\right) = \begin{cases} f_N / f_{N,ref}, & f_N \le f_{N,ref} \\ f_{N,mx} / f_{N,ref}, & f_N > f_{N,mx} \end{cases} \tag{3.14}$$

According to this function, $f_{Pm,N}$ increases linearly as the N concentration increases to the maximum value, above which there is no further increase in the rate of photosynthesis.

Although N concentration is expressed in terms of plant carbon, The default parameter values

$$\begin{aligned} &\mathrm{C}_3: \quad f_{N,ref} = f_{N,mx} = \frac{0.04}{F_C} \text{ kg N } \left(\text{kg C}\right)^{-1} \\ &\mathrm{C}_4: \quad f_{N,ref} = f_{N,mx} = \frac{0.03}{F_C} \text{ kg N } \left(\text{kg C}\right)^{-1} \end{aligned} \tag{3.15}$$

are used, where F_C is the carbon fraction of dry weight which is taken to be 0.45 kg C (kg d.wt)$^{-1}$, as given by eqn (1.69) in Chapter 1, Section 1.5. The values 0.04 and 0.03 correspond to 4% and 3% respectively in the familiar units of N content as a percentage of dry weight. The lower values for C_4 plants reflects the fact that these species generally have lower nitrogen concentration than C_3.

The basic generic temperature response function that was described in Chapter 1, section 1.3.5 is used, that is

$$f_T\left(T\right) = \begin{cases} 0, & T \le T_{mn} \\ \left(\dfrac{T - T_{mn}}{T_r - T_{mn}}\right)^q \left(\dfrac{(1+q)T_{opt} - T_{mn} - qT}{(1+q)T_{opt} - T_{mn} - qT_r}\right), & T_{mn} < T < T_{mx} \\ 0 & T \ge T_{mx} \end{cases} \tag{3.16}$$

where T_r is a reference temperature, so that

$$f_T\left(T_r\right) = 1 \tag{3.17}$$

and T_{mx} is given by

$$T_{mx} = \frac{(1+q)T_{opt} - T_{mn}}{q} \tag{3.18}$$

The function takes its maximum value at T_{opt} and is zero outside the range T_{mn} to T_{mx}.

The optimum temperature for photosynthesis is seen to increase in response to atmospheric CO_2 concentration and so the combined T and C function, $f_{Pm,TC}(T,C)$, uses eqn (3.16), but with T_{opt} defined by

$$T_{opt,Pm} = T_{opt,Pm,amb} + \gamma_{Pm}\left[f_C\left(C\right) - 1\right] \tag{3.19}$$

where $f_C(C)$ is again given by the CO_2 response function described in Chapter 1, and the parameter γ_{Pm} has default value

$$\gamma_{Pm} = 10^{\circ}\mathrm{C} \tag{3.20}$$

C_3 and C_4 species are treated in the same way, with the exception that for C_4 species the constraint

$$\mathrm{C}_4: \quad f_{Pm,TC}(T,C) = f_{Pm,TC}\left(T_{opt,Pm},C\right), \quad \text{for } T > T_{opt,pm} \tag{3.21}$$

applies, so that the temperature response does not fall when temperatures exceed the optimum. The decline in photosynthesis for C_3 plants at high temperature is due to the shift from photosynthesis to photorespiration, while, for C_4 plants, photorespiration is generally negligible. In practice, there may be a decline in photosynthesis at high temperatures due to water stress. Also, since, as discussed below, respiration does increase with temperature, there will be a decline in net photosynthesis at high temperatures for C_4 plants.

Default values

$$\begin{aligned} &\mathrm{C}_3: \quad T_{ref} = 20^{\circ}\mathrm{C}, \quad T_{mn} = 3^{\circ}\mathrm{C}, \quad T_{opt,Pm,amb} = 23^{\circ}\mathrm{C} \\ &\mathrm{C}_4: \quad T_{ref} = 25^{\circ}\mathrm{C}, \quad T_{mn} = 12^{\circ}\mathrm{C}, \quad T_{opt,Pm,amb} = 35^{\circ}\mathrm{C} \end{aligned} \tag{3.22}$$

are used, although these may vary for different species.

Photosynthetic efficiency, α

Now consider the leaf photosynthetic efficiency, α, which is defined by

$$\begin{aligned} &\mathrm{C}_3: \quad \alpha = \alpha_{amb,15} f_{\alpha,C}(C) f_{\alpha,TC}(T,C) f_{\alpha,N}(f_N) \\ &\mathrm{C}_4: \quad \alpha = \alpha_{amb,15} f_{\alpha,C}(C) f_{\alpha,N}(f_N) \end{aligned} \tag{3.23}$$

where $\alpha_{amb,15}$ mol CO_2 (mol photons)$^{-1}$ is the value of α at ambient CO_2 concentration, C_{amb}, and 15°C, with default value

$$\alpha_{amb,15} = 50 \text{ mmol } \mathrm{CO}_2 \ (\text{mol photons})^{-1} \tag{3.24}$$

The function $f_{\alpha,C}(C)$ in eqn (3.23) captures the direct influence of C on α and is given by the same generic response function that is used for P_m in eqn (3.8).

The function $f_{\alpha,TC}(T,C)$ in eqn (3.23)defines the temperature response on α and the influence of C on this response as given by

$$f_{\alpha,TC}(T,C) = \begin{cases} 1 - \lambda_{\alpha} \dfrac{C_{amb}}{C}\left(T - T_{opt,\alpha}\right), & T \geq T_{opt,\alpha} \\ 1, & T < T_{opt,\alpha} \end{cases} \tag{3.25}$$

where λ is a constant and

$$T_{opt,\alpha} = 15 + \gamma\left[f_C(C) - 1\right] \tag{3.26}$$

where, again, the generic CO_2 response function is used. Note that eqn (3.25) will not be valid for very small values C as the term C_{amb}/C will become infinitely large. Rather than address this issue to deal with unrealistic CO_2 concentrations, the theory is restricted to CO_2 concentrations greater than 100 μmol mol^{-1}, and subject to

$$f_{\alpha,TC}(T,C) \geq 0 \text{ for all } T \text{ and } C \tag{3.27}$$

Default parameter values are

$$\lambda_\alpha = 0.02\,^\circ\text{C} \quad \text{and} \quad \gamma_\alpha = 6\,^\circ\text{C} \tag{3.28}$$

With these values, $T_{opt,\alpha}$ increases from its ambient value of 15°C by 3°C for a doubling of CO_2 from ambient.

The function for $f_{\alpha,fN}$ defines the protein response for α and is assumed to be a simple ramp function:

$$f_{\alpha,N}(f_N) = \begin{cases} 0.5 + 0.5\, f_N / f_{N,ref}, & f_N \leq f_{N,ref} \\ 1, & f_N > f_{N,ref} \end{cases} \tag{3.29}$$

where the values for $f_{N,ref}$ are given in eqn (3.15). This equation will not be valid for very low f_N but, for that situation, photosynthesis will be primarily restricted by the influence on P_m.

According to these equations, photosynthetic efficiency α increases with increasing C for both C_3 and C_4 species, but for C_3 plants there is also a decline for temperatures above 15°C. The increase in α in response to C reflects the greater availability of CO_2, while the decline in response to temperature for C_3 species indicates a shift towards photorespiration as temperature increases, while this shift is reduced at increasing C. The lack of temperature response for C_4 species is due to the lack of photorespiration in those plants.

The curves are not illustrated in detail here as they can be explored in DairyMod and the SGS Pasture Model and, for more detail, in PlantMod (Johnson 2013). Figure 3.3 shows the leaf gross photosynthetic response for C_3 and C_4 leaves at their reference N concentration and for T = 20, 30° and $C = C_{amb}, 2C_{amb}$, where C_{amb} = 380 ppm. It can be seen that there is little impact of elevated CO_2 on C_4 photosynthesis, whereas the response is quite noticeable for C_3 plants. Also, while C_4 photosynthesis is quite high for C_4 plants at 30°C, it should be noted that high temperatures are often associated with significant water stress and so these rates may not occur very often in practice. Indeed, possible direct benefits to elevated CO_2 are likely to be offset by corresponding impacts due to temperature and water stress.

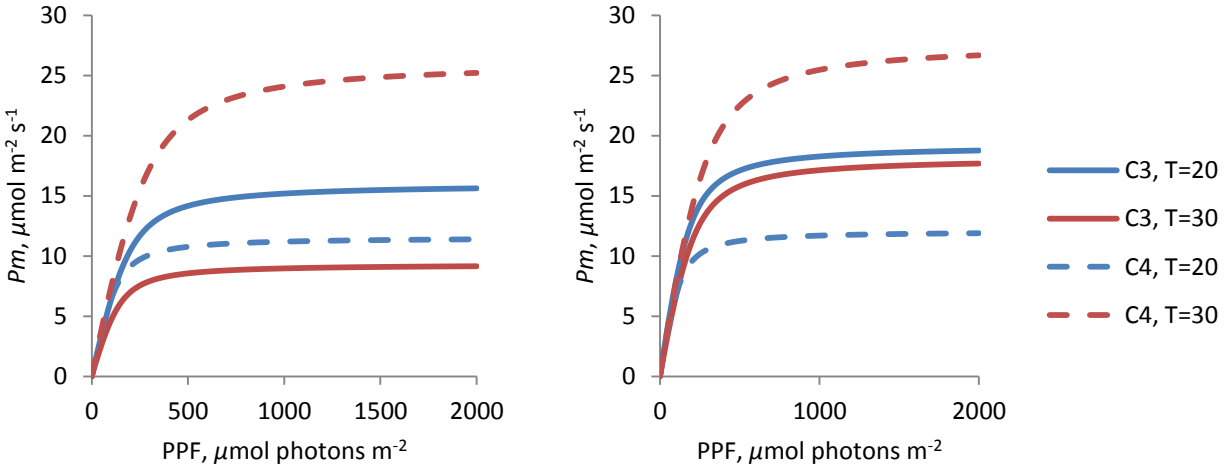

Figure 3.3. Leaf gross photosynthetic response for C_3 and C_4 leaves at 20°C and 30°C as indicated and at ambient CO_2, left, and double ambient CO_2, right.

3.3.3 Instantaneous canopy gross photosynthesis

The rate of instantaneous canopy gross photosynthesis, P_g μmol CO_2 (m^{-2} ground) s^{-1}, is calculated by summing the leaf photosynthetic rate over all leaves in the canopy, and is given by

$$P_g = \int_0^L P_\ell\left(I_\ell\right)\mathrm{d}\ell \tag{3.30}$$

where P_ℓ μmol CO_2 (m^{-2} leaf) s^{-1}, is the rate of leaf gross photosynthesis as discussed above, and I_ℓ μmol photons (m^2 leaf)$^{-1}$ s^{-1}, is the photosynthetic photon flux (PPF) incident on the leaf (Chapter 2), L (m^2 leaf) (m^{-2} ground) is the total canopy leaf area index, and ℓ is a dummy variable defining the cumulative leaf area index through the depth of the canopy.

In Chapter 2 the direct and diffuse components of PPF were discussed. It is important to account for these components since, as seen earlier, the leaf photosynthetic response to PPF is non-linear and so taking the average PPF rather than separate direct and diffuse components can lead to an over-estimate of canopy photosynthesis. For more discussion see Johnson *et al.* (2010) and Johnson (2013).

Separating the leaves into those in direct and diffuse PPF, eqn (3.30) can be written

$$P_g = \int_0^{L_s} P_\ell\left(I_{\ell,s}\right)\mathrm{d}\ell_s + \int_0^{L_d} P_\ell\left(I_{\ell,d}\right)\mathrm{d}\ell_d \tag{3.31}$$

which, using eqns (2.19) and (2.20) in Chapter 2 for ℓ_s and ℓ_d becomes

$$P_g = \int_0^L P_\ell\left(I_{\ell,s}\right)e^{-k\ell}\mathrm{d}\ell + \int_0^L P_\ell\left(I_{\ell,d}\right)\left(1-e^{-k\ell}\right)\mathrm{d}\ell \tag{3.32}$$

Equation (3.32) is the key equation for calculating the rate of canopy gross photosynthesis which, combined with the previous theory, incorporates the effects of PPF, temperature, leaf nitrogen, atmospheric CO_2 concentration and total leaf area index.

The integrals in eqn (3.32) are difficult to solve analytically although quite straightforward to solve numerically by summing through the canopy according to

$$P_g = \sum_{i=1}^{i=n}\left[P_\ell\left(I_{\ell_i,s}\right)e^{-k\ell_i} + P_\ell\left(I_{\ell_i,d}\right)\left(1-e^{-k\ell_i}\right)\right]\Delta\ell \tag{3.33}$$

where

$$\ell_i = \left(i-1\right)\Delta\ell + \frac{\Delta\ell}{2} = \left(2i-1\right)\frac{\Delta\ell}{2}, \quad i = 1 \text{ to } n \tag{3.34}$$

and

$$n = \frac{L}{\Delta\ell} \tag{3.35}$$

According to this scheme, the canopy is divided into layers of depth $\Delta\ell$ and $f_p(L)$ is evaluated at the mid-point of each layer and the total enzyme content of the layer is this value multiplied by the layer depth. This is a common scheme for numerical integration and, while more elaborate numerical techniques can be applied, it works well for the present purposes. The value

$$\Delta\ell = 0.1 \tag{3.36}$$

is used throughout.

3.3.4 Daily canopy gross photosynthesis

The daily canopy gross photosynthesis, $P_{g,day}$ kg C (m^{-2} ground) d^{-1} is given by the integral of P_g throughout the day:

$$P_{g,day} = 0.012 \times 10^{-6} \int_0^{\tau} P_g \mathrm{d}t \tag{3.37}$$

where t is time (s), τ (s) is the daylight period in seconds, the factor 10^{-6} converts from μmol CO_2 to mol CO_2, and the factor 0.012 converts from mol CO_2 to kg CO_2. This equation can be applied with any daily distribution of PPF and temperature. For constant PPF, I_0, and temperature, T, it is

$$P_{g,day} = 0.012 \times 10^{-6} \tau P_g \left(I_0, T\right) \tag{3.38}$$

where Δt is a small time-step,

$$t_i = \left(i-1\right)\Delta t + \frac{\Delta t}{2} = \left(2i-1\right)\frac{\Delta t}{2}, \quad i = 1 \text{ to } n \tag{3.39}$$

and

$$n = \frac{\tau}{\Delta t} \tag{3.40}$$

Essentially, this scheme sums P_g as evaluated at regular intervals throughout the day. The accuracy of the numerical scheme will increase as the time step (Δt) gets smaller, or the number of time steps (n) gets larger, although the computation will take longer. However, continuing to decrease Δt to very small values can cause numerical errors to increase and the scheme actually becomes less accurate. A general strategy is to start with a relatively small value for n and with Δt calculated from eqn (3.40), gradually increase n until the estimate of $P_{g,day}$ in eqn (3.38) starts to change. This sets a lower limit on n. In the present model, the mean daytime PPF and temperature values are used and so eqn (3.38) applies.

3.3.5 Daily canopy respiration rate

It is now necessary to calculate the daily respiration rate. Respiration, excluding photorespiration (which is incorporated directly into the calculation of gross photosynthesis) is calculated using the McCree (1970) approach, that has been further developed by Thornley (1970), Johnson (1990), and is widely used. This identifies the growth and maintenance components of respiration. These components are helpful in understanding the respiratory demand by the plants, although the actual underlying respiratory process whereby ATP is produced from sugars with a respiratory efflux of CO_2 is common to both growth and maintenance respiration. Growth respiration is the respiration associated with the synthesis of new plant material, while maintenance is the respiration required primarily to provide energy for the re-synthesis of degraded proteins. Consequently, growth respiration is related to the growth rate of the plant, or daily carbon assimilation, whereas maintenance respiration is proportional to the plant dry weight or, more specifically, the actual protein content which may vary in response to plant nutrient status, particularly nitrogen. For a background on this treatment of respiration, see Johnson (1990), Thornley and Johnson (2000), Johnson (2013). The respiratory costs of nitrogen (N) uptake and N fixation are also incorporated.

Maintenance respiration

Maintenance respiration is generally regarded to be related to the plant live dry weight. However, maintenance respiration is primarily related to the resynthesis of degraded proteins. There are other maintenance costs, such as the energy required for phloem loading, but these are not considered explicitly, so that it is assumed that enzyme concentration is an indicator of overall maintenance costs. In addition, as a rate process, it is strongly temperature dependent. Incorporating these features, the maintenance respiration is assumed to be given by

$$R_{m,day} = m_{ref} f_m(T) \frac{f_N}{f_{N,ref}} W \tag{3.41}$$

where $f_m(T)$ is a maintenance temperature response function which takes the value unity at the reference temperature T_{ref}, W (kg C m^{-2}) is shoot mass, f_N is the canopy N concentration kg N (kg C)$^{-1}$ as used above in the discussion of the influence of protein on the light saturated rate of leaf gross photosynthesis, P_m, $f_{N,ref}$ is the reference N concentration, and m_{ref} (d^{-1}) is the maintenance coefficient at the reference temperature and N content, with default value

$$m_{ref} = 0.025 \text{ d}^{-1} \tag{3.42}$$

The maintenance temperature response function, $f_m(T)$, is defined to take the value unity at the reference temperature T_{ref}, so that

$$f_m\left(T = T_{ref}\right) = 1 \tag{3.43}$$

A simple linear response is used, as given by

$$f_m(T) = \frac{T - T_{m,mn}}{T_{ref} - T_{m,mn}} \tag{3.44}$$

with default values

$$\begin{aligned} &\text{C}_3: \quad T_{mn} = 3^{\circ}\text{C} \\ &\text{C}_4: \quad T_{mn} = 12^{\circ}\text{C} \end{aligned} \tag{3.45}$$

and the same reference temperature as in eqn (3.22).

Growth respiration

According to the standard theory for the definition of growth respiration, one unit of substrate that is utilised for growth results in Y units of plant structural material and $(1 - Y)$ units of respiration, where Y is the growth efficiency. Thus, for 1 unit of growth, this can be represented by the scheme in Fig. 3.4:

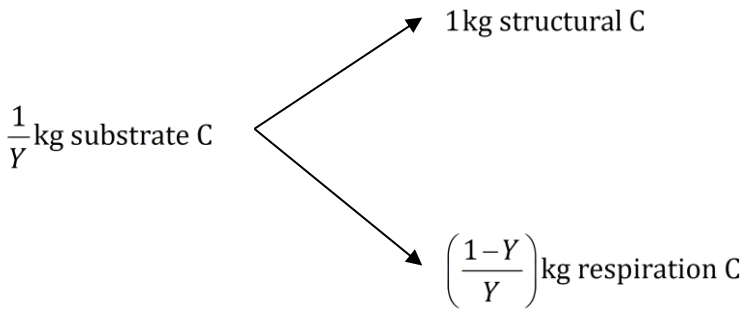

Figure 3.4: Schematic representation of growth respiration.

Thus, for growth G kg C m^{-2} d^{-1}, the corresponding growth respiration is

$$R_g = \left(\frac{1-Y}{Y}\right)G \tag{3.46}$$

The respiratory costs for cell wall and protein synthesis are different, with the costs of the more complex protein molecules being greater – a detailed discussion can be found in Thornley and Johnson (2000). The plant composition components discussed in Section 1.5 in Chapter 1, are used, so that the plant structure comprises cell wall, protein and sugars, with molar concentrations f_w, f_p and f_s respectively, and where

$$f_w + f_p + f_s = 1 \tag{3.47}$$

It is readily shown that, if the growth efficiencies for cell wall and protein are Y_w, and Y_p, then these are related to the overall growth efficiency, Y, by

$$\left(\frac{1-Y}{Y}\right) = \left(\frac{1-Y_w}{Y_w}\right)f_w + \left(\frac{1-Y_p}{Y_p}\right)f_p \tag{3.48}$$

from which

$$Y = \frac{1}{1+\left(\frac{1-Y_w}{Y_w}\right)f_w + \left(\frac{1-Y_p}{Y_p}\right)f_p} \tag{3.49}$$

This allows for the direct influence of plant structure on the overall growth efficiency directly. The model defaults are:

$$Y_w = 0.85;\ \ Y_p = 0.55 \tag{3.50}$$

so that, for example, with 20% sugars, 25% protein and 55% cell wall (on a mole basis), $Y = 0.81$, whereas, if the protein content is reduced to 20% and the cell wall increased to 60%, this becomes $Y = 0.83$. Values for Y that are observed experimentally are generally in the range 0.75 to 0.85. For more discussion, see Johnson (1990), Thornley and Johnson (2000), Thornley and France (2007), Johnson (2013).

Respiratory cost of nitrogen uptake and fixation

Nitrogen uptake involves energy costs (eg Johnson, 1990) and it is assumed that this is given by $R_{N,up}$ where

$$R_{N,up} = \lambda_{N,up} N_{up} \tag{3.51}$$

where N_{up} is the daily N uptake, kg N m^{-2} and $\lambda_{N,up}$, kg C (kg N)$^{-1}$ is the N uptake respiration coefficient with default value

$$\lambda_{N,up} = 0.6 \text{ kg C } (\text{kg N})^{-1} \tag{3.52}$$

The corresponding respiratory cost of N fixation in legumes is given by

$$R_{N,fix} = \lambda_{N,fix} N_{fix} \tag{3.53}$$

where N_{fix} is the daily N fixation, kg N m^{-2} and $\lambda_{N,fix}$, kg C (kg N)$^{-1}$ is the N fixation respiration coefficient with default value

$$\lambda_{N,fix} = 6 \text{ kg C } (\text{kg N})^{-1} \tag{3.54}$$

The fact that $\lambda_{N,fix}$ is greater than $\lambda_{N,up}$ reflects the fact that the respiratory costs associated with N fixation are significantly higher than for N uptake.

3.3.6 Daily carbon fixation

The previous section describes daily canopy gross photosynthesis and respiration. These are now combined to give the daily carbon fixation, or net growth rate as given by

$$G = P_{g,day} - R_g - R_m - R_N \tag{3.55}$$

where R_N is the respiratory cost of N acquisition and, is

$$\begin{aligned} &\text{non-legumes:} \quad R_N = R_{N,up} \\ &\text{legumes:} \quad\quad R_N = R_{N,up} + R_{N,fix} \end{aligned} \tag{3.56}$$

There is a circularity problem with the analysis here since growth depends on the respiratory cost of N uptake, but this cost depends on growth. In order to avoid unnecessary complexity, and since this is a daily time-step model, the value for R_N from the previous day is used in the calculations.

Using eqn (3.46), eqn (3.55) becomes

$$G = Y\left(P_{g,day} - R_m - R_N\right) \tag{3.57}$$

which defines the net pasture growth rate, or carbon fixation, including roots.

3.3.7 Influence of temperature extremes on photosynthesis

The influence of temperature on leaf photosynthesis and respiration has been described above, but temperature extremes may also affect photosynthetic capacity. For example, winter daytime temperatures in southern Queensland may be suitable for a C_4 species such as kikuyu, but low night temperatures may prevent growth occurring. To accommodate this possibility, low and high cumulative temperature functions can be defined and implemented in terms of the maximum and minimum daily temperatures.

First consider the low-temperature stress function. Two critical temperatures are defined, $T_{mn,high}$ and $T_{mn,low}$, where $T_{mn,high}$ is the critical temperature below which low-temperature stress will occur, and $T_{mn,low}$ is the critical temperature at which the low-temperature stress is maximum. The low-temperature stress function calculations are defined for situations where the minimum daily temperature, T_{mn}, is either greater than or less than $T_{mn,high}$

On day i, If $T_{mn} < T_{mn,high}$ then the temperature stress coefficient is calculated as

$$\xi_{T,low,i} = \begin{cases} \dfrac{T_{mn} - T_{mn,low}}{T_{mn,high} - T_{mn,low}}, & T_{mn} > T_{mn,low} \\ 0, & T_{mn} \le T_{mn,low} \end{cases} \tag{3.58}$$

which varies between 0 and 1 from $T_{mn,low}$ to $T_{mn,high}$.

Conversely, if $T_{mn} \geq T_{mn,high}$ the recovery coefficient is calculated according to

$$\zeta_{T,low,i} = \frac{T_{mean}}{T_{sum,low}} \tag{3.59}$$

where $T_{sum,low}$ is a critical temperature sum for recovery from low temperature stress.

Starting with $\xi_{T,low,0} = 1$, either eqn (3.58) or (3.59) is calculated depending on the minimum daily temperature. If $T_{mn} < T_{mn,high}$ then the cumulative temperature stress function is calculated as

$$\tau_{T,low} = \prod \xi_{T,low,i} \tag{3.60}$$

whereas, if $T_{mn} \geq T_{mn,high}$ then the cumulative stress function is now calculated as

$$\tau_{T,low} = \min\left(1, \tau_{T,low} + \zeta_{T,low,i}\right) \tag{3.61}$$

The daily gross photosynthesis, $P_{g,day}$ is then multiplied by $\tau_{T,low}$ to incorporate the influence of cumulative low temperatures or recovery from low temperatures.

In practice, low temperature stress increases in response to a sequence of low temperature and then the plant can recover as temperature increases. Full recovery from full stress, that is when $\xi_{T,low}$ is zero, will occur when there are no further days with $T_{mn} < T_{mn,high}$ and when the temperature sum of the mean daily temperature exceeds $T_{sum,low}$.

The default parameter values are

$$\begin{aligned} \mathrm{C}_3: &\quad T_{mn,low} = 0^{\circ}\mathrm{C}, \quad T_{mn,high} = 5^{\circ}\mathrm{C}, \quad T_{sum,low} = 100^{\circ}\mathrm{C} \\ \mathrm{C}_4: &\quad T_{mn,low} = 3^{\circ}\mathrm{C}, \quad T_{mn,high} = 7^{\circ}\mathrm{C}, \quad T_{sum,low} = 100^{\circ}\mathrm{C} \end{aligned} \tag{3.62}$$

although it should be noted that, by default, low temperature stress is not implemented for C_3 plants.

The effect of high temperature stress is defined in an analogous way to low temperatures, but now the critical temperature sum for recovery is defined by

$$\zeta_{T,high,i} = \sum \left[\frac{\max\left(0, 25 - T_{mean}\right)}{T_{sum,high}} \right] \tag{3.63}$$

Default parameter values are

$$\begin{aligned} \mathrm{C}_3: &\quad T_{mx,high} = 35^{\circ}\mathrm{C}, \quad T_{mx,low} = 30^{\circ}\mathrm{C}, \quad T_{sum,high} = 100^{\circ}\mathrm{C} \\ \mathrm{C}_4: &\quad T_{mx,high} = 38^{\circ}\mathrm{C}, \quad T_{mx,low} = 35^{\circ}\mathrm{C}, \quad T_{sum,high} = 100^{\circ}\mathrm{C} \end{aligned} \tag{3.64}$$

although it should be noted that, by default, high temperature stress effects are not implemented.

Although this treatment of low and high temperature stresses on photosynthesis is completely empirical, it captures the influence of temperature extremes and subsequent recovery.

3.4 Root distribution

The distribution of roots is important because of its influence on factors such as water and nutrient uptake as well as the input to the soil organic matter. For vegetative species, root depth is taken to be constant, whereas for annual species it increases to its maximum value at anthesis (flowering), as described later.

The relative root distribution by weight is shown in Fig 3.5, and is defined by:

$$f_r(z) = \frac{1}{1 + \left(\frac{z}{d_{r,h}} \right)^{q_r}} \tag{3.65}$$

where $d_{r,h}$ is the depth for 50% relative root mass and q_r is a scaling parameter. This is a convenient empirical approach, whereby $f_r = 0.5$ when $z = d_{r,h}$.

Root distribution has also been described according to an exponential equation, as used by Gerwitz and Page (1974) when they analysed a large range of root distribution data. However, the data are very variable and the sigmoidal pattern is probably preferable as it allows for a concentration of roots near the surface, sometimes referred to as the plough layer.

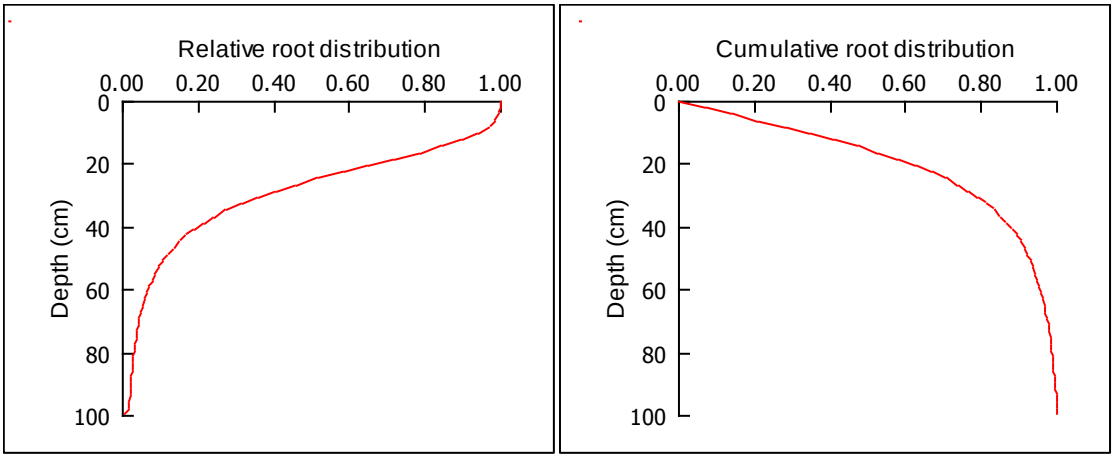

Figure 3.5: Relative root distribution, and corresponding cumulative root distribution as a function of depth using eqn (4.17), with $d_{r,h} = 25$ cm, q_r=3, and a total root depth of 100 cm.

3.5 Nitrogen remobilisation, uptake, and fixation

Nitrogen is available for growth from soil inorganic NO_3 and NH_4, N_{up}; N fixation in the case of legumes, N_{fix}; and any remobilised N from senescent material, N_{remob}, and can be written

$$N_{avail} = N_{up} + N_{fix} + N_{remob} \tag{3.66}$$

where all terms have units kg N m^{-2}. For non-legumes, N_{fix} is obviously zero.

Remobilisation of N is accounted for in the model by recycling N from senescent tissue, and is taken to be proportional to senescence, and so is given by

$$N_{remob} = f_{N,remob} \left. \frac{\mathrm{d}W_{dead}}{\mathrm{d}t} \right|_{gross} \tag{3.67}$$

where the derivative term is the gross production of dead material prior to, for example, losses from standing dead to litter.

Nitrogen uptake from soil inorganic NO_3 or NH_4 are treated on a *pro-rata* basis. Thus, if the concentration of inorganic nitrogen in any layer is $[N]_\ell$, kg N (kg soil)$^{-1}$, and the root fraction is $W_{r,\ell}$, kg root C m^{-2}, the potential N uptake is

$$N_{up} = \xi_N \sum_\ell [N]_\ell W_{r,\ell} \tag{3.68}$$

where ξ_N, kg soil (kg root C)$^{-1}$ d^{-1} is a nitrogen uptake coefficient. This parameter, while quite simple, is not particularly intuitive to work with. In the model, it has been calculated in relation to reference available N and root dry weight, with default value

$$\xi_N = 200 \text{ gN } (\text{t root d.wt})^{-1} N_{ppm}{}^{-1} d^{-1} \quad (3.69)$$

where N_{ppm} is the soil N concentration expressed as ppm, or mg N (kg soil)$^{-1}$. Thus, in these units, if the soil N concentration is 10 ppm, 1 t roots ha^{-1} will take up 2 kg N.

N fixation in legumes is an important source of nitrogen in many crop and pasture systems. The treatment of N fixation in the model is quite simple and is structured to ensure that legumes can obtain the required N for the optimum N concentration in new growth. Thus,

$$N_{fix} = \max\left[0, N_{req,opt} - \left(N_{remob} + N_{up}\right)\right] \quad (3.70)$$

So that N acquisition in legumes meets optimum requirement. It is apparent from this equation that if the available N from remobilisation and uptake is sufficient for optimum demand then there will be no fixation.

Once the total N available for growth is known, it is possible to define a nitrogen limiting factor, analogous to that for water (eqn (3.5)), as

$$\Omega_N = \min\left(1, \frac{N_{avail}}{N_{req,opt}}\right) \quad (3.71)$$

which is used later when considering the partitioning of growth between shoots and roots.

3.6 Pasture growth, senescence and development

The analysis so far defines the carbon inputs through photosynthesis and respiration as well as nitrogen remobilisation, uptake and, in the case of legumes, fixation. It now remains to describe overall canopy growth in terms of shoot and root growth and senescence, as well as the leaf and sheath components of shoot growth. A key feature of the treatment of pasture growth here is the turnover of plant tissue, which has been shown to have a major impact on pasture growth and utilisation (eg Parsons, 1988), and is widely used. The flow of tissue through the system is shown schematically in Fig. 3.6:

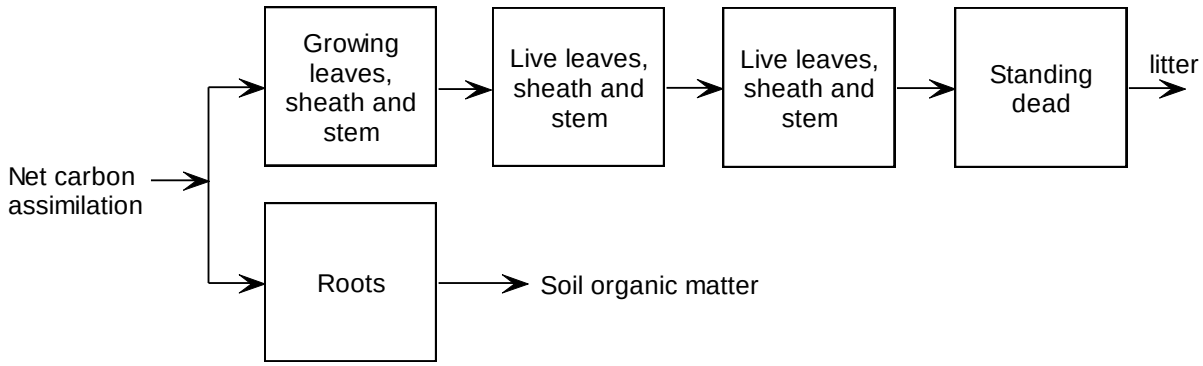

Figure 3.6: Schematic representation of growth, tissue turnover and senescence.

According to this scheme there are leaf categories, including the associated sheath and stem, corresponding to growing leaves, two categories of live leaves, and standing dead. New growth goes to the growing leaf box. There is a flow of tissue through the categories until it is transferred to the litter. Carbon is also partitioned to the roots, although separate root categories are not included. Root senescence passes straight to the soil organic matter pool.

The net carbon assimilation was described in detail in the previous section and the dynamics of growth, partitioning, tissue turnover and senescence are now considered.

First, the basic state variables in the model are define:

Live leaf:	$W_{live,\ell,i},\ i=1\text{to}3$	(3.72)
Total live leaf:	$W_{live,\ell}=\sum_{i=1}^{3}W_{live,\ell,i}$	(3.73)
Live sheath + stem	$W_{live,s,i},\ i=1\text{to}3$	(3.74)
Total live sheath+stem:	$W_{live,s}=\sum_{i=1}^{3}W_{live,s,i}$	(3.75)
Total live shoot:	$W_{live,shoot}=W_{live,\ell}+W_{live,s}$	(3.76)
Dead leaf	$W_{dead,\ell}$	(3.77)
Dead sheath + stem	$W_{dead,s}$	(3.78)
Root live	W_r	(3.79)

3.6.1 Shoot:root partitioning

Shoot:root partitioning is important in terms of the plant's ability to access water and nutrients, its impact on shoot, and therefore harvestable, growth, and also on the supply of organic matter to the soil for soil organic matter and inorganic nutrient dynamics. Various models of shoot:root partitioning are discussed in Thornley and Johnson (2000). The models partition growth in a way that attempts to balance the requirements between resources acquired by the shoot and root respectively. For example, if water is limiting then plants will partition a greater proportion of growth to the roots to attempt to increase water uptake.

The partitioning of new growth to the shoot, G_{shoot} kg C m^{-2} d^{-1}, is defined as

$$G_{shoot}=\rho_{shoot,ref}\left(\Omega_{water}\Omega_N\right)^{1/2}G \tag{3.80}$$

where the growth limiting factors, Ω_{water} and Ω_N are given by eqns (3.5) and (3.71), and G is the total plant growth rate, eqn (3.57). According to this equation, the proportion of new growth partitioned to the shoot declines as water or nitrogen stress increases. The square root term moderates the response and has been seen to give realistic partitioning patterns. Note that for legumes, Ω_N always takes the value unity.

Root growth, G_{root} kg C m^{-2} d^{-1}, is then simply

$$G_{root}=G-G_{shoot} \tag{3.81}$$

3.6.2 Leaf:sheath partitioning and leaf growth

Once the proportion of shoot growth is defined by eqn (3.80) it is partitioned linearly between the leaf and sheath, so that

$$\begin{aligned}G_\ell&=\rho_\ell G_{shoot}\\G_s&=\rho_s G_{shoot}\end{aligned} \tag{3.82}$$

where G_ℓ and G_s, kg C m^{-2} d^{-1} are the daily rates of leaf and sheath growth.

Equation (3.82) defines the leaf mass growth, and it now remains to define the associated leaf area index production. The specific leaf area, σ m^2 leaf (kg C)$^{-1}$, is defined as

$$\sigma = \frac{L}{W_\ell} \tag{3.83}$$

where L, m^2 leaf (m^2 ground)$^{-1}$ is the leaf area index and W_ℓ, kg C (m^2 ground)$^{-1}$ is the leaf mass. σ is seen to depend on atmospheric CO_2 concentration and, following Johnson *et al.* (2010), is taken to be

$$\sigma = \frac{\sigma_{amb}}{\sqrt{f_C(C)}} \tag{3.84}$$

where σ_{amb} is the value of σ at ambient CO_2 and $f_C(C)$ is the generic CO_2 response function used earlier in the treatment of leaf photosynthesis, and discussed in Chapter 1, Section 1.3.4. σ is quite variable for different species, but as an example and on a dry weight basis the default value for perennial ryegrass is equivalent to 20 m^2 leaf (kg d.wt)$^{-1}$.

3.6.3 Growth dynamics

Figure 3.6 shows the scheme for tissue turnover and senescence. Define the flux parameter as γ, d^{-1}, (with subscript $dead$ for the flux from standing dead to litter), the flux of material between each category can be defined as:

$$flux(1 \to 2) = 2\gamma W_{live,1} \tag{3.85}$$

$$flux(2 \to 3) = \gamma W_{live,2} \tag{3.86}$$

$$flux(3 \to dead) = \gamma W_{live,3} \tag{3.87}$$

$$flux(dead \to litter) = \gamma_{dead} W_{dead} \tag{3.88}$$

The factor 2 in eqn (3.85) allows for the fact that the mean d.wt of leaves in the growing leaf category will be about half of the fully grown leaves in that category. It is assumed that the flux between the live leaf categories are lower for the sheath than the leaf.

The growth dynamics equations can now be written

Leaf

$$\frac{dW_{live,\ell,1}}{dt} = \rho_\ell G_{shoot} - 2\gamma_\ell W_{live,\ell,1} \tag{3.89}$$

$$\frac{dW_{live,\ell,2}}{dt} = 2\gamma_\ell W_{live,\ell,1} - \gamma_\ell W_{live,\ell,2} \tag{3.90}$$

$$\frac{dW_{live,\ell,3}}{dt} = \gamma_\ell W_{live,\ell,2} - \gamma_\ell W_{live,\ell,3} \tag{3.91}$$

$$\frac{dW_{dead,\ell}}{dt} = \gamma_\ell W_{live,\ell,3} - \gamma_{dead} W_{dead,\ell} \tag{3.92}$$

Sheath + stem

$$\frac{dW_{live,s,1}}{dt} = (1-\lambda_\ell) G_{shoot} - 2\gamma_s W_{live,s,1} \tag{3.93}$$

$$\frac{dW_{live,s,2}}{dt} = 2\gamma_s W_{live,s,1} - \gamma_s W_{live,s,2} \tag{3.94}$$

$$\frac{\mathrm{d}W_{live,s,3}}{\mathrm{d}t} = \gamma_s W_{live,s,2} - \gamma_s W_{live,s,3} \tag{3.95}$$

$$\frac{\mathrm{d}W_{dead,s}}{\mathrm{d}t} = \gamma_s W_{live,s,3} - \gamma_{dead} W_{dead,s} \tag{3.96}$$

Root

$$\frac{\mathrm{d}W_r}{\mathrm{d}t} = G_{root} - \gamma_r W_r \tag{3.97}$$

In the model, a scale factor is defined to relate γ_s and γ_r to γ_ℓ although individual values could be prescribed if necessary.

The rate constant, γ_ℓ, can be related to the number of live leaves per tiller, number of boxes in Fig. 3.6, and the leaf appearance rate, ϕ_ℓ d^{-1}, and is

$$\gamma_\ell = \phi_\ell \frac{\text{number of boxes}}{\text{live leaves per tiller}} \tag{3.98}$$

which can be helpful in defining the flux parameters. In the model, which has 3 leaf age category boxes, the leaf appearance interval and live leaves per tiller are defined and, since the leaf appearance interval is the reciprocal of leaf appearance rate, this defines γ_ℓ.

Nitrogen

The equations for plant dynamics above apply to nitrogen as well as carbon, but now scale factors for N concentration in non-leaf shoot material and root material are defined, which are both 0.5 by default. Furthermore, remobilisation of N from senescent tissue is an additional flux into the growing leaf.

3.6.4 Influence of temperature on growth dynamics

The rate of leaf appearance is strongly temperature dependent and so the γ rate constants are related to mean daily temperature by

$$\gamma = f_\gamma(T)\gamma_{ref} \tag{3.99}$$

where $f_\gamma(T)$ again uses the temperature response function with an asymptote, eqn (1.41) discussed in Chapter 1, Section 1.3.6. Default parameters for perennial ryegrass are

$$\phi_\ell = 1/8;\ T_{mn} = 3^\circ C;\ T_{opt} = 20^\circ C;\ q = 2 \tag{3.100}$$

with this value of ϕ_ℓ corresponding to a leaf appearance interval of 8 d at 20°C. Both the leaf appearance rate and interval are illustrated in Fig.3.7 for these parameter values.

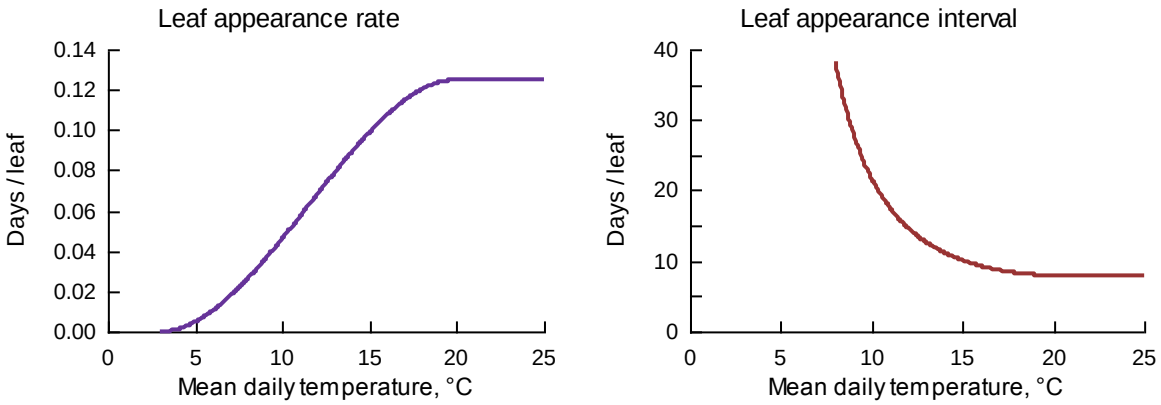

Figure 3.7: Leaf appearance rate and interval for the default parameter values for perennial ryegrass as given in eqn (3.100)

3.7 Mixed swards

The analysis so far has considered a single species and we now consider mixed swards, which involves defining light interception and photosynthesis in mixtures, as well as allowing for root distribution of multiple species.

3.7.1 Light interception and attenuation

The theory is based on Johnson *et al.* (1989) and Thornley and Johnson (2000) but is developed to allow for canopies of different heights.

First, the relationship between canopy leaf area index, L, and height, h, is defined using the non-rectangular hyperbola discussed in Chapter 1, Section 1.3.2, which in terms of L and h variables, can be written

$$h = \frac{1}{2\xi}\left[\alpha L + h_m - \left\{(\alpha L + h_m)^2 - 4\alpha\xi h_m L\right\}^{1/2}\right] \tag{3.101}$$

where, as discussed in Section 1.3.2, α is the initial slope of the response, h_m the asymptote, which is the maximum canopy height, and ξ a curvature parameter between 0 and 1. This equation was used above for the leaf photosynthetic light response curve. A characteristic of the present model is to try to express the underlying equations in terms of parameters that have some underlying physiological interpretation. For the relationship between $h(L)$, the initial slope of the curve is not easy to estimate. However, by defining the value of L for half-maximum height, L_{half}, it is readily shown after some algebra that

$$\alpha = h_m \frac{(2-\xi)}{2L_{half}} \tag{3.102}$$

so that, instead of prescribing α, L_{half} can be defined instead. In the model, a fixed value for the curvature parameter is used, which is

$$\xi = 0.9 \tag{3.103}$$

The maximum height, and consequently L_{half} are likely to vary significantly between species, and the default values for perennial ryegrass are

$$h_m = 0.5\text{m}, \quad L_{half} = 2\,\text{m}^2\text{leaf}\left(\text{m}^2\text{ground}\right)^{-1} \tag{3.104}$$

The response is shown in Fig. 3.8 for these parameter values.

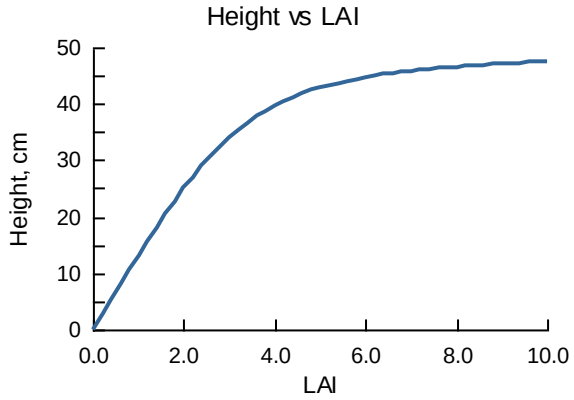

Figure 3.8. Relationship between canopy height and LAI as given by eqns (3.101) to (3.104).

The procedure now is to adapt the light attenuation and interception theory that was described in Chapter 2, Section 2.4.5, and that was applied above for a single species. The procedure is numerical and uses the LAI increment δL where, for the calculations,

$$\delta L = 0.1 \tag{3.105}$$

and then sums through the canopy at these LAI increments to the total canopy LAI. Thus, the total number of layers is

$$n_L = \frac{L_{tot}}{\delta L} \tag{3.106}$$

where L_{tot} is the sum of the LAI for each species. Each species is then assumed to be distributed through the canopy on a *pro-rata* basis of their height. Thus, if the canopy height is h_{mx}, which is the height of the species with maximum height, then the starting layer for each species is

$$n_{start,p} = 1 + \text{round}\left(\frac{h_{mx} - h_p}{h_{mx}}\right) \tag{3.107}$$

where p denotes the s*p*ecies and 'round' is a programming technique to round floating point values to integer, since $n_{start,p}$ must be integer. The LAI increment for each species now becomes

$$\delta L_p = \frac{L_p}{n_L - n_{start,p}} \tag{3.108}$$

Thus, we now know the LAI increments for each species and which layer, from the top, where they first occur in the canopy.

The procedure is now to integrate through the canopy to calculate the light interception on each species in each canopy layer. Following Johnson *et al* (1989), an 'effective' light extinction coefficient for each layer is defined as

$$k_{e,i} = \frac{\sum k_p \delta L_p}{\sum \delta L_p} \tag{3.109}$$

where the summations are over all species and a species is only included in the summation if

$$n_{start,p} \geq i \tag{3.110}$$

Extending the theory in Chapter 2, Section 2.4.5, the direct and diffuse components of PPF in any layer, denoted by i are given by

$$J_{s,i} = J_{s,i-1}\left(1-k_e \delta L_i\right) \tag{3.111}$$

and

$$J_{d,i} = J_{d,i-1}\left(1-k_e \delta L_i\right) \tag{3.112}$$

respectively, where

$$\delta L_i = \sum \delta L_p \tag{3.113}$$

is the total LAI in the layer and, again, a species is only included in the summation if eqn (3.110) applies.

Equations (3.111) and (3.112) are then used in the canopy photosynthetic integrals given by eqn (3.32) or, more precisely the numerical procedure defined immediately after that equation.

3.7.2 Root distribution

Root distribution for each species was discussed above in Section 3.4. The uptake of both water and nutrients for multiple species on any particular day is calculated for each species as if the other species were not present. The rationale for this is that the relative amount of water or nutrients that is removed from the soil on any one day is generally a small fraction of the total available. However, on the next day, the pool of available soil resources will have been depleted by the amount used by all species. A minor problem may be that if a large proportion of resources is removed on any one day then the order in which species are treated may have a small effect on the simulation. In order to avoid any problems in the unlikely event that this occurs, each species is allocated a maximum possible amount of available water or nitrogen in each soil layer which is based on their fractional root mass in that layer.

3.8 Concluding remarks

The model for pasture growth described here is a physiologically based carbon assimilation model in response to environmental conditions. Daily growth rate is estimated by starting with leaf photosynthesis, summing this over the canopy and accumulating over the day. Dark respiration components for maintenance, nitrogen uptake and, for legumes, nitrogen fixation are incorporated. In addition, generic parameters for C_3 and C_4 pastures are included. Multiple species interactions are also incorporated. The model includes the effects of tissue turnover, phase development, annual and perennial species as well as legumes. In addition, the nutrient composition of live and dead tissue is calculated which is used both in the treatment of nutrient cycling and also animal nutrition. Water and nutrient dynamics interact with the soil water and nutrient balances in a consistent manner.

3.9 References

Cannell MGR, Thornley JHM. (1998). Temperature and CO2 responses of leaf and canopy photosynthesis: a clarification using the non-rectangular hyperbola model of photosynthesis. *Annals of Botany,* **82,** 883-892.

Gerwitz A and Page ER (1974). An empirical mathematical model to describe plant root systems. *Journal of Applied Ecology,* **11,** 773 – 781.

Johnson IR (2013). PlantMod: exploring the physiology of plant canopies. IMJ Software, Dorrigo, NSW, Australia. www.imj.com.au/software/plantmod.

Johnson IR, Thornley JHM, Frantz JM, Bugbee B (2010). A model of canopy photosynthesis incorporating protein distribution through the canopy and its acclimation to light, temperature and CO_2. *Annals of Botany*, **106,** 735-749.

Johnson IR (1990). Plant respiration in relation to growth, maintenance, ion uptake and nitrogen assimilation. *Plant, Cell and Environment,* **13,** 319-328.

Johnson IR, Parsons AJ and Ludlow MM (1989). Modelling photosynthesis in monocultures and mixtures. *Australian Journal of Plant Physiology*, **16,** 501-516.

Johnson IR and Thornley JHM (1983). Vegetative crop growth model incorporating leaf area expansion and senescence, and applied to grass. *Plant, Cell and Environment,* **6,** 721-729.

Johnson IR and Thornley JHM (1985). Dynamic model of the response of a vegetative grass crop to light, temperature and nitrogen. *Plant, Cell & Environment* **8,** 485–499.

Johnson IR and Parsons AJ (1985). A theoretical analysis of grass growth under grazing. *Journal of Theoretical Biology,* **112,** 345-367.

McCree KJ (1970). An equation for the respiration of white clover plants grown under controlled conditions. In *Prediction and Measurement of Photosynthetic Productivity* (ed. I. Setlik), pp 221 – 229. Pudoc, Wageningen.

Parsons AJ (1988). The effects of season and management on the growth of grass swards. In: *The Grass Crop - the Physiological Basis of Production* (eds MB Jones and A Lazenby). Chapman Hall, London, 243-275.

Parsons AJ, Johnson IR and Harvey A (1988). The use of a model to optimise the interaction between the frequency and severity of intermittent defoliation and to provide a fundamental comparison of the continuous and intermittent defoliation of grass. *Grass and Forage Science,* **43,** 49-59

Parsons AJ, Carrere P and Schwinning S (2000). Dynamics of heterogeneity in a grazed sward. In: *Grassland Ecophysiology and Grazing Ecology* (eds G Lemaire, *et al*). CAB International, Wallingford (UK).

Passioura JB and Stirzaker RJ (1993). Feedforward responses of plants to physically inhospitable soil. *International Crop Science* I, pp 715 – 719. Crop Science Society of America, Madison, WI.

Robson MJ and Sheehy JE (1981). Leaf area and Light Interception. In *Sward Measurement Handbook* (eds J Hodgson, R D Baker, A Davies, A S Laidlaw and J D Leaver), pp 115 – 139. British Grassland Society, Hurley.

Sands PJ (1995). Modelling canopy production. I. Optimal distribution of photosynthetic resources, *Australian Journal of Plant Physiology*, **22,** 593-601.

Thornley JHM (1970). Respiration, growth and maintenance in plants. *Nature* **227,** 304 – 305.

Thornley, JHM (1998). *Grassland Dynamics, An Ecosystem Simulation Model.* CAB International, Wallingford, UK.

Thornley JHM and Johnson IR (2000). *Plant and Crop Modelling.* Reprint of 1990 Oxford University Press edition. www.blackburnpress.com.

Thornley JHM and France J (2007). *Mathematical Models in Agriculture.* CABI, Oxford.

4 Water dynamics

4.1 Introduction

The water balance in pasture and crop systems involves an intricate interaction between rainfall, evapotranspiration, runoff and infiltration. The general scheme is presented in Fig. 4.1:

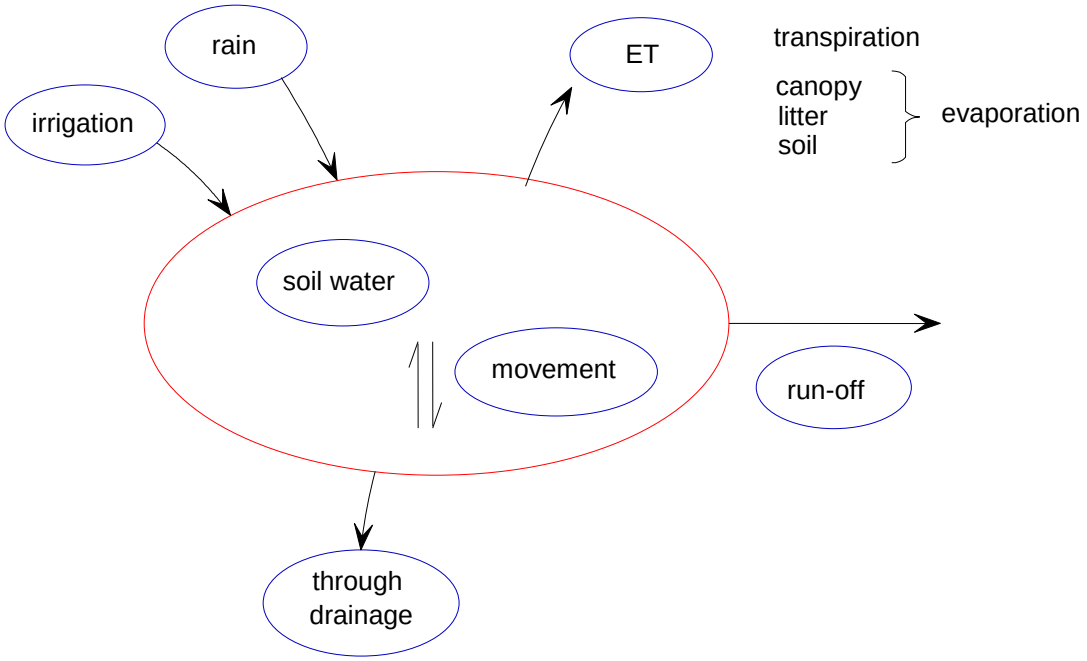

Figure 4.1: Schematic representation of the soil water balance.

In this diagram, the processes that are included in the model are shown. Some of these are quite readily measured, whereas others are more difficult. For example, while rainfall can be measured quite accurately, it is much more difficult to measure actual evapotranspiration.

The individual processes are now considered in turn.

4.2 Potential transpiration

The theory of canopy transpiration has received much attention, and the most widely used model is the Penman-Monteith (PM) equation (Penman (1948) and Monteith (1965)). This approach is based on sound physical principles, and describes the influence of radiation, temperature, vapour deficit, windspeed and canopy structure on water use. As with any theory, there is always scope to incorporate greater complexity, but the PM equation provides an ideal description of canopy water use for most crop and pasture physiological studies, and is widely used in crop and pasture models. For further discussion see Monteith (1973), or the later edition Monteith and Unsworth (2008), Campbell (1977), or the later edition Campbell and Norman (1998), Jones (1992), Allen *et al.* (1998), Thornley and Johnson (2000), Thornley and France (2007), Johnson (2013). Background definitions for water vapour and conductance are given in Chapter 1, while the canopy radiation balance was discussed in Chapter 2: this material will be referred to frequently throughout this Chapter. Canopy transpiration is influenced by canopy temperature which, in turn, is affected by the prevailing environmental conditions. A key part of the analysis for canopy transpiration is the elimination of canopy temperature so that transpiration is defined in terms of air temperature and other environmental factors. For a complete derivation of the PM equation as used here,

see Thornley and Johnson (2000) or Johnson (2013). The approach here is to define potential transpiration and use this in conjunction with available soil water to estimate the actual transpiration by the plant canopy, as discussed in Chapter 3, Section 3.2.

For daily crop and pasture models that work with standard meteorological data, transpiration is generally required in units of mm d^{-1} to be consistent with rainfall. However, transpiration is also presented in mol units in the literature. The conversion is straightforward with

1 mol water ≡ 0.018 kg water (4.1)

and

1 kg water m^{-2} ≡ 1 mm water (4.2)

so that

1 mol water m^{-2} ≡ 0.018 mm water (4.3)

The PM equation involves defining conductances for water vapour which can be prescribed either as m s^{-1} or mol m^{-2} s^{-1}. The present theory is presented using mass rather than mol units.

4.2.1 Penman-Monteith equation

The PM equation defines the canopy transpiration rate in terms of climatic conditions and canopy parameters. It can also be adapted to define evaporation from soil, litter or the canopy surface. The general approach in deriving and using the PM equation is to start with the instantaneous rate of transpiration (mm s^{-1}) and then scale that up to get daily values. The general formulation for the PM equation for daily transpiration, assumed to occur during daylight hours, can be written as

$$E_T = \frac{sR_{n,day} + 86,400 f_{day} c_p \rho_a g_a \Delta e_{v,a}}{\lambda\left[s + \gamma\left(1 + g_a / g_c\right)\right]} \quad (4.4)$$

where the symbols (some of which have been defined in Chapter 2), with units, are defined by:

E_T	Daily transpiration rate	mm water d^{-1}
$R_{n,day}$	Canopy net radiation balance	J m^{-2} d^{-1}
f_{day}	Daylight fraction	-
$\Delta e_{v,a}$	Vapour pressure deficit	Pa
λ	Latent heat of vaporization	2.45 x 10^6 J kg^{-1}
s	Slope of the saturated vapour pressure as a function of temperature relative to P	Pa K^{-1}
γ	Psychrometric parameter	Pa K^{-1}
c_p	Specific heat capacity of dry air	J kg^{-1} K^{-1}
ρ_a	Density of dry air	1.2 kg m^{-3}
g_c	canopy conductance	m s^{-1}
g_a	boundary layer conductance	m s^{-1}

Vapour pressure deficit was discussed in Chapter 1, Section 1.6.2; the slope of the saturated vapour pressure as a function of temperature, s, is calculated by differentiating the Tetens formula, eqn (1.97) in Chapter 1, and is

$$s = \frac{2.58\times10^6}{(T+241)^2}\exp\left(\frac{17.5T}{T+241}\right) \tag{4.5}$$

Density of dry air is related to temperature according to

$$\rho = \frac{352.9}{T+273.2} \tag{4.6}$$

The psychrometric parameter, γ, is given by

$$\gamma = \frac{c_p P_{atm}}{\varepsilon\lambda} \tag{4.7}$$

where P_{atm} is atmospheric pressure, taken to be

$$P_{atm} = P_{atm,sea}\left(1-\frac{0.1}{1000}\right)\Lambda \tag{4.8}$$

where Λ, m, is the altitude and the atmospheric pressure at sea level is

$$P_{atm} = 101{,}325 \text{ Pa} \tag{4.9}$$

so that P_{atm} falls by 10% for every 1000m increase in altitude. The final parameter in eqn (4.7) is ε ,the ratio of the relative molecular mass of water to that of dry air and is (eg, Thornley and Johnson, 2000), with value

$$\varepsilon = 0.622 \tag{4.10}$$

It now remains to define the canopy and boundary layer conductances, which are the conductances of water vapour across the leaf stomata and from the surface of the leaves to the bulk air stream respectively.

Canopy conductance

Canopy conductance is generally defined as the product of the leaf stomatal conductance and the conducting leaf area of the canopy. In the present model, there is no attempt to simulate leaf stomatal conductance and so canopy conductance is taken to be a constant value appropriate for well watered leaves. This means that eqn (4.4) applies to plants that are not under water stress. This is then used in eqn (3.5) in Chapter 3 where plant response to transpiration demand is discussed. The constant values for stomatal conductance are:

$$\begin{aligned} &C_3: \quad g_c = 0.015 \text{ m s}^{-1} \\ &C_4: \quad g_c = 0.01 \quad \text{m s}^{-1} \end{aligned} \tag{4.11}$$

where the C_3 value is similar to that used by Allen *et al.* (1998) and the lower C_4 value is because these plants have a lower internal leaf CO_2 concentration due to the C_4 photosynthetic mechanism which results in a lower stomatal conductance.

Boundary layer conductance

There is considerable discussion of boundary layer conductance in the literature, although not without problems, as discussed in Johnson (2013). Rather than attempt to add greater complexity to the theory, a

much simpler approach is used here to capture the general characteristics of the expected behaviour for canopy conductance. g_a is assumed to be related to mean daily windspeed, u (m s^{-1}), and canopy height, h (m), given by

$$g_a = g_{a,0} + \left(g_{a,ref} - g_{a,0}\right)\frac{u}{u_{ref}}\left(\frac{h}{h_{ref}}\right)^{0.5} \tag{4.12}$$

where $g_{a,ref}$ is the value of g_a at the reference windspeed u_{ref} and canopy height h_{ref}. The reference values for windspeed and canopy height are taken to be

$$\begin{aligned} u_{ref} &= 2 \text{ m s}^{-1} \\ h_{ref} &= 0.3 \text{ m} \end{aligned} \tag{4.13}$$

and the default conductance parameters are

$$\begin{aligned} g_{a,0} &= 0.002 \text{ m s}^{-1} \\ g_{a,ref} &= 0.01 \quad \text{m s}^{-1} \end{aligned} \tag{4.14}$$

These values are consistent with Allen *et al.* (1998).

4.3 Potential daily evaporation

Potential evaporation of water sitting on the surface of the leaves, litter or soil is treated in a similar fashion to transpiration but now there is no resistance to water movement through the leaf stomata, so that the term $1/g_c \to 0$ in eqn (4.4) and hence

$$E_v = \frac{sR_{n,day} + 86,400 f_{day} c_p \rho_a g_a \Delta e_{v,a}}{\lambda\left(s+\gamma\right)} \tag{4.15}$$

Although there may be some nighttime evaporation, the reverse may also occur, with deposition of dew. Neither of these are likely to be significant and are not considered in the model.

4.4 Soil water infiltration and redistribution

The description of soil water infiltration and redistribution is crucial in the study of water movement in soils. The aim of this section is to consider some approaches and issues relating to this topic. There is a large body of theory on modelling soil water dynamics, and so the objective here is to give a brief account of some of the principal approaches and then discuss the particular options that are available in the present model.

The most widely used mechanistic model for soil water infiltration is the Richards equation, which combines Darcy's law for water movement along a water potential gradient with mass balance. There is considerable appeal to the Richards equation, but it does pose significant challenges in solving it for soils with variable soil hydraulic properties. While earlier versions of the SGS Pasture Model and DairyMod had the option of using the Richards equation, we have now moved to the more flexible and robust 'capacitance' model, and so the Richards equation is not discussed here.

The flux of water, q m water d^{-1}, is given by

$$q = K_{sat}\left(\frac{\theta}{\theta_{sat}}\right)^{\sigma} \tag{4.16}$$

where θ m^3 water (m^3 soil)$^{-1}$ is volumetric soil water content, θ_{sat} saturated water content, K_{sat} m d^{-1} is the saturated hydraulic conductivity which is the value of q when $\theta = \theta_{sat}$, and σ is a flux coefficient which is discussed below.

θ_{sat} is calculated from soil bulk density, ρ_b kg (m^3 soil)$^{-1}$, and soil particle bulk density, ρ_b kg m^{-3}, where

$$\theta_{sat} = 1 - \frac{\rho_b}{\rho_p} \tag{4.17}$$

which simply assumes that when the soil is saturated all pore spaces are occupied by water. The standard default value

$$\rho_p = 2{,}650 \text{ kg m}^{-3} \tag{4.18}$$

is used.

The 'field capacity', θ_{fc}, sometimes referred to as 'drained upper limit' is defined here such that

$$q\left(\theta = \theta_{fc}\right) = q_{fc} \tag{4.19}$$

where q_{fc} is a very small flow rate, taken to be

$$q_{fc} = 0.1 \text{ mm d}^{-1} \tag{4.20}$$

parameter σ is then derived from eqn (4.16) as

$$\sigma = \frac{\ln\left(q_{fc}/K_{sat}\right)}{\ln\left(\theta_{fc}/\theta_{sat}\right)} \tag{4.21}$$

The model has low, medium and high textured soils, as well as a duplex, as defaults. Default values for the medium textured soil are:

$$\begin{aligned} K_{sat} &= 0.15 \text{ m d}^{-1} \\ \rho_b &= 1.2 \text{ g cm}^{-3} \\ \theta_{fc} &= 0.4 \end{aligned} \tag{4.22}$$

which, with eqns (4.17) and (4.21) give

$$\begin{aligned} \theta_{sat} &= 0.55 \\ \sigma &= 23.3 \end{aligned} \tag{4.23}$$

These values are used to illustrate the flux, q, in Fig. 4.2. According to this approach:

- only water in excess of the drainage point can move, and all movement is downwards;
- the flux decreases as the available water for movement declines, as controlled by σ, which in turn is derived from the water holding capacity of the soil.

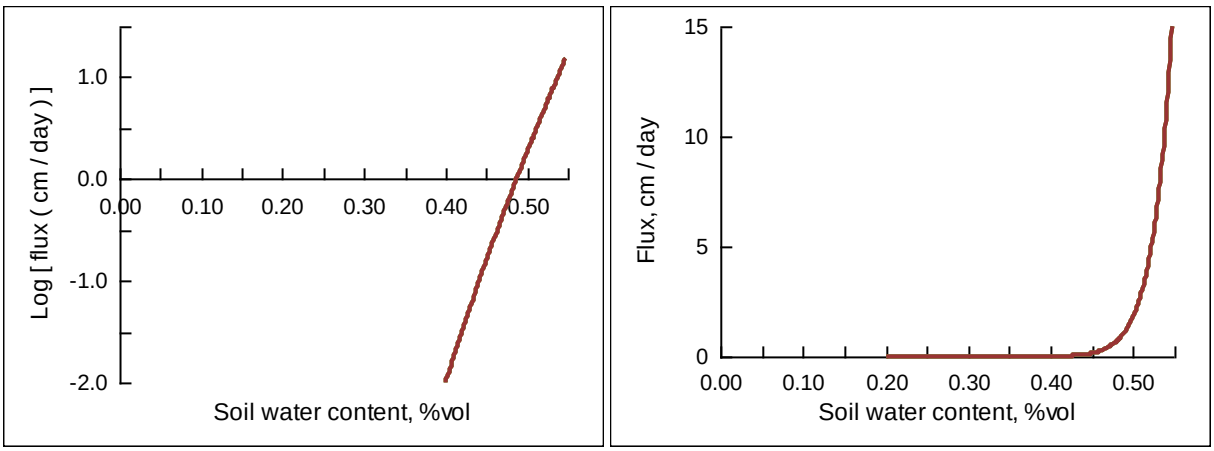

Figure 4.2: Water flux, q, eqn (4.16), in relation to soil water content for the parameters in eqns (4.22) and (4.23)

The method is applied by divide the soil into layers – in the present model, the first four are each 5cm and then subsequent layers are 10cm. A sub-daily time-step is then calculated to ensure the water movement from any layer does not exceed that which is available. This requires evaluating the variable

$$\xi_\ell = \frac{K_{sat,\ell}}{\left(\theta_{sat,\ell} - \theta_{fc,\ell}\right)\delta z_\ell} \tag{4.24}$$

where ℓ refers to the soil layer and δz_ℓ, m, is the layer thickness. The number of time increments in the day is then chosen to ensure that it is greater than all of the ξ_ℓ values. To avoid any likelihood of problems, the number of time-steps is then increased by 50%.

A further constraint applies in selecting the daily time increments in that it must be an exact multiple of the sub-daily time increment for the prescription of daily rainfall distribution as discussed in Chapter 2, Section 2.2. By default, rainfall is divided into hourly distributions and so the daily time increments for infiltration must be a multiple of 24.

This model is readily implemented numerically and is formulated in terms of easily characterised soil parameters. On the interface where the parameters are prescribed, the wilting point and air-dry water content are also included. These are used for plant water use and soil water evaporation respectively and not directly for infiltration.

The main difference between this model and the more commonly used tipping-bucket model is the use of hydraulic conductivity and a fairly fine depth layer distribution. In the tipping-bucket model, the layers are generally coarser and water in excess of field capacity is assumed to move from one layer to the next in a day (although variations on this are to be found).

4.5 Runoff

There are several approaches in the literature for the treatment of runoff, depending on the general objectives of the model as well as the spatial- and time-scales. For the present purposes, it is necessary to be able to calculate the flux of water off the paddock on a time-scale that is consistent with the treatment of rainfall inputs, infiltration and evapotranspiration, which are calculated at sub-daily intervals.

Two widely used, and quite similar, approaches are the Manning equation and Horton's equation. Manning's equation states that the speed of water movement across the surface, v (m s^{-1})

$$v = \frac{D^{2/3} S^{1/2}}{n} \tag{4.25}$$

where D (m) is the depth of water on the surface, S is the profile slope (%), and n (s $m^{-1/3}$) is the 'Manning coefficient', with typical values of around 0.04 for pastures and 0.1 for bare soil. Horton's equation is similar in structure to eqn (5.18a). The main disadvantage in using eqn (4.25) is that n depends on the ground cover characteristics which will vary throughout the simulation and so a simplified approach is used.

While runoff will clearly depend on the depth of water on the soil surface, it will also depend on the ground cover, and so it is assumed that:

$$v = \lambda \left(D - D_0 \right) S^{1/2} \tag{4.26}$$

where D (m) is the depth of water on the surface, D_0 is the surface detention (amount of water that the bare soil surface can hold with no runoff), and λ (s^{-1}) is related to the relative ground cover (from 0 to 1) by

$$\lambda = \lambda_0 + \left(\lambda_{mx} - \lambda_0 \right) \times \text{cover} \tag{4.27}$$

This approach captures the essence of runoff in that it increases with profile slope and depth of water on the surface (above a threshold value), while increasing ground cover will decrease runoff. The parameters λ_0 and λ_{mx} can be prescribed on the model interface. Note that the ground cover components are derived in Chapter 3, Section 3.3.

The runoff speed, as given by eqns (4.26), (4.27) is shown in Fig. 4.3.

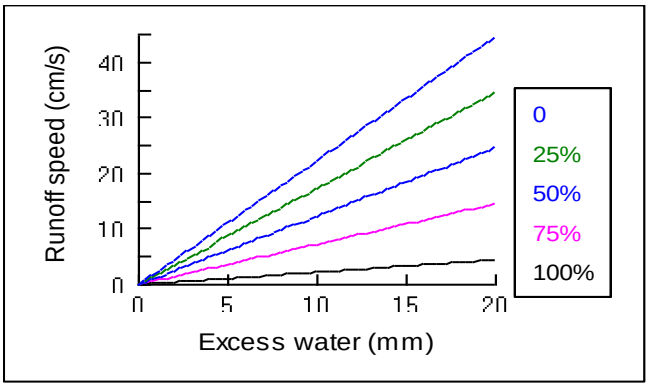

Figure 4.3: Runoff speed as a function of excess surface water for a range of ground covers as shown. The parameters are: $S = 5\%$, $\lambda_0 = 100$ 100 s^{-1} and $\lambda_{mx} = 10$ 10 s^{-1}.

4.6 Evaporation

Water can evaporate from the canopy, litter or soil. Evaporation from the canopy occurs if there is any free standing water on the canopy. The potential evaporation is defined by eqn (4.15). Water can evaporate from the canopy, litter and soil. These are considered in turn

4.6.1 Canopy

It is assumed that any water sitting on the canopy surface (leaves) is available for evaporation at the potential rate. If the amount of water on the canopy surface is H_{canopy}, then the actual evaporation of water from the canopy is simply:

$$E_{v,canopy} = \max\left(H_{canopy}, f_g E_v \right) \tag{4.28}$$

where f_g is the total ground cover by the canopy, eqn (2.23) in Chapter 2, and E_v is the potential daily evaporation from a free surface, as given by eqn (4.15).

4.6.2 Litter

As for the canopy, it is assumed that if there is any water held in the litter then it is available for evaporation. It is therefore necessary to define the ground cover due to the presence of litter, W_{litter} kg d.wt m^{-2}, which is defined as

$$f_{g,litter} = \exp\left(-0.69\frac{W_{litter}}{W_{litter,h}}\right) \tag{4.29}$$

where the -0.69 factor is ln(2) and ensures that

$$f_{g,litter}\left(W_{litter} = W_{litter,h}\right) = 0.5 \tag{4.30}$$

However, the evaporative demand is attenuated in relation to canopy cover. Thus, if the amount of water held by the litter is H_{litter}, then the actual evaporation of water from the litter is

$$E_{v,litter} = \max\left\{H_{litter}, \left(1-f_g\right) f_{g,litter} E_v\right\} \tag{4.31}$$

Where, as above, f_g is the total ground cover by the canopy, eqn (2.23) in Chapter 2, and E_v is the potential daily evaporation from a free surface, as given by eqn (4.15).

4.6.3 Soil

Soil evaporation is the flux of water from the soil to the atmosphere in response to evaporative demand, ground cover and soil water content. It is assumed that the potential to evaporate from the soil declines with depth according to the function

$$\mu_\ell = \exp\left(-0.69\frac{z_\ell}{z_h}\right)\left(\frac{\min\left(\theta_\ell, \theta_{fc,\ell}\right) - \theta_{ad,\ell}}{\theta_{fc,\ell} - \theta_{ad,\ell}}\right)^\sigma \tag{4.32}$$

where z_ℓ (m) is the mid-point of the depth of layer ℓ, the potential declines by 50% at z_h, θ_ℓ is water content in the layer, θ_{fc} as discussed above is field capacity, θ_{ad} is the air-dry water content so that soil water content cannot fall below this value, and σ is the coefficient used in the infiltration characteristics above, eqn (4.21).

The water available for evaporation in each layer is given by

$$H_{evap,\ell} = \mu_\ell\left(\theta_\ell - \theta_{fc,\ell}\right)\delta z_\ell \tag{4.33}$$

Potential evaporation is then defined as

$$E_{v,soil} = \left(1-f_g\right)\left(1-f_{g,litter}\right)E_v \tag{4.34}$$

The model then works through the layers starting at the top and removes water from each layer according to eqn (4.33) up to the potential limit given by (4.34).

This empirical approach captures the characteristics of soil evaporation restricted by the canopy and litter, as well as the reduction due to available soil water and depth of water in the soil.

4.7 Concluding remarks

A detailed account of the water dynamics has been presented. Evapotranspiration is based on the widely used Penman-Monteith equation and the details of prescribing the net radiation balance as well as canopy and boundary layer conductance have been discussed. A versatile treatment of soil water infiltration has been described that uses readily available soil hydraulic parameters. Likewise, the description of runoff is straightforward to parameterize.

Water balance is an interaction between a range of complex flows. The model structure should allow the user to explore these fluxes and so gain understanding into the underlying behaviour of the system.

4.8 References

Allen RG, Pereira LS, Raes D, and Smith M (1998). FAO irrigation and drainage paper no. 56: crop evapotranspiration. http://www.kimberly.uidaho.edu/ref-et/fao56.pdf

Campbell GS (1977). *An introduction to environmental biophysics*. Springer-Verlag, New York, USA.

Campbell GS and Norman JM (1998). *An Introduction to environmental biophysics*, second edition. Springer, New York, USA.

Johnson IR (2013). *PlantMod: exploring the physiology of plant canopies*. IMJ Software, Dorrigo, NSW, Australia.

Jones HG (1992). *Plants and microclimate*. Cambridge University Press, Cambridge, UK.

Monteith JL (1965). Evaporation and environment. *Symposium of the Society for Experimental Biology,* **19,** 205-234.

Monteith JL (1973). *Principles of environmental physics,* Edward Arnold, London.

Monteith JL & Unsworth MH (2008). *Principles of environmental physics,* third edition. Elsevier, Oxford, UK.

Penman HL (1948). Natural evaporation from open water, bare soil and grass. *Proceedings of the Royal Society of London, Series A*, **193,** 120-145.

Thornley JHM and France J (2007). *Mathematical models in agriculture*. CAB International, Wallingford, UK.

Thornley JHM and Johnson IR (2000). *Plant and Crop Modelling.* Reprint of 1990 Oxford University Press edition. www.blackburnpress.com.

5 Soil organic matter and nitrogen dynamics

5.1 Introduction

The soil nutrient dynamics component of this model includes organic matter turnover and inorganic nitrogen (N) mineralization or immobilization, movement in the soil (leaching), adsorption in the soil, and atmospheric losses. The turnover of organic matter (OM) is important both for the carbon balance of the system and also the mineralization and immobilization of inorganic N. The model requires the initial organic and inorganic status to be defined in order to start the simulation, which are defined graphically on the interface. For inorganic NO_3 that is subject to leaching it is common to find a bulge somewhere down the profile where N can accumulate through leaching. The interface allows the user to construct such a bulge for the initial status. The supply of organic matter is from litter (dead plant material), dung and dead roots. There are three soil organic matter pools (in addition to surface litter, dung and live roots): fast and slow turnover, and inert. The inert material does not decay but must be accounted for as it will show up in experimental measurements. The only source of organic matter to the inert pool is through fire. The organic matter and inorganic N dynamics of the model are illustrated schematically in Fig. 5.1. The model described here is relatively simple in structure compared with many other soil organic models, although it does capture the general processes involved.

Since measurements of soil nutrients are made much less frequently than those for soil water, care must be taken in data analysis. For example, the nitrification of ammonium (that is, the transformation from NH_4 to NO_3) is affected by water status and temperature. Since most organic matter is near the surface, and since organic matter breakdown involves the production of NH_4 which is then transformed to NO_3, the time at which these components are measured in relation to climatic conditions will be important. This is compounded by the fact that NO_3 leaches freely with water movement, whereas there is very little movement of NH_4. Furthermore, both volatilization and denitrification (atmospheric losses of NH_4 and NO_3 respectively) are very episodic and so are extremely difficult to measure.

In the analysis, all pool dynamics are defined for the same layer distribution as is used in the soil water dynamics. Organic matter is expressed as kg C m^{-3}, with the associated N component as kg N m^{-3}, and inorganic NO_3 and NH_4 have units kg N m^{-3}. However, on the model interface, percent is also used and, for the inorganic N, mg N kg^{-1} which is equivalent to parts per million (ppm).

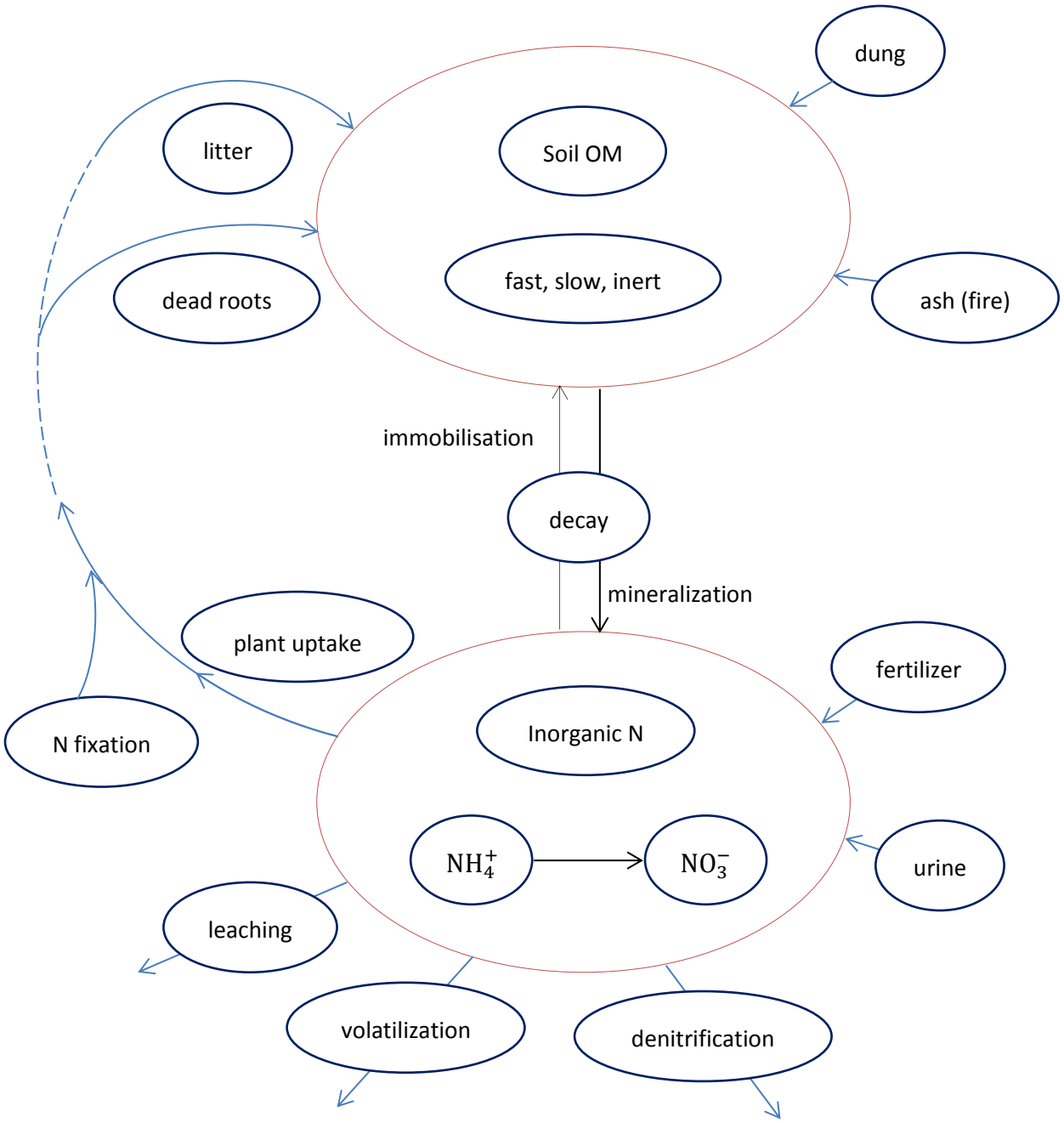

Figure 5.1: Schematic representation of the organic matter and nitrogen dynamics.

5.2 Organic matter dynamics

5.2.1 Overview

Soil organic matter dynamics are generally modelled by using pools of organic matter with different turnover rates. Early models of this type were developed by Van Veen & Paul (1981) and Van Veen *et al.* (1984, 1985), McCaskill and Blair (1988), Parton *et al.* (1988). Since then, the multi-pool approach has been extensively applied with well-known models being APSIM (Probert *et al.* 1998), RothC (Jenkinson 1990),

CENTURY (Parton *et al.* 1998), and SOCRATES (Grace *et al.,* 2006). A fundamental challenge with soil carbon models comprising several pools is that it is possible to get similar overall carbon dynamics with different rates of input and turnover, and so we must continually assess all aspects of the soil carbon dynamics in the model including the description of plant growth and senescence as it feeds into the soil carbon.

The approach in the present model has been to simplify the description of soil organic matter dynamics to include dynamic fast and slow turn-over pools, plus an inert component. The fast and slow pools are sometimes referred to as *particulate organic matter* and *humus soil carbon*. The inert carbon pool, which is essentially charcoal, is not subject to turnover. Keeping the model relatively simple avoids having to define a large number of parameters that are likely to have strong interactions and are difficult to estimate. The only parameters required are the decay rate constants for the fast and slow pools (proportion that decays per unit time), their efficiency of decay (proportion of carbon respired during decay), and the transfer rate from the fast to slow pool. The N concentration of the inputs are also required, and are calculated dynamically in the model. Soil carbon dynamics are also affected by temperature and soil water status. Soil carbon dynamics are driven by inputs from the plant material, and its digestibility.

5.2.2 Organic matter turnover

The model is illustrated in Fig. 5.2. There are two dynamic pools representing fast and slow turnover carbon, $W_{F,soil}$ and $W_{S,soil}$ kg C m^{-3}, and a third inert pool which is primarily charcoal. Note that SI units are used throughout the model, although results are converted to familiar units (such as t C ha^{-1} in the top 30cm soil). Inputs from dead plant material and dung are transferred to $W_{F,soil}$. This is subject to decay and also transfer to $W_{S,soil}$, which also decays but at a slower rate. During decay, carbon is respired as CO_2, with the remainder going to the fast turnover pool. Note that restricting the analysis to these three pools is consistent with current recommended measureable soil carbon pools (Skjemstad *et al.* 2004). Although the model only considers two dynamic pools, the decay characteristics of $W_{F,soil}$ are related to the digestibility of the inputs so that litter and dead roots from less digestible pastures will decay at a slower rate than more digestible inputs.

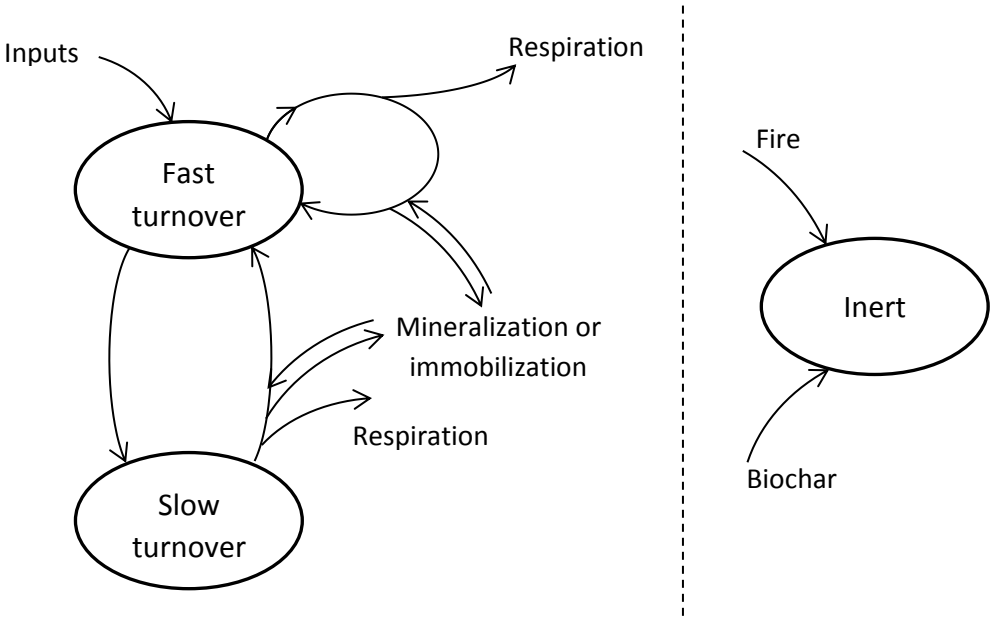

Figure 5.2. Overview of the soil carbon dynamics.

The process of breakdown involves utilization of carbon to produce microbial biomass with an associated respiratory loss. If the rate constant for pool decay is k, and the efficiency of breakdown Y, then for every kg of carbon in this pool that decays, the production of microbial biomass is Y kg with the remaining $(1-Y)$ being lost to respiration, as illustrated in Fig. 5.3. This general structure is applied to both the fast and slow turnover pools.

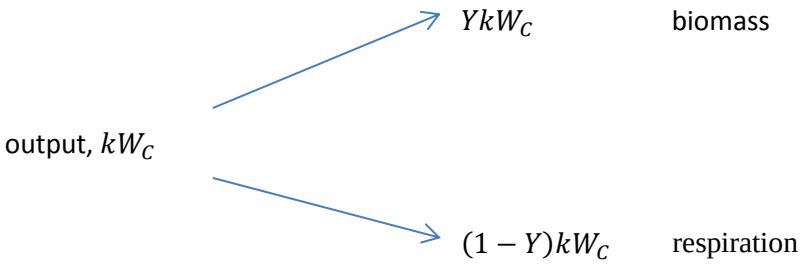

Figure 5.3: Schematic representation of OM breakdown. See text for details.

Denoting the carbon mass in the fast and slow turn-over pools by $W_{F,C}$ and $W_{S,C}$ kg C m^{-3} respectively, applying the general structure illustrated in Fig. 5.3, their dynamics are described by

$$\frac{\mathrm{d}W_{F,C}}{\mathrm{d}t} = I_C - k_{FS}W_{F,C} - k_F\left(1-Y_F\right)W_{F,C} + Y_S k_S W_{S,C} \tag{5.1}$$

$$\frac{\mathrm{d}W_{S,C}}{\mathrm{d}t} = k_{FS}W_{F,C} - k_S W_{S,C} \tag{5.2}$$

where k_F and k_S (d^{-1}) are the decay rates for the fast and slow pools, k_{FS} (d^{-1}) is the transfer coefficient for movement from the fast to slow pool, Y_F and Y_S are the dimensionless efficiencies of fast and slow organic matter decay, and I_C (kg C m^{-3} d^{-1}) is the rate of carbon input, and t (d) is time. The corresponding respiration is

$$R = \left(1-Y_F\right)k_F W_{F,C} + \left(1-Y_S\right)k_S W_{S,C} \tag{5.3}$$

Now consider the associated nitrogen dynamics. The decay of organic matter is assumed to be through digestion by biomass. The biomass pool is not modelled explicitly, and is taken to be part of the fast pool. Defining the N fraction of the biomass as $f_{B,N}$, kg N (kg C)$^{-1}$ which is taken to be a fixed quantity, and the corresponding N fractions for the pools as $f_{F,N}$ and $f_{S,N}$, which will be variables that depend on the inputs and decay parameters, the nitrogen dynamics corresponding to eqns (5.1) and (5.2) are

$$\frac{\mathrm{d}W_{F,N}}{\mathrm{d}t} = I_N - k_{FS}W_{F,N} - k_F W_{F,N}\left(1-Y_F\frac{f_{B,N}}{f_{F,N}}\right) + Y_S k_S \frac{f_{B,N}}{f_{S,N}} \tag{5.4}$$

$$\frac{\mathrm{d}W_{S,N}}{\mathrm{d}t} = k_{FS}W_{F,N} - k_S W_{S,N} \tag{5.5}$$

The associated N mineralization rate, which is the flux of N from the soil organic matter into the ammonium pool, is

$$M_N = k_F W_{F,N}\left(1-Y_F\frac{f_{B,N}}{f_{F,N}}\right) + k_S W_{S,N}\left(1-Y_S\frac{f_{B,N}}{f_{S,N}}\right) \tag{5.6}$$

If this is negative then immobilization of inorganic nitrogen occurs and it is assumed that this nitrogen can be supplied either from the NH_4 or NO_3 pools.

These relatively simple equations completely define the soil organic matter dynamics, including carbon assimilation and respiration as well as nitrogen mineralization or immobilization. I have used nitrogen fractions of organic matter and biomass rather than C:N ratios which are more common. The analysis is clearer to work with using fractions, although the C:N ratio is the inverse of the N fraction. Thus, the default value for $f_{B,N}$ is taken to be 1/8 which is equivalent to a C:N ratio in biomass of 8. In the simulations, results are shown as C:N ratios.

5.2.3 Effects of water and temperature

Organic matter dynamics are influenced by soil water status and temperature (eg Davidson *et al.*, 2000). The rate constants k_{FS}, k_F, k_S are defined by

$$k = \phi_H \phi_T k_{ref} \tag{5.7}$$

where ϕ_H and ϕ_T are dimensionless water and temperature functions respectively, and k_{ref} is a reference value for each of the rate constants defined at non-limiting soil water conditions and 20°C. Estimating these responses from experimental data is difficult owing to variation in the data.

It is assumed that soil biological processes are unrestricted by available water at water potentials greater than -100kPa (RE White, *personal communication*). Using the widely used Campbell water retention function (Campbell, 1974) to relate soil water content to potential, it is readily shown that for a wide range of soil types, the soil water content corresponding to -100kPa occurs close to the average of field capacity and wilting point. As in Chapter 4, which discusses water dynamics in detail, denote the volumetric soil water content by θ m^3 water $(m^3$ soil$)^{-1}$, with field capacity and wilting points θ_{fc} and θ_w respectively, so that the soil water content at -100kPa, θ_{100} can be approximated by

$$\theta_{100} = 0.5\left(\theta_w + \theta_{fc}\right) \tag{5.8}$$

A versatile equation for ϕ_H which is based on the temperature functions discussed in Section 1.35 in Chapter 1, which increases from zero to 1 over the soil water content 0 to θ_{100} is

$$\phi_H = \begin{cases} \left(\dfrac{\theta}{\theta_{100}}\right)^q \left(\dfrac{\theta_{fc} - \theta}{\theta_{fc} - \theta_{100}}\right)^p, & \theta \le \theta_{100} \\ 1, & \theta > \theta_{100} \end{cases} \tag{5.9}$$

where q is a curvature coefficient and

$$p = q\left(\frac{\theta_{fc} - \theta_{100}}{\theta_{100}}\right) \tag{5.10}$$

The temperature function, ϕ_T is taken to be given by eqn (1.41) in Section 1.35 of Chapter 1, with reference temperature 20°C.

ϕ_H and ϕ_T are illustrated in Fig. 5.4: the illustration for where ϕ_H is for generic soil hydraulic properties and that for where ϕ_T is for the model defaults parameter values.

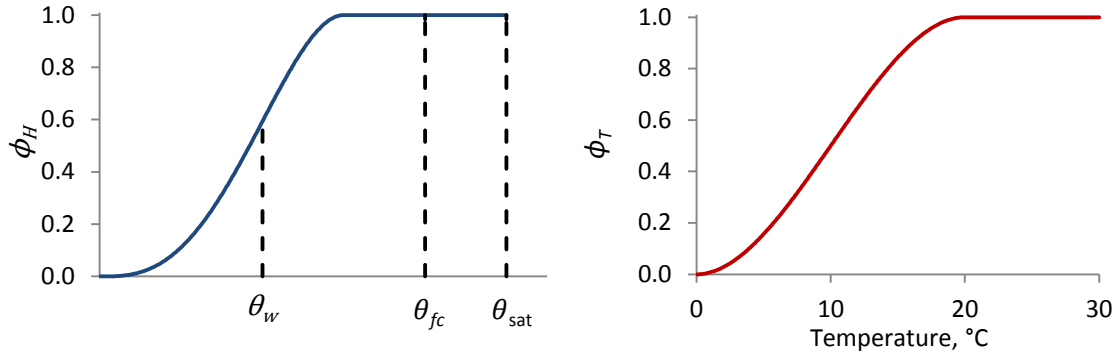

Figure 5.4: Soil water (left) and temperature (right) response functions ϕ_H and ϕ_T respectively. ϕ_H is shown for generic soil hydraulic properties, with $q = 3$ while the illustration for ϕ_T uses the model default values where both the reference and optimum temperatures are 20°C and the curvature coefficient is 2.

5.2.4 Influence of inputs on organic matter dynamics

Now consider the influence of the quality of organic matter inputs through plant and root senescence on organic matter dynamics. For each plant species, the digestibility of both the live and dead plant tissue is prescribed. The value for the dead material is taken to influence the decay coefficient, k_F, of the fast pool. This is done on a pro-rata basis, so that the decay coefficient on day t is related to the value on day t-1 by

$$k_{F,t} = \left[k_{F,ref} \Delta W_{C,in} \frac{\delta_{in}}{\delta_{ref}} + k_{F,t-1} W_{F,C} \right] \Big/ \left(W_{F,C} + \Delta W_{C,in} \right) \qquad (5.11)$$

where $W_{F,C}$ is the initial mass of carbon in the fast pool, $\Delta W_{C,in}$ is the carbon input with digestibility δ_{in}, δ_{ref} is a reference digestibility (taken to be 0.4), and k_{ref} is the reference decay rate for material with digestibility δ_{ref}.

It is assumed that the decay rates for the fast and slow pools are independent of soil type, whereas the transfer from the fast to slow pool is taken to be related to the soil clay fraction. Thus,

$$k_{FS} = k_{FS,ref} \frac{\gamma}{\gamma_{ref}} \qquad (12)$$

where γ is the clay fraction and γ_{ref} is a reference value so that $k_{FS} = k_{FS,ref}$ when $\gamma = \gamma_{ref}$. By default, γ_{ref}=0.3. In the model, the actual clay fraction is defined in the water module.

This completely defines the soil organic matter dynamics including carbon accumulation and respiration, N mineralization and immobilization, and the influence of soil water, temperature, and quality of inputs. The decay rate of the fast turnover pool will decline with decreasing quality of organic matter inputs, as defined by digestibility.

5.2.5 Half-life and mean-residence time

The above analysis is formulated in terms of decay rates, k d^{-1}, that is proportion per day, for the soil organic matter pools. These decay rates are generally very small – for example, the model defaults for the fast and slow turnover pools are 10^{-3} and 4×10^{-5} d^{-1}. However, these parameters do not lend themselves to intuitive biophysical interpretation. For linear decay systems of the form used here, where the time course of pool W with decay coefficient k, with no inputs to the system, is

$$\frac{\mathrm{d}W}{\mathrm{d}t} = -kW \tag{5.13}$$

which has solution

$$W = W_0 e^{-kt} \tag{5.14}$$

where W_0 is the initial value of W. This is, of course, exponential decay. The *half-life*, h, is the time taken for W to reach half its initial value, and is simply given by

$$h = \frac{\ln(2)}{k} = \frac{0.69}{k} \tag{5.15}$$

h has units that are the reciprocal of k and so, in the present model, h has units of d. For pools with slow turnover, it is common to convert this to years: for example, the default value of 4×10^{-5} d^{-1} for the slow turnover pool is equivalent to 47.5 years. The model interface presents the half-lives for the fast turnover pool as days and slow turnover pool as years.

Mean residence time (MRT) is also used. This again is derived from exponential decay in refers to the mean time that an element, or constituent, of the pool remains in the pool, and is given by

$$r = \frac{1}{k} \tag{5.16}$$

so that

$$r = \frac{h}{0.69} \tag{5.17}$$

Thus the terms are linearly related.

My preference is for half-life and this is used in the present model.

5.2.6 Initialization

The organic matter pools need to be initialized at the start of the simulation. There are three generic default soil organic matter types referred to as 'Low OM', 'Medium OM' and 'High OM' which refer to the initial organic matter status. Initial values for the fast and slow turnover pools, as well as the inert pool, are defined for the top and base of the soil profile, along with a curvature and depth for 50% decline. The interface then displays the organic matter to 30 cm as t C ha^{-1} as well as a percentage value. The C:N ratio of each pool is also defined, along with the value for the biomass. The default initial soil carbon distribution for the 'Medium OM' default soil type is shown in Fig. 5.5

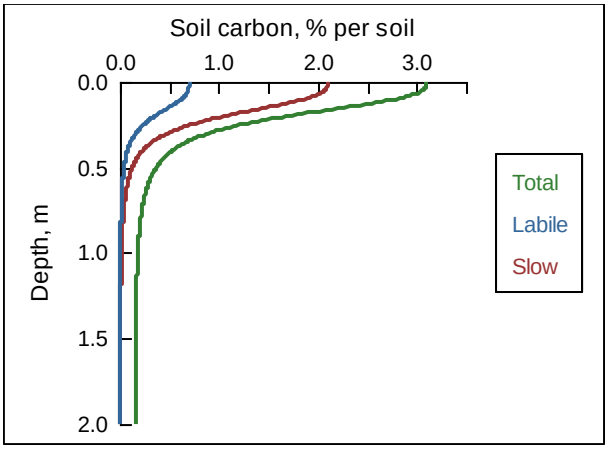

Figure 5.5: Initial soil carbon distribution for the default 'Medium OM' soil type. The 'labile' pool is the fast turnover pool. Note that the inert carbon is not shown as it does not affect carbon dynamics.

5.2.7 Illustration

System dynamics will, of course, depend on climate, plant growth and organic matter inputs to the soil, and variation in soil water content. Also, since soil carbon dynamics generally have low decay rates the influence of initial conditions, in particular the mass of soil organic matter in the soil, may influence the simulations for many years or decades. To demonstrate the general behaviour of the model, a simple simulation is available on the model interface for fixed soil water and temperature effects and constant organic matter inputs. This simulation is illustrated for the default 'Medium OM' soil (see the program interface), a combined impact of soil water and temperature given by

$$\phi_H \phi_T = 0.5 \tag{5.18}$$

and a daily input of 15 kg dwt ha (10cm)$^{-1}$ d^{-1} with C:N ratio 25 and digestibility 0.4. The soil carbon percent and C:N ratio are shown in Fig. 5.6 where the simulation has been run for 3650 days (approximately 10 years)

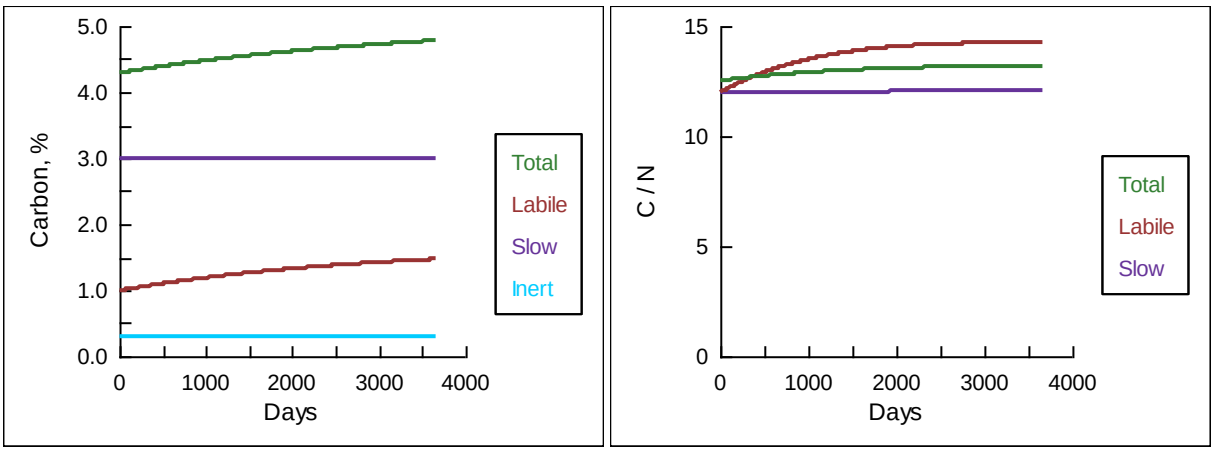

Figure 5.6: Sample simulation for soil organic matter dynamics under constant conditions as discussed in the text. Left: soil carbon percent of each pool as well as the total. Right: C:N ratio of the total, fast (labile) and slow turnover pools. Note that the C:N ratio of the inert pool, which has default value 30, is not shown.

5.2.8 Surface litter and dung

Surface litter and dung turnover dynamics are treated the same as the fast turnover soil organic matter pool. As litter and dung decay, carbon is respired with that remaining being transferred to the fast turnover pool in the surface soil layer. The scale function of water, ϕ_H is also taken to be that of the surface layer. Individual decay rate and efficiency parameters for litter and dung are defined on the model interface.

There is also physical incorporation of litter and dung into the soil. Again, this follows linear dynamics with incorporation rates being defined for both the litter and dung.

Surface litter is treated exactly the same as organic matter as described above, but with the following considerations:

- It is assumed that the turnover rate for litter is half that of soil organic matter. This is because of lower microbial levels.
- The water content in the surface soil layer is used in the expression for the effect of water status on litter turnover – that is $g(\theta)$ in the above analysis.
- There is a physical transfer of litter from the soil surface to the soil.

The depth to which litter can be transported and the rate constant for this transfer (proportion per day) are prescribed. Litter is then transferred evenly to this depth at this rate.

5.3 Inorganic nutrient dynamics

5.3.1 Overview

Plants acquire N from the inorganic NO_3 and NH_4 pools. The mineralization, and possibly immobilization, through organic matter dynamics has been described above. The other processes in the model are inputs from fertilizer or urine, nitrification of ammonium, gaseous losses of N through denitrification of nitrate and volatilization of ammonium, leaching and plant uptake. N uptake by the plants is described in the Chapter 3, Section 3.5.

5.3.2 Nitrogen inputs

Nitrogen inputs can occur from urine or fertilizer. Urea inputs from fertilizer or urine are assumed to be hydrolyzed immediately and incorporated in the surface soil NH_4 pool, although some details apply. Fertilizer inputs of nitrate or ammonium are transferred directly to the relevant surface inorganic N pool.

The partitioning of nutrients between dung and urine may play an important role in nutrient dynamics and the associated plant response, since urine returns are readily available whereas for dung the process of organic matter decay delays the release. This partitioning is discussed in Chapter 6. Urine N inputs are transferred directly to the soil NH_4 pool. While nutrient dynamics in urine patches are likely to differ from the bulk soil due to the greater concentrations of nutrient in the patches, no explicit treatment for urine patch dynamics is considered here. For urine inputs, the user specifies a maximum depth and scale factor to distribute nutrient inputs.

5.3.3 Nitrification of ammonium

Nitrification of ammonium, which is the conversion of NH_4 to NO_3 is described using a Michaelis-Menten response to available soil ammonium, so that the rate of nitrification is

$$\zeta = V_{mx,NH_4}\left(\frac{[NH_4]}{[NH_4]+K_{NH_4}}\right)\phi_H\phi_T\gamma_C \tag{5.19}$$

where $[NH_4]$ is the ammonium concentration in the soil, mg N kg^{-1}, V_{mx,NH_4} is the maximum rate of nitrate production, mg N kg^{-1} day^{-1}, K_{NH_4} is the NH_4 concentration for half maximal response to ammonium concentration, the ϕ functions are the water and temperature responses that are discussed I section 5.2.3 above, and γ_C represents the effect of soil microbial mass as described below.

According to this approach, the nitrification rate is linear in response to available soil ammonium at low concentrations and then curves to an asymptote as the concentration increases. It is apparent from (5.19) that at low concentrations

$$\zeta \approx \frac{V_{mx,NH_4}}{K_{NH_4}}[NH_4]\phi_H\phi_T\,\gamma_C \tag{5.20}$$

The default parameters are

$$V_{mx,NH_4} = 1 \text{ mg N kg}^{-1}\text{ day}^{-1} \text{ and } K_{NH_4} = 100 \text{ mg N kg}^{-1} \tag{5.21}$$

The response with no limitations due to temperature, water or carbon is shown in Fig. 5.7.

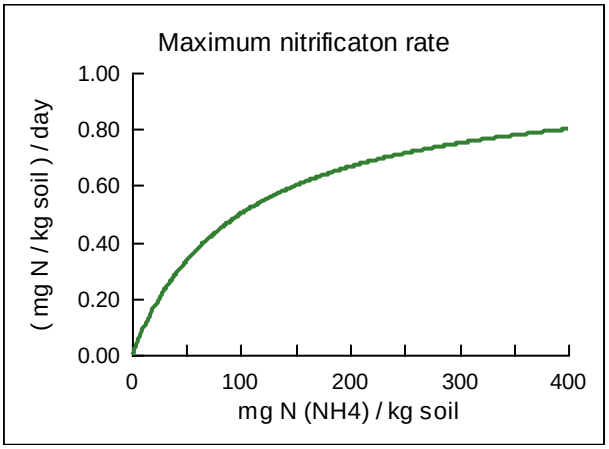

Figure 5.7: The rate of nitrification as a function of available soil ammonium for non-limiting water, temperature and carbon conditions as defined in eqn (5.19) with parameters in eqn (5.21) and $\phi_H = \phi_T = 1$ – see text for discussion.

Since there is no direct treatment of the soil microbial pool, it is assumed that the labile soil carbon (fast turnover) reflects the level of microbes, so that

$$\gamma_{C,L} = \frac{\left[W_{f,C}(L)\right]}{\left[W_{f,C,ref}\right]} \tag{5.22}$$

where L represents the soil layer, and [.] indicates mg kg^{-1}. The reference soil carbon concentration in the fast turnover pool is

$$\left[W_{f,C,ref}\right] = 5000\,\text{mg kg}^{-1} \equiv 0.5\% \tag{5.23}$$

5.3.4 Denitrification of nitrate

Denitrification is the conversion of nitrate to nitrous oxide and nitrogen gas and, while the actual denitrification losses may be relatively small in terms of the overall nitrogen dynamics in the system, the fact that nitrous oxide is such a major greenhouse gas (the CO_2 equivalent value is currently taken to be 310), care must be taken with these calculations. It is generally assumed that denitrification responds to temperature in an analogous manner to nitrification but that, since it is an anaerobic process, it only occurs in wet soils and increases towards saturation. Furthermore, as the soil gets wetter, there is a shift from losses from N_2O to N_2. In addition, as this is a microbial process, it is necessary to include the effect of soil microbial mass. The dynamics of denitrification are now considered.

Denitrification is described using Michaelis-Menten dynamics for the response to available nitrate. As for nitrification, denitrification is also related to temperature and soil water, and can be written as:

$$\rho = V_{mx,NO_3}\left(\frac{[NO_3]}{[NO_3] + K_{NO_3}}\right)\phi_T f_\rho(\theta)\gamma_C \qquad (5.24)$$

where $[NO_3]$ is the concentration of NO_3 in the soil layer, mg N kg^{-1}, V_{mx,NO_3} is the maximum rate of nitrate production, mg N kg^{-1} day^{-1}, K_{NO_3} is the NO_3 concentration for half maximal response to nitrate concentration, ϕ_T is the temperature response function discussed in Section 5.2.3 above, $f_\rho(\theta)$ is the water response function , and γ_C again represents the effect of soil microbial mass as described by eqn (5.22). The default parameters are:

$$V_{mx,NO_3} = 0.1 \text{ mg N kg}^{-1} \text{ day}^{-1} \text{ and } K_{NO_3} = 20 \text{ mg N kg}^{-1} \qquad (5.25)$$

and the rate of denitrification with these parameters is shown in Fig. 5.8.

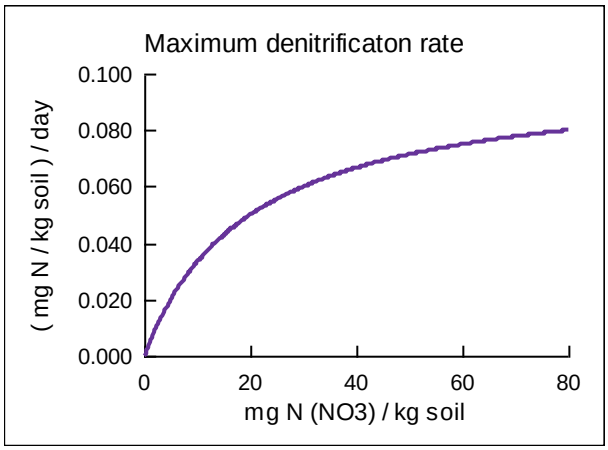

Figure 5.8: Rate of denitrification, eqn (5.24) with the parameters in eqn (5.25).

The effect of water is a bit more complex and is an area that can have important implications on the calculations of denitrification. The following approach is designed to allow flexibility in exploring the effects of soil water content on denitrification. Water filled pore space rather than volumetric soil water content is used, which is defined as

$$\phi = \frac{\theta}{\theta_{sat}} \qquad (5.26)$$

where (as usual) θ is the volumetric soil water content and θ_{sat} is the saturated water content. According to this definition, ϕ ranges between 0 (no water in the soil, which is generally not possible) to 1 at saturation. It is now assumed that the water function, $f_\rho(\theta)$, in eqn (5.24) is given by

$$f_\rho(\theta)=\begin{cases}\sin\left(\frac{\pi}{2}\left(\frac{\phi-\phi_{mn,dn}}{1-\phi_{mn,dn}}\right)^{q_\rho}\right), & \phi\geq\phi_{mn,dn};\\ 0, & \phi<\phi_{mn,dn}.\end{cases} \tag{5.27}$$

where q_ρ is a curvature coefficient. The default parameters are

$$\phi_{mn,dn}=0.6 \text{ and } q_\rho=2. \tag{5.28}$$

The partitioning of denitrification between N_2O and N_2 is defined according to the scheme described by Granli and Bockman (1994) according to which by assuming that:

- initially as the soil wets up all losses are to N_2O – this occurs between $\phi_{mn,dn}$ and ϕ_{mn,N_2}
- as the soil gets wetter there is a linear shift towards N_2 losses – this occurs between ϕ_{mn,N_2} and ϕ_{mn,N_2O}
- at water contents greater than ϕ_{mn,N_2O} all denitrification losses are as N_2.

Granli and Bockman (1994) described these dynamics qualitatively and for the present model I have adopted the following mathematical scheme, whereby the functions for partitioning total denitrification $f_v(\theta)$ into N_2O and N_2 components, $f_{v,N_2O}(\theta)$ and $f_{v,N_2}(\theta)$ respectively, are given by

$$\begin{aligned}f_{v,N_2O}(\theta)&=\lambda f_v(\theta),\\ f_{v,N_2}(\theta)&=(1-\lambda)f_v(\theta),\end{aligned} \tag{5.29}$$

where

$$\lambda=\begin{cases}1, & \phi_{mn,dn}\leq\phi\leq\phi_{mn,N_2},\\ \frac{\phi_{mx,N_2O}-\phi}{\phi_{mx,N_2O}-\phi_{mn,N_2}}, & \phi_{mn,N_2}\leq\phi\leq\phi_{mx,N_2O},\\ 0, & \phi\geq\phi_{mx,N_2O}.\end{cases} \tag{5.30}$$

The default parameters are

$$\phi_{mn,N_2}=0.7 \text{ and } \phi_{mx,N_2O}=0.9, \tag{5.31}$$

with $\phi_{mn,dn}$ prescribed in (5.28).

The full denitrification function, with partitioning between N_2O and N_2 is illustrated in Fig. 5.9

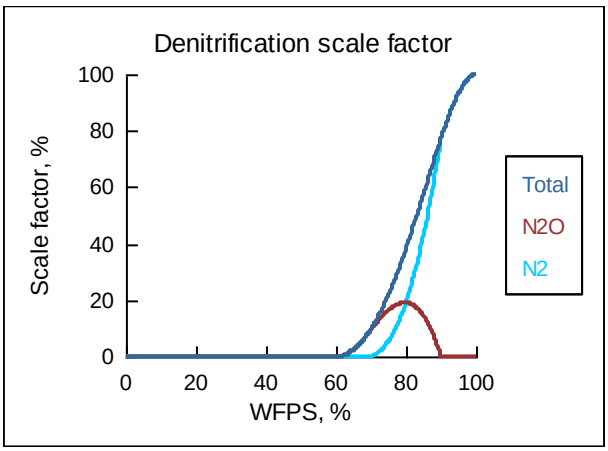

Figure 5.9: Total N denitrification function, including N_2O and N_2 components, as functions of water filled pore space, with parameters given by eqns (5.28), (5.31).

It is interesting to note that with this treatment of denitrification, soils with field capacity close to saturation may be susceptible to more denitrification than soils where there is quite a difference between saturation and field capacity. For example, if the saturated water content is 55% and field capacity is 45%, then field capacity occurs at a WFPS of 80% which means that denitrification occurs at field capacity and below (down to WFPS of 60% with the defaults here). Alternatively, if the field capacity is 30%, then this corresponds to a WFPS of 54%, and denitrification will not occur. This means that once the soils are wet, those soils with field capacity greater than the cut-off WFPS for denitrification may have greater rates of denitrification.

A characteristic of the mathematical treatment is that by changing the exponent q_ρ, not only does the shape of the total denitrification curve change, but so does the partitioning. This is illustrated in Fig. 5.10 which shows the responses for $q_\rho = 1$ and $q_\rho = 3$.

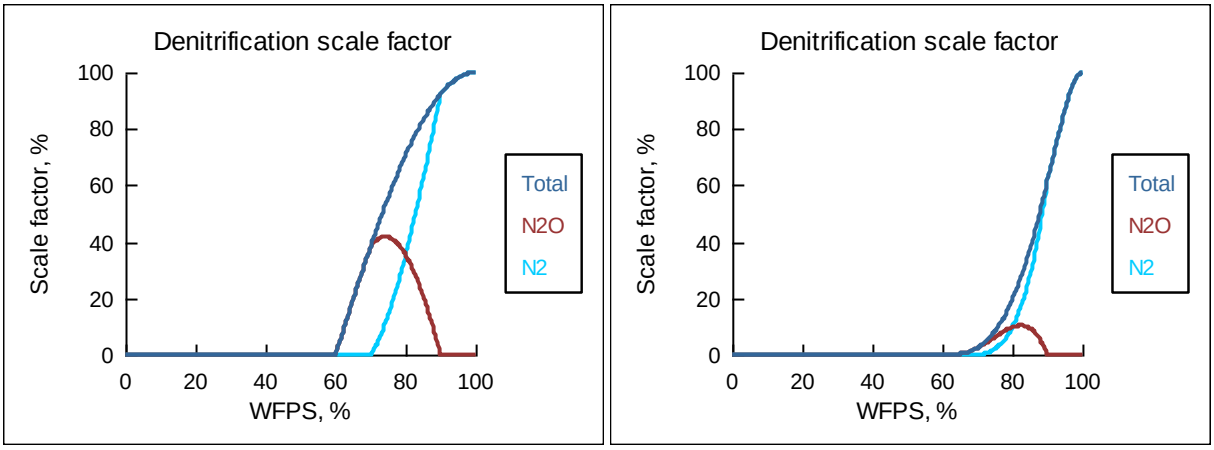

Figure 5.10: Total N denitrification function, along with the N_2O and N_2 components, corresponding to Fig. 5.9, but with $q_\rho = 1$ (left) and 3 (right). See text for details.

The empirical approach used here for partitioning denitrification into N_2O and N_2 components captures the general characteristics described by Granli and Bockman (1994) and is quite straightforward to implement in terms of parameters that have direct biophysical interpretation.

5.3.5 Volatilization of ammonium

Volatilization, the conversion of ammonium to ammonia gas, mainly occurs from urine patches, from urea fertilizer shortly after application, and from the bulk soil ammonium pool in the top soil layer. Volatilization is assumed to occur in relation to evapotranspiration, E_{ET} mm d^{-1}, and the scale parameter

$$\xi = \max\left(0, \frac{E_{ET} - R}{E_{ET,ref}}\right) \tag{5.32}$$

where R mm d^{-1} is the daily rainfall and $E_{ET,ref}$ is a reference evapotranspiration rate with default value

$$E_{ET,ref} = 5 \text{ mm d}^{-1} \tag{5.33}$$

Volatilization from urea inputs either from fertilizer or urine, denoted by Ω_{urea} kg N m^{-2} d^{-1} is assumed to be given by

$$\Omega_{urea} = \xi \omega_{urea} U_N \tag{5.34}$$

where U_N, kg N m^{-2} d^{-1}, is the daily urea N input and ω_{urea} is a dimensionless parameter that defines the proportion of urea N lost as volatilization with default value.

$$\Omega_{urea} = 0.2 \tag{5.35}$$

According to this approach, urea N losses to volatilization are proportional to the inputs and evapotranspiration in excess of rainfall.

Volatilization from the surface layer of the bulk soil NH_4 pool is treated in a similar way and is taken to be

$$\Omega_{NH4} = \xi \omega_{NH4} W_{NH4,1} \tag{5.36}$$

where, $W_{NH4,1}$ kg N m^{-2}, is the inorganic NH4 in the surface soil layer and, again, ω_{NH4} is a dimensionless parameter with default value

$$\omega_{NH4} = 0.01 \tag{5.37}$$

which is equivalent to 1% per day.

5.3.6 Nutrient adsorption

Nutrient adsorption is a key component in the movement of nutrients through the profile: nitrate does not adsorb and so is prone to leaching, whereas for many soil types most of the ammonium is adsorbed and so is less likely to leach, although this may not be true for very sandy soils. Note that in this section, all analysis uses SI units – that is kg rather than mg – although solute concentrations are generally discussed in mg nutrient (kg soil)$^{-1}$ or mg nutrient L^{-1} for solution in water. Mixing units can create problems with the analysis and, while these are not insurmountable, it is better practice to use SI units and make conversions at the end. The following analysis is general for any inorganic nutrient that is subject to adsorption and so the analysis is described for any inorganic nutrient. Indeed, much of the work in this field has been done for phosphorous.

Two commonly applied approaches for describing nutrient adsorption are to use either the Freundlich equation or the Langmuir equation.

The Freundlich equation is a power law, as given by:

$$C_a = \lambda C_s^q \tag{5.38}$$

where, for any nutrient nu, C_a is the nutrient concentration in the soil, kg nu (kg soil)$^{-1}$, C_s is the nutrient concentration in solution, kg nu (kg water)$^{-1}$, a and s refer to adsorbed and solution respectively, and λ and q are empirical parameters, with q usually in the range 0.4 to 0.5 for a wide range of soils. Note that the reciprocal of q is sometimes used.

The Langmuir equation is a form of the rectangular hyperbola, and can be written as:

$$C_a = \frac{\alpha C_{a,mx} C_s}{\alpha C_s + C_{a,mx}} \tag{5.39}$$

where α [kg nu (kg soil)$^{-1}$] [kg nu (kg water)$^{-1}$]$^{-1}$ is the initial slope of the curve at low values of C_s, and $C_{a,mx}$ kg nu (kg soil)$^{-1}$ is the maximum adsorption capacity of the soil at saturation. The parameters can be expressed mathematically as:

$$C_a \to \alpha C_s \text{ as } C_s \to 0, \text{ and } C_a \to C_{a,mx} \text{ when } C_s >> \alpha C_s. \tag{5.40}$$

With either of these equations, the analysis relates adsorbed to solution nutrient concentrations. However, since the model defines total inorganic nutrient mass, it is necessary to calculate each of these components from the total. An advantage of the rectangular hyperbola is that it allows analytical solution of the individual concentrations in terms of the total nutrient in the soil, whereas the use of the power law, eqn (5.38), requires a numerical approach. A second advantage is that the linear characteristic of the adsorption curve at low nutrient levels is generally more realistic. Figure 5.11 shows the rectangular hyperbola eqn (5.39) fitted to the data of Moody and Bolland. (1999) for phosphorous adsorption in three contrasting soils, and it can be seen that the curve gives a good fit to each data set.

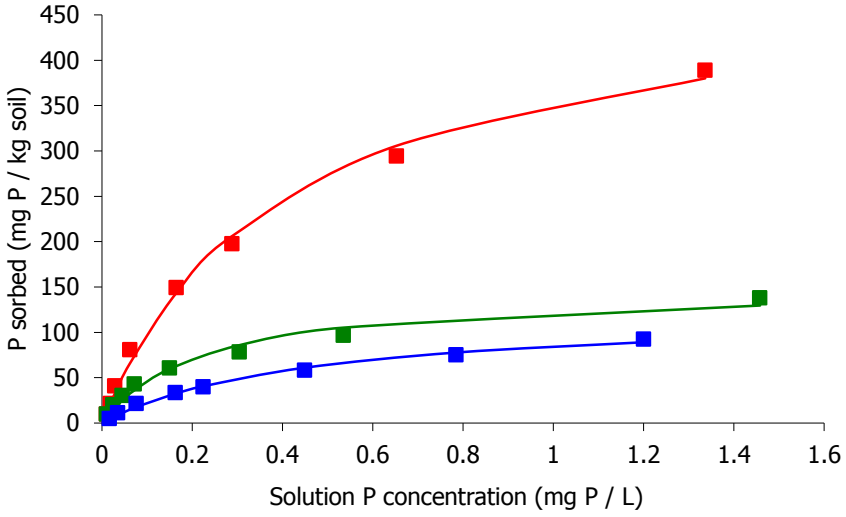

Figure 5.11: Phosphorous sorption curves using eqn (5.39) along with data from Moody and Bolland (1999) for a Ferrosol (red), Vertosol (green), Podosol (blue).

The parameters for the soil types in Fig. 5.7 are

	α (soln / sorbed at low P)	$C_{a,mx}$ (max P sorption capacity)
Ferrosol	1225	495
Vertosol	661	150
Podosol	270	123

Equation (5.39) is used in the model to define the sorption characteristics of NH_4 – it is assumed that NO_3 does not adsorb and is all in solution. The default values for NH_4 adsorption are

$$\alpha = 1000 \text{ adsorbed NH4 concentration } \left(\text{solution NH4 concentration}\right)^{-1}$$
$$C_{a,mx} = 500 \text{ mg NH4 } \left(\text{kg soil}\right)^{-1} \tag{5.41}$$

The NH_4 sorption curve with default parameters is shown for in Fig 5.12.

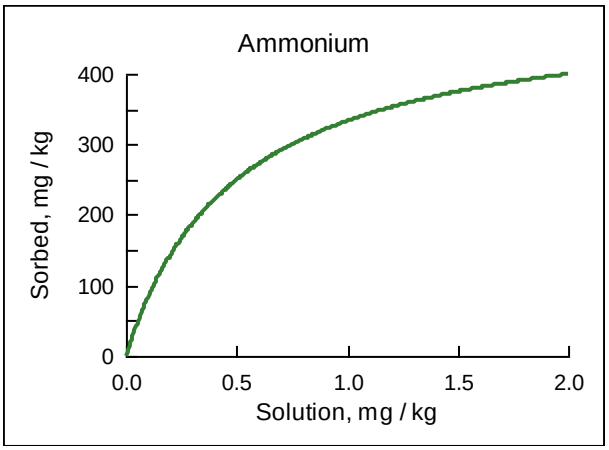

Figure 5.12: Solution NH_4 as a function of sorbed NH_4 using eqn (5.39) with default parameters given by eqn (5.41).

The analysis for deriving the sorbed and solution nutrient components from the total nutrient content of any soil layer is now presented. This analysis is presented for any generic nutrient, nu, although only NH_4 is considered in the model at present. If the mass of nutrient in any layer of depth Δz (m) is M kg nu m^{-2}, then the adsorbed and solution components are

$$M_a = C_a \, \Delta z \, \rho_b \tag{5.42}$$

and

$$M_s = C_s \, \Delta z \, \theta \, \rho_w \tag{5.43}$$

where ρ_b, kg soil m^{-3} is the soil bulk density, ρ_w, kg water m^{-3} is the density of water, and θ (m^3 water) (m^3 soil)$^{-1}$ is the volumetric soil water content, and

$$M = M_a + M_s \tag{5.44}$$

is the total mass of nutrient in the layer.

It now remains to calculate the concentration components in terms of the total nutrient mass. Writing

$$m = M / \Delta z \tag{5.45}$$

it is readily shown that

$$\alpha\theta\rho_w C_s^2 + \left[C_{a,mx}\left(\alpha\rho_b + \theta\rho_w\right) - \alpha m\right] C_s - m C_{a,mx} = 0 \tag{5.46}$$

which is a quadratic equation for C_s as a function of m. While this has two solutions, one of them is always negative, and so the positive solution defines C_s: it is simple to calculate this solution.

In the model, plant uptake is described in terms of total inorganic nutrient and not the actual solution component. While nutrient in solution is the source for the plant, there is a continual flux from sorbed sites

to the solution. It is likely that the roots are physically close to the soil particles so that the nutrient concentration in the region near the roots may well differ from that in the bulk soil water. Furthermore, for NH_4 (highly adsorbing), the actual nutrient in solution at any particular time is only sufficient for a few hours growth, so that there is a continual flux from sorbed to solution to the plant. The principal role of nutrient adsorption in the model is in the description of nutrient leaching, with plant uptake being described in relation to total nutrient. Consequently, N leaching will be dominated by the flux of NO_3 which is assumed not to adsorb.

5.3.7 Nutrient leaching

It is assumed that nutrients in solution can move with the water as the water moves through the soil profile. Thus, in the in the soil water infiltration and redistribution dynamics discussed in Chapter 4, Section 4.4, the proportion of water moving from one layer to the next in each sub-daily time-step, Δt d^{-1} is calculated and the corresponding proportion of solution nutrient that moves is taken to be the same.

5.4 Concluding remarks

The treatment of soil nutrients has covered organic and inorganic dynamics, leaching, nitrogen transformations, and gaseous nitrogen losses. The aim has been to avoid unnecessary complexity and yet to encapsulate the key processes.

Care must be taken in analysing soil nutrient data since, the observed data for variables such as organic carbon or inorganic nutrient concentration result from a series of fluxes. Since different combinations of these fluxes can lead to similar system state variables, attention should focus on the fluxes and not just the state variables. For example, if the rate of root growth and senescence is greater than actually occurs, but the rate of organic matter turnover is also greater than occurs, then the actual soil organic matter values from the model may agree well with observational data. Similarly, if the observations and data differ, then this could be due either to errors in estimates of inputs to the pools or to fluxes out of the pools.

The study of soil nutrient dynamics is particularly complex since data are often hard to obtain due to the slow turnover rates that are involved. The model provides a sound structure for analysing nutrient dynamics, and for interpreting observational data.

5.5 References

Campbell GS (1974). A simple model for determining unsaturated conductivity from moisture retention data. *Soil Science*, **117,** 311 – 314.

Davidson EA, Verchot LV, Cattanio, JH, Ackerman, IL, Carvalho JEM (2000). Effects of soil water content on soil respiration in forests and cattle pastures of eastern Amazonia. *Biogeochemistry* **48,** 53-69.

Grace PR, Jeffrey JN, Robertson GP, Gage SH (2006). SOCRATES—A simple model for predicting long-term changes in soil organic carbon in terrestrial ecosystems. *Soil Biology & Biochemistry* **38,** 1172–1176.

Granli T and Bockman OC (1994). Nitrous oxide from agriculture.

Nor. J. Agric. Sci. (Suppl. 12): 128 Jones CA, Cole AN, Sharpley AN, and Williams JR (1984). A simplified soil and plant phosphorus model: 1. Documentation. *Soil Science Society of America Journal.* **48,** 800-805.

Karpinets TV, Greenwood DJ, and Ammons JT (2004). Predictive mechanistic model of soil phosphorus dynamics with readily available inputs. *Soil Science Society of America Journal.* **68,** 644-653.

McCaskill MR (1987). *Modelling S, P and N Cycling in Grazed Pastures.* PhD Thesis, University of New England, Armidale, NSW, Australia.

McCaskill MR, and Blair GJ (1988). Development of a simulation model of sulfur cycling in grazed pastures. *Biogeochemistry* **5,** 165-181.

Moody PW and Bolland MDA (1999). Phosphorus. In *Soil analysis: an interpretation manual*. (Eds KI Peverill, LA Sparrow, DJ Reuter) pp. 187–220. (CSIRO Publishing: Melbourne)

Parton WJ, Steward JBW, Cole CV (1988). Dynamics of C, N, P and S in grassland soils: a model. *Biogeochemistry* **5,** 109-131.

Parton WJ, Stewart JWB, Cole CV (1998). Dynamics of C, N, P and S in grassland soils: a model. *Biogeochemistry* **5,** 109-131.

Probert ME, Dimes JP, Keating BA, Dalal RC, Strong WM (1998). APSIM's water and nitrogen modules and simulation of the dynamics of water and nitrogen in fallow systems. *Agricultural Systems* **56(1),** 1-28.

Skjemstad, JO, Spouncer, LR, Cowie, B, Swift, RS (2004) Calibration of the Rothamsted organic carbon turnover model (RothC ver. 26.3), using measurable soil organic carbon pools. *Australian Journal of Soil Research* **42,** 79-88.

Thornley JHM (1998). *Grassland Dynamics, An Ecosystem Simulation Model.* CAB International, Wallingford, UK.

Thornley JHM and Johnson IR (2000). *Plant and Crop Modelling.* www.blackburnpress.com.

Van Veen JA, Paul EA (1981). Organic carbon dynamics in grassland soils. 1. Background information and computer simulation. *Canadian Journal of Soil Science* **61,** 185-20.

Van Veen JA, Ladd JN, Frissel MJ (1984). Modelling C and N turnover through the microbial biomass in soil. *Plant and Soil* **76,** 257-74.

Van Veen JA, Ladd JN, Amato M (1985). Turnover of carbon and nitrogen through the microbial biomass in a sandy loam and a clay soil incubated with C-14 glucose and N-15 ammonium sulfate under different moisture regimes. *Soil Biology and Biochemistry* **17,** 747-56.

6 Animal growth and metabolism

6.1 Introduction

Animal growth and metabolism is obviously a central component of DairyMod and the SGS Pasture Model. Animal processes are modelled at different levels of complexity, ranging from detailed ruminant nutrition models to simple growth curve response (for a discussion see Thornley and France, 2007). Detailed models of rumen metabolism, while offering an understanding of processes such as animal response to feed composition (e.g., Baldwin et al., 1987; Dijkstra et al., 1992; Dijkstra, 1994; Baldwin, 1995; Gerrits et al., 1997; Thornley and France, 2007), may be too complex to be readily parameterized for different animal types and breeds, or to apply routinely in biophysical pasture simulation models. Similarly, describing animal growth directly with growth functions, such as the Gompertz equation, may give a reliable description of experimental data, but this approach alone cannot be applied directly to conditions of variable available pasture. For a whole-system biophysical model, striking a balance among complexity, realism, and versatility allows the model to be applied quite readily to different animal breeds and respond dynamically to pasture availability and quality.

The present model is based on the animal growth model described by Johnson *et al.* (2012) and is adapted to pregnancy and lactation, as well as responses to combined pasture, concentrate, mixed ration and forage feed supply. It is an energy-driven model of animal growth and metabolism that has been developed specifically to be appropriate for a whole-system biophysical pasture simulation model.

The model describes animal growth and energy dynamics for cattle and sheep in response to available energy, and includes body protein, water, and fat. Model parameters have direct physiological interpretation, which facilitates prescribing parameter values to represent different animal species and breeds. Animal protein weight is taken to be the primary indicator of metabolic state, while fat is regarded as a potential source of metabolic energy for physiological processes, such as the resynthesis of degraded protein. The growth of protein is defined using a Gompertz equation, which is widely used in animal modelling for sigmoidal growth responses, and was discussed in Section 1.3.6 in Chapter 1. Fat growth is secondary and depends on current protein weight, as well as maximum potential fat fraction of body weight (BW), which varies throughout the growth of the animal as defined by total BW. Protein is subject to turnover. Therefore, maintaining current protein reserves requires the resynthesis of degraded proteins. This maintenance, along with the energy required for activity, takes precedence over growth of new tissue. New growth of fat depends on current protein weight, as well as the maximum potential fat fraction of BW, with this maximum varying throughout the growth of the animal. While the Gompertz equation could also be used to describe fat growth as done by Emmans (1997), the present approach allows the model to be adapted to respond to restricted energy intake by viewing fat as a stored source of energy. Therefore, body composition during growth and at maturity is determined by available energy with (as will be seen) reduced fat fraction generally occurring when energy is restricted. The release of energy reserves from fat during lactation is an important aspect of energy dynamics, particularly in dairy cows, and details are presented describing the priority for milk production following parturition.

Animal intake in response to available pasture and pasture quality is described, as well as intake from supplementary feeding in relation to quality. The composition of pasture, silage, hay or concentrate during animal intake have a direct effect on animal growth and metabolism, including lactation, as well as nutrient dynamics and the nitrogen contents of dung and urine. The model is formulated using standard information on feed composition, and parameters relating to the energy dynamics in the animal, including methane emissions during fermentation and the energy costs of dung and urine.

Energy dynamics in the animal are affected by the digestibility of the feed and also include costs for excreted urine N and dung. The metabolic energy of feed is therefore also related to diet quality and N composition and this is calculated in the model.

6.2 Body composition during growth

Denoting empty BW by W kg, and protein, water, and fat components by W_P, W_H, W_F kg respectively, these are related by

$$W = W_P + W_H + W_F \tag{6.1}$$

The ash component of BW is not specifically included as it is generally a small proportion of the total and is proportional to protein (Williams, 2005). It is assumed that water and protein weights are in direct proportion, so that

$$W_H = \lambda W_P \tag{6.2}$$

where λ is a dimensionless constant. Thus, eqn (6.1) becomes

$$W = (1+\lambda) W_P + W_F \tag{6.3}$$

The ratio of water to protein is assumed to be different for sheep and cattle (Johnson *et al.*, 2012) and default values are

$$\begin{aligned} &\text{sheep:} \quad \lambda = 3.5 \\ &\text{cattle:} \quad \lambda = 3 \end{aligned} \tag{6.4}$$

Protein is the primary component of growth with fat being related to protein. Defining body fat fraction as

$$f_F = \frac{W_F}{W} \tag{6.5}$$

kg fat (kg empty BW)$^{-1}$, eqns (6.3) and (6.5) can be combined to give the individual protein, water, and fat components as

$$\begin{aligned} W_P &= \left(\frac{1-f_F}{1+\lambda}\right) W; \\ W_H &= \lambda \left(\frac{1-f_F}{1+\lambda}\right) W; \\ W_F &= f_F W. \end{aligned} \tag{6.6}$$

Body fat fraction is generally seen to increase with BW (e.g., Fox and Black, 1984; Lewis and Emmans, 2007). Normal growth conditions are defined as those under which intake is sufficient for potential protein growth and associated fat growth, with the corresponding fat fraction at maturity denoted by $f_{F,mat,norm}$. It is assumed that during growth, the normal fat fraction increases linearly so that

$$f_{F,norm} = \frac{W_{F,norm}}{W} = f_{F,b} + \left(f_{F,mat,norm} - f_{F,b}\right)\left(\frac{W_{norm} - W_b}{W_{mat,norm} - W_b}\right) \tag{6.7}$$

where W_b, kg, is the birth weight, $f_{F,b}$ is the fat fraction at birth and subscripts mat and $norm$ refer to 'mature' and 'normal'. Combining eqns (6.3) and (6.7) gives a quadratic equation for $W_{F,norm}$ as a function of W_P, which is

$$aW_{F,norm}{}^2 + bW_{F,norm} + c = 0 \tag{6.8}$$

where the coefficients are

$$\begin{aligned} a &= \left(\frac{f_{F,mat,norm} - f_{F,b}}{W_{mat,norm} - W_b} \right) \\ b &= \left(f_{F,b} - 1 \right) + a\left[2W_P \left(1 + \lambda \right) - W_b \right] \\ c &= f_{F,b} W_P \left(1 + \lambda \right) + aW_P \left(1 + \lambda \right)\left[W_P \left(1 + \lambda \right) - W_b \right] \end{aligned} \tag{6.9}$$

which is solved in the standard way, with the physiologically valid solution being

$$W_{F,norm} = \frac{1}{2a}\left(-b - \sqrt{b^2 - 4ac} \right) \tag{6.10}$$

to give the normal fat weight, $W_{F,norm}$, as a function of current protein weight, W_P, the birth fat fraction, $f_{F,b}$, and the normal mature fat fraction, $f_{F,mat,norm}$.

For growth above normal, BW increases are entirely in the form of fat so that at maximum mature BW, $W_{mat,max}$, the protein weight is the same as that at normal mature BW, and hence

$$\left(1 - f_{F,mat,norm} \right) W_{mat,norm} = \left(1 - f_{F,mat,max} \right) W_{mat,max} \tag{6.11}$$

where $f_{F,mat,max}$ is the maximum fat fraction at maximum mature empty BW, $W_{mat,max}$, which gives

$$W_{mat,max} = \left(\frac{1 - f_{F,mat,norm}}{1 - f_{F,mat,max}} \right) W_{mat,norm} \tag{6.12}$$

for $W_{mat,max}$ in terms of the normal mature BW and corresponding prescribed fat fractions, so that $W_{mat,max}$ is a derived quantity and not a prescribed parameter. With the default values for cattle and sheep (see below), the mature maximum weight is 27% and 12% greater than the normal for cattle and sheep respectively. Finally, during growth, the ratio of the maximum fat component of empty BW to that during normal growth is taken to be constant, so that

$$W_{F,max} = \frac{f_{F,mat,max}}{f_{F,mat,norm}} \left(\frac{1 - f_{F,mat,norm}}{1 - f_{F,mat,max}} \right) W_{F,norm} \tag{6.13}$$

These equations completely define the normal and maximum empty BW during growth, as well as the water and fat components, in terms of the fat fractions at birth, normal mature weight, and maximum mature weight ($f_{F,b}$, $f_{F,mat,norm}$, $f_{F,mat,max}$, respectively) in terms of the current protein weight (W_P) and normal mature weight ($W_{mat,norm}$).

Default body fat composition parameters for sheep and cattle are:

$$\begin{aligned} &\text{cattle:} \quad f_{F,b} = 0.06, \quad f_{F,mat,norm} = 0.3, \quad f_{F,mat,max} = 0.45 \\ &\text{sheep:} \quad f_{F,b} = 0.1, \quad f_{F,mat,norm} = 0.25, \quad f_{F,mat,max} = 0.33 \end{aligned} \tag{6.14}$$

with units kg fat (kg BW)$^{-1}$.

Values for birth weights (used below) and normal mature weights will vary between different animal types and breeds, with the default values in the model being

$$\begin{aligned} &\text{cattle:} \quad W_b = 50 \text{ kg}, \quad W_{mat,norm} = 600 \text{ kg} \\ &\text{sheep:} \quad W_b = 6 \text{ kg}, \quad W_{mat,norm} = 60 \text{ kg} \end{aligned} \tag{6.15}$$

6.3 Growth and energy dynamics

For potential protein growth, the net accumulation of protein, which includes protein synthesis and degradation, is assumed to be defined by the Gompertz equation (see Section 1.3.6 in Chapter 1), which can be written

$$\frac{\mathrm{d}W_P}{\mathrm{d}t} = \mu W_P \mathrm{e}^{-Dt} \tag{6.16}$$

where t (d) is time, μ (d^{-1}) is the initial specific growth rate for W_P, and D (d^{-1}) is a parameter defining the decay with time of the specific growth rate. This equation has solution

$$W_P = W_{P,b} \exp\left[\frac{\mu\left(1-\mathrm{e}^{-Dt}\right)}{D}\right] \tag{6.17}$$

where $W_{P,b}$ is the initial, or birth, protein mass. The mature, or asymptotic, protein weight is

$$W_{P,mat} = W_{P,b}\mathrm{e}^{\mu/D} \tag{6.18}$$

so that

$$D = \frac{\mu}{\ln\left(W_{P,mat}/W_{P,b}\right)} \tag{6.19}$$

Although eqn (6.17) is an analytical solution for W_P through time for potential growth, the model needs to address the situation where intake demand is not satisfied, and so it is convenient to write eqn(6.16) for protein growth rate as a rate-state equation so that it is independent of time. This is readily derived by eliminating the term e^{-Dt} by using eqn (6.17) giving

$$\frac{\mathrm{d}W_P}{\mathrm{d}t} = DW \ln\left(\frac{W_{P,mat}}{W_P}\right) \tag{6.20}$$

For more details, see Section 1.3.6 in Chapter 1. According to this formulation, the Gompertz equation for W_P is written in terms of its final value, $W_{P,mat}$, and parameter D, eqn (6.19), which depends on the initial value $W_{P,b}$ and growth coefficient μ. The default values for μ are

$$\begin{aligned} &\text{cattle:} \quad \mu = 0.012 \text{ d}^{-1} \\ &\text{sheep:} \quad \mu = 0.04 \text{ d}^{-1} \end{aligned} \tag{6.21}$$

with $W_{P,b}$ evaluated from eqn (6.6).

In the following analysis, energy costs associated with growth are calculated according to the standard approach whereby if the energy content of body tissue is ε MJ kg^{-1} and the efficiency of growth is Y, then the energy required per unit growth, E MJ kg^{-1}, is

$$E = \frac{\varepsilon}{Y} \tag{6.22}$$

The corresponding energy lost as heat during the synthesis of 1 kg due to respiration, R MJ kg^{-1}, is

$$R = \varepsilon\left(\frac{1-Y}{Y}\right) \tag{6.23}$$

where heat loss is accompanied by respiration of CO_2. Default values for energy contents and efficiencies for protein and fat synthesis are

$$\begin{aligned} &\text{protein:} \quad \varepsilon_P = 23.6 \text{ MJ kg}^{-1}, \quad Y_P = 0.48 \\ &\text{fat:} \quad\quad\ \varepsilon_F = 39.3 \text{ MJ kg}^{-1}, \quad Y_F = 0.71 \end{aligned} \tag{6.24}$$

with the same values being used for sheep and cattle. See Johnson *et al.* (2012) for a discussion of the derivation of these values. It can be seen that the energy costs of synthesising 1 kg of protein, excluding the costs of resynthesis of degraded protein and fat are 49.2 and 55.4 MJ kg^{-1}, respectively. However, because protein growth also is associated with accumulation of body water (as discussed later), increasing total BW by 1 kg with no actual fat growth requires substantially less energy. Therefore, it is important when discussing the energy cost of growth to be clear as to the composition of the growth. As the animal grows from birth to maturity, the fat composition generally increases and so the overall energy required per unit of total BW gain will increase, as found by Wright and Russell (1984).

Once potential protein and fat growth are known, as well as energy costs for the resynthesis of degraded protein and activity costs, the actual growth is calculated in relation to available energy intake. Under restricted intake, fat catabolism may occur in order to supply energy for other processes.

Using eqn (6.22), the daily energy cost (MJ d^{-1}) associated with protein growth as given by eqn (6.20) is

$$E_{P,g,req} = \frac{\varepsilon_P}{Y_P}\frac{\mathrm{d}W_P}{\mathrm{d}t} \tag{6.25}$$

It is assumed that protein is subject to continual breakdown, with linear decay rate k_P d^{-1}, so that the protein decay rate is

$$k_P W_P \tag{6.26}$$

and the energy required to resynthesis this protein (MJ d^{-1}) is

$$E_{P,maint,req} = \frac{1}{Y_P}\varepsilon_P k_P W_P \tag{6.27}$$

Default values for k_p are

$$\begin{aligned} &\text{cattle:} \quad k_p = 0.023 \text{ d}^{-1} \\ &\text{sheep:} \quad k_p = 0.03 \text{ d}^{-1} \end{aligned} \tag{6.28}$$

Also, it is assumed that not all energy is released to the animal metabolic energy pool during protein decay, but that some is lost as heat. Denoting this by $Y_{P,d}$, during protein decay the energy returned to the energy pool is

$$E_{P,d} = Y_{P,d}\varepsilon_P k_P W_P \tag{6.29}$$

while the remainder of the energy is lost as heat, with the default value

$$Y_{p,d} = 0.9 \tag{6.30}$$

Combining eqns (6.27) and (6.29), the net energy required for protein resynthesis (MJ d^{-1}) is

$$E_{P,maint,net,req} = E_{P,maint,req} - E_{P,d}$$
$$= \left(\frac{1}{Y_P} - Y_{P,d} \right) k_P \varepsilon_P W_P \quad (6.31)$$

which is referred to as the protein maintenance energy requirement.

Now consider the growth of the fat component where it is assumed that

$$\frac{\mathrm{d}W_F}{\mathrm{d}t} = k_{F,g} W_P \left(1 - \frac{W_F}{W_{F,max}} \right) \quad (6.32)$$

where $k_{F,g}$, kg fat (kg protein)$^{-1}$ d^{-1}, is a fat growth parameter, with default values

$$\begin{aligned} &\text{cattle:} \quad k_{F,g} = 0.03 \text{ kg fat } (\text{kg protein})^{-1} \text{ d}^{-1} \\ &\text{sheep:} \quad k_{F,g} = 0.2 \text{ kg fat } (\text{kg protein})^{-1} \text{ d}^{-1} \end{aligned} \quad (6.33)$$

According to this equation, fat growth approaches the current potential maximum ($W_{F,max}$) asymptotically, with fat growth potential being directly related to current protein weight, W_P, so that absolute potential fat growth increases as protein weight increases. Fat growth potential is related to protein weight because of the assumption that metabolic state is defined by protein weight.

The energy required for fat growth, $E_{F,g,req}$ (MJ d^{-1}), is, using eqn (6.22)

$$E_{F,g,req} = \frac{\varepsilon_F}{Y_F} \frac{\mathrm{d}W_F}{\mathrm{d}t} \quad (6.34)$$

The final energy component to be included is that associated with animal physical activity, which is assumed to be given by

$$E_{act} = \alpha_{act} W \quad (6.35)$$

(MJ d^{-1}) where parameter α_{act} MJ kg^{-1} d^{-1} is the energy requirement for animal activity per unit of BW. Increasing this parameter will be appropriate, for example, for animals on hilly terrain. The default value for both sheep and cattle is

$$\alpha_{act} = 0.025 \text{ MJ kg}^{-1} \text{ d}^{-1} \quad (6.36)$$

so that, for example, with a 600 kg steer E_{act}=15 MJ d^{-1}, whereas for a 60 kg sheep, it is 1.5 MJ d^{-1}. While other maintenance costs such as maintaining body temperature are not specifically included, these could be included in this term if necessary.

Combining protein maintenance costs, eqn (6.31) with (6.35), gives the total maintenance energy requirement as

$$E_{maint,req} = E_{P,maint,net,req} + E_{act} \quad (6.37)$$

Equation (6.32) for the potential fat growth rate allows body fat to accumulate to the maximum. The actual energy required to grow to normal fat weight during time Δt (d) is simply

$$E_{F,g,norm,req} = \frac{\varepsilon_F}{Y_F} \left(\frac{W_{F,norm} - W_F}{\Delta t} \right) \quad (6.38)$$

where, for a daily time-step model, Δt=1 d. Of course, this will only be satisfied if

$$E_{F,g,norm,req} \le E_{F,g,req} \tag{6.39}$$

Similarly, to grow to maximum fat weight, the energy required is

$$E_{F,g,max,req} = \frac{\varepsilon_F}{Y_F}\left(\frac{W_{F,max} - W_F}{\Delta t}\right) \tag{6.40}$$

with

$$E_{F,g,max,req} \le E_{F,g,req} \tag{6.41}$$

Finally, the energy required for normal growth is

$$E_{req,norm} = E_{P,g,req} + E_{maint,req} + E_{F,g,norm,req} \tag{6.42}$$

and for maximum growth

$$E_{req,max} = E_{P,g,req} + E_{maint,req} + E_{F,g,max,req} \tag{6.43}$$

6.4 Model solution in relation to available energy

The model described so far, describes growth rates for protein, the associated water and fat, as well as the corresponding energy costs. In practice, growth is dictated by available energy and the theory is now applied to this more general situation. Equations (6.25) and (6.34) define the energy required for prescribed protein and fat growth rates, but they can be inverted to define growth rates in relation to available energy, that is

$$\frac{\mathrm{d}W_P}{\mathrm{d}t} = E_{P,g,avail}\frac{Y_P}{\varepsilon_P}; \quad E_{P,g,avail} \le E_{P,g,req} \tag{6.44}$$

and

$$\frac{\mathrm{d}W_F}{\mathrm{d}t} = E_{F,g,avail}\frac{Y_F}{\varepsilon_F}; \quad E_{F,g,avail} \le E_{F,g,req} \tag{6.45}$$

Forward differences with a daily time-step are used to calculate protein and fat components on day t (d) to their values and growth rates on day t-1 according to

$$\begin{aligned} W_{P,t} &= W_{P,t-1} + \Delta t\frac{\mathrm{d}W_{P,t-1}}{\mathrm{d}t} \\ W_{F,t} &= W_{F,t-1} + \Delta t\frac{\mathrm{d}W_{F,t-1}}{\mathrm{d}t} \end{aligned} \tag{6.46}$$

where Δt is the time-step with

$$\Delta t = 1 \text{ d} \tag{6.47}$$

Three sets of circumstances are now considered where the available intake energy, E_{in} (MJ d^{-1}), exceeds requirements for normal growth, is less than or equal to that for normal growth, but exceeds maintenance requirements, or is less than maintenance requirements.

6.4.1 E_{in} exceeds requirements for normal growth

If the available energy from intake, E_{in}, exceeds requirements for normal growth then

$$E_{req,norm} < E_{in} \le E_{req,max} \tag{6.48}$$

Protein growth and all maintenance costs are met, with any remaining energy being used for fat growth, so that

$$\begin{aligned} E_{maint} &= E_{maint,req} \\ E_{P,g} &= E_{P,g,req} \\ E_{F,g} &= E_{in} - \left(E_{P,g} + E_{maint} \right) \end{aligned} \tag{6.49}$$

with $E_{P,g}$ and $E_{F,g}$ being used in eqns (6.44) to (6.47) to calculate $W_{P,t}$ and $W_{F,t}$.

6.4.2 E_{in} is between maintenance requirement and normal growth requirement

Under these circumstances

$$E_{maint} \le E_{in} < E_{req,norm} \tag{6.50}$$

and it is assumed that maintenance costs are met with the remainder of the available energy being fat and growth, so that growth is reduced. The energy available for growth is partitioned between protein and fat on a *pro-rata* basis according to requirement, so that

$$\begin{aligned} E_{maint} &= E_{maint,req} \\ E_{P,g} &= \left(E_{in} - E_{maint,req} \right) \left(\frac{E_{P,g,req}}{E_{P,g,req} + E_{F,g,norm,req}} \right) \\ E_{F,g} &= \left(E_{in} - E_{maint,req} \right) \left(\frac{E_{P,g,req}}{E_{P,g,req} + E_{F,g,norm,req}} \right) \end{aligned} \tag{6.51}$$

and, again, $E_{P,g}$ and $E_{F,g}$ are used in eqns (6.44) to (6.47) to calculate $W_{P,t}$ and $W_{F,t}$.

6.4.3 E_{in} is less than maintenance requirement

These animals do not have sufficient energy to grow, with all available energy being used for activity and maintenance. For this scenario, ME intake is constrained by

$$E_{in} < E_{maint,req} \tag{6.52}$$

and fat catabolism can occur.

As for fat growth, fat catabolism is assumed to be related to animal protein weight, which is an indication of its metabolic state, and also related to available body fat. Therefore, it is assumed that the maximum rate of fat catabolism is given by

$$\Delta F_{d,mx} = k_{F,d} W_P \left(\frac{W_F - W_{F,mn}}{W_{F,mx} - W_{F,mn}} \right) \tag{6.53}$$

(kg fat d^{-1}) where $k_{F,d}$ [kg fat (kg protein)$^{-1}$ d^{-1}] is a fat decay parameter, so that the maximum daily rate of fat catabolism is equivalent to the fraction $k_{F,d}$ of total protein weight at maximum fat composition. During breakdown, there will be some energy lost as heat and so taking the efficiency of breakdown to be $Y_{F,d}$, the ME available from fat catabolism is

$$E_{F,d,mx} = Y_{F,d} \varepsilon_F \Delta F_{d,mx} \tag{6.54}$$

Default values for cattle and sheep are

$$k_{F,d} = 0.005 \text{ kg fat } (\text{kg protein})^{-1} \text{ d}^{-1} \quad Y_{F,d} = 0.95 \tag{6.55}$$

The actual daily fat catabolism is now simply

$$E_{F,d} = \min\left(E_{F,d,mx}, E_{m,req} - E_{in}\right) \tag{6.56}$$

so that maintenance costs will be satisfied if there is sufficient energy available from fat catabolism, otherwise the maximum energy available from fat will be utilized for partial satisfaction of maintenance requirements.

According to this approach, if available energy from intake and fat catabolism does not meet maintenance requirements there will be a reduction in protein weight and less activity. The reduction in activity is consistent with reduced grazing. Note that fat catabolism does not occur to support new protein growth, only the maintenance of existing protein.

6.5 Illustrations of animal growth dynamics

The following illustrations are presented to demonstrate the overall characteristics of the model as applied to the growth of cattle and sheep. These illustrations are also discussed by Johnson *et al.* (2012).

The first set of illustrations consider growth and body composition for cattle and sheep under maximum growth conditions, which allows us to compare the model results with observations summarised by Fox and Black (1984) for cattle and Lewis and Emmans (2007) for sheep. In these papers the authors collated experimental data and summarised relationships between body components with fitted empirical curves. Summarising large amounts of experimental data in this way is one of the primary applications of empirical models, as discussed by Thornley and France (2007). The default body composition and growth parameters presented in the previous section have been selected based on these empirical responses, although the specific mathematical formulation of those responses have not been used in the present model structure.

Figure 6.1 shows total empty BW growth, as well as protein, water, and fat components for sheep and cattle for maximum growth. It should be noted that Fox and Black (1984) fitted polynomial curves for protein, water, and fat as functions of total weight, whereas Lewis and Emmans (2007) related water and fat to protein by using allometric equations. Consequently, the figures show the fitted curves for each body component for cattle, but only water and fat for sheep. It can be seen from these figures that there is virtually complete agreement between the present model and the curves that have been fitted to data, to the extent that the dashed lines representing the data are largely obscured by the model responses. Apart from this agreement, the general shapes of the responses are consistent with expected characteristics.

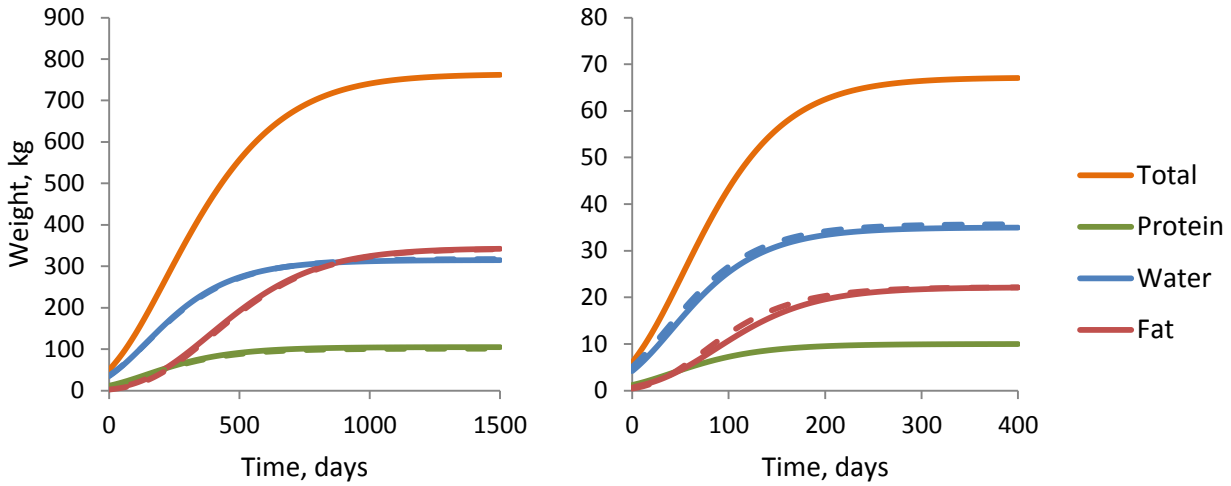

Figure 6.1: Empty BW and composition for cattle (left and sheep (right) from birth to maturity for maximum growth. The solid lines are the model and the broken lines are the regression curves derived by Fox and Black (1984) for cattle and Lewis and Emmans (2007) for sheep. Fox and Black reported protein, water, and fat as functions of BW, while Lewis and Emmans gave fat and water as functions of protein. Note that the model and observed response curves are virtually identical and the response curves (broken lines) are almost completely obscured by the model (solid lines).

The energy dynamics for cattle and sheep, corresponding to the growth characteristics in Fig. 6.1, are illustrated in Fig. 6.2. It can be seen that energy requirement for protein growth peaks earlier than that for fat growth, but as the requirements for protein growth decline the cost of protein maintenance increases and reaches a greater value than the peak cost for new protein growth. In addition, maximum energy requirement occurs prior to the animal reaching its maximum weight. Energy costs for the resynthesis of degraded protein are considerably greater than activity costs, although this behaviour depends on the choice of parameters for the protein degradation rate k_P and activity costs, α_{act}. One characteristic difference apparent from Fig 6.2 is that the relative amount of energy required for maintenance is greater in cattle than sheep.

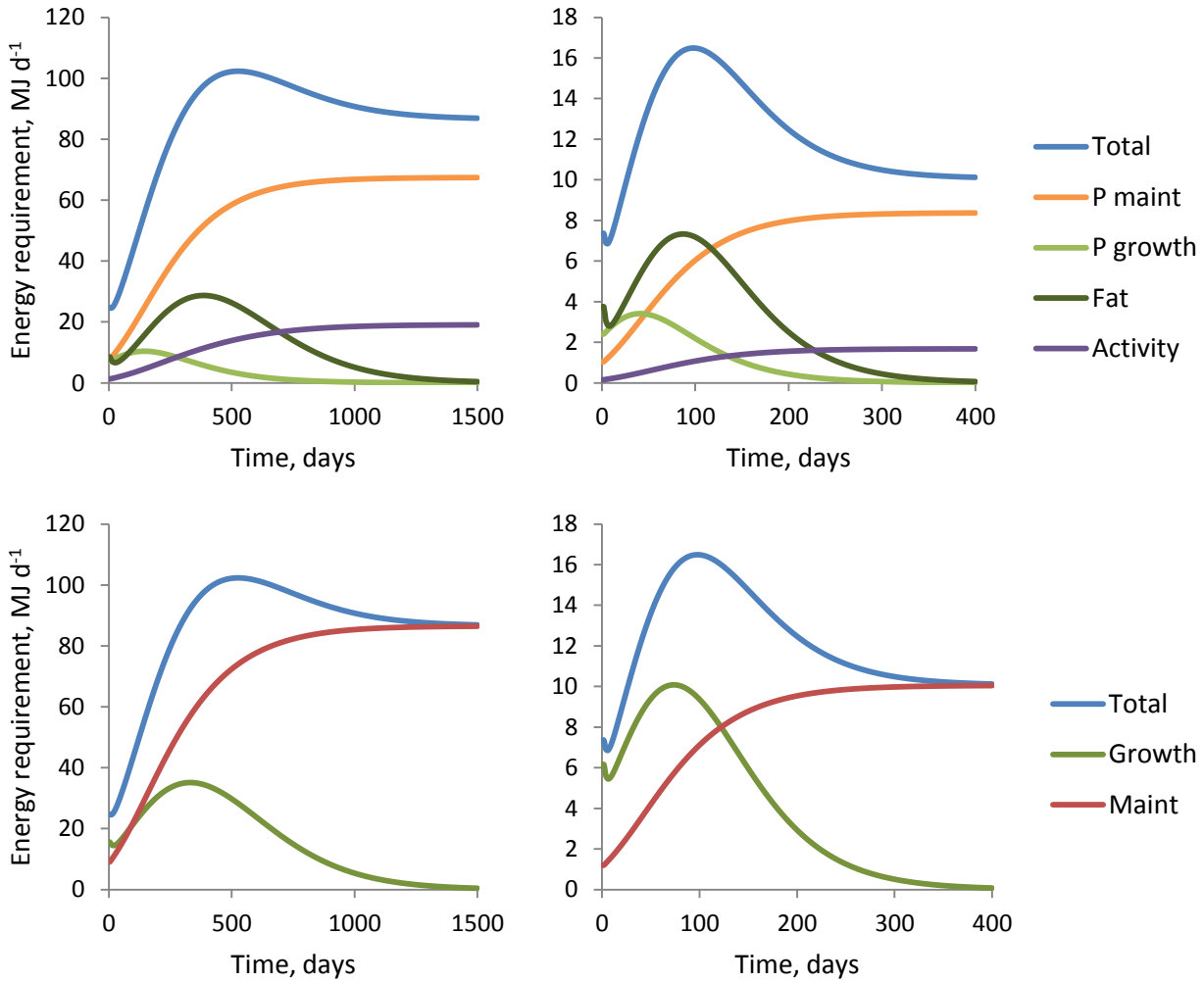

Figure 6.2: Top: growth energy dynamics for cattle (left) and sheep (right) from birth to maturity, corresponding to Fig. 6.1. The total energy required, as well as the individual requirements for protein growth, protein maintenance, fat growth, and activity are indicated. Bottom: the combined growth and maintenance components are shown. Note the different scales for cattle and sheep.

It is instructive to look at energy dynamics in relation to BW as well as through time. The responses for growth, maintenance and total energy required, corresponding to Fig. 6.2, are shown in Fig. 6.3. There is a non-linear relationship between the energy required for maintenance and total empty BW, which is often characterised by an empirical allometric response. Although not shown here, this response is very similar to the bodyweight raised to the power between 0.73 and 0.75, which is widely used in feed evaluation systems and simulation models (ARC, 1981; Finlayson et al., 1995; National Research Council, 2001).

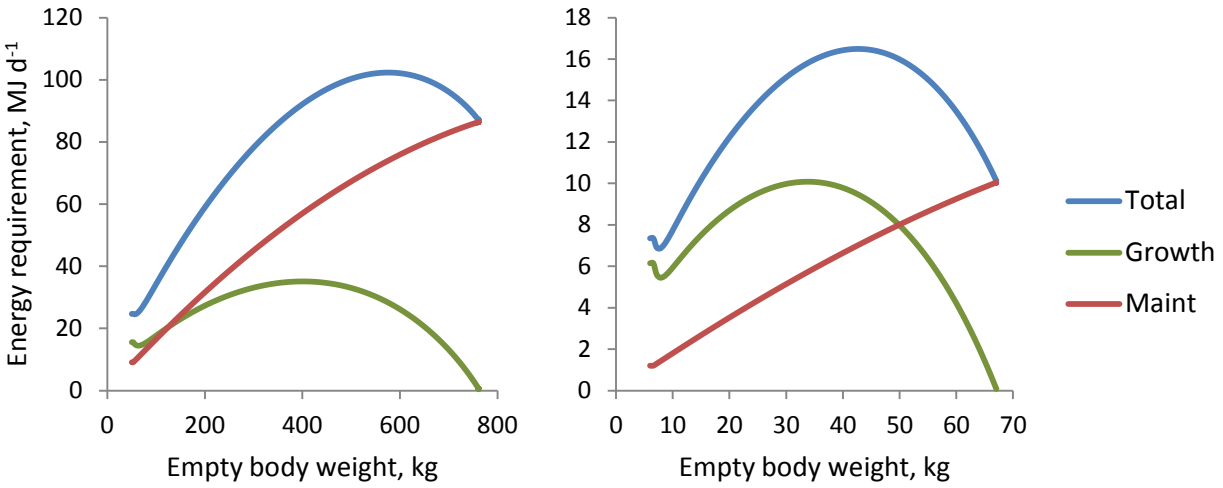

Figure 6.3: Total energy requirements, and the growth and maintenance components as functions of empty body weight, for cattle (left) and sheep (right), corresponding to Fig. 6.2.

The analysis so far has considered growth under optimal conditions of non-limiting intake as defined by E_{req}, eqn (6.43) and now consider the situation where intake does not satisfy maximum demand. It may be neither desirable nor practical for animals to grow to their absolute maximum, due to restricted feed or the fact that maximum body fat may only be achieved through supplementary feeding. The illustrations in Fig. 6.4 show animal growth with energy intake at maintenance plus 100%, 90%, 80%, 70% of potential growth (protein and fat) energy requirement during animal growth, as given by eqn (6.42). The results are as expected with growth being reduced under restricted intake. For example, the time to reach half mature BW at full intake is 270 d for cattle and 70 d for sheep whereas with 70% intake requirement it is 342 d and 99 d, which correspond to increases of 27% and 41%, respectively.

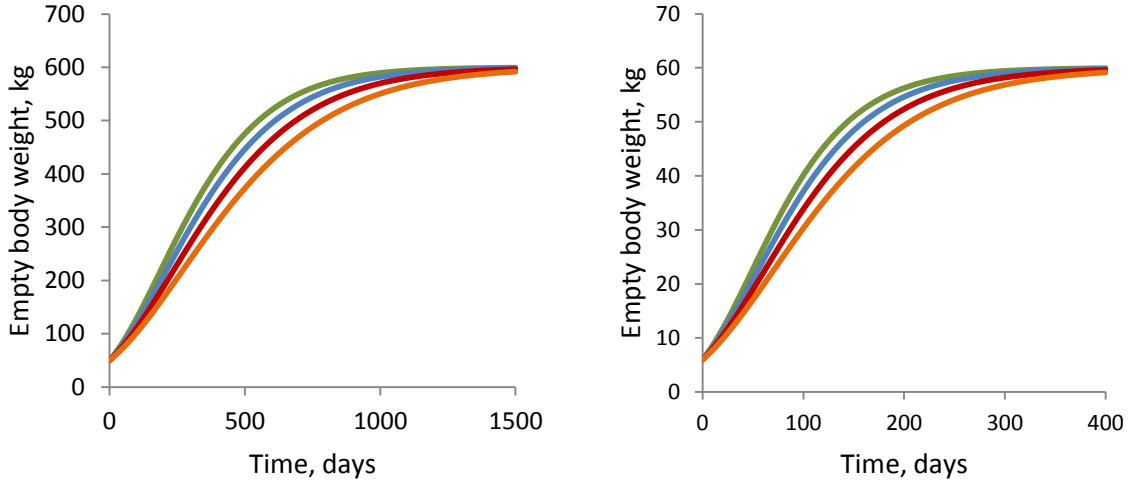

Figure 6.4: Growth dynamics for growing cattle (left) and sheep (right) for intake either at full requirement (100%) or maintenance plus 90%, 80%, and 70% growth requirement as indicated. Note the different scales.

Animal growth rate and that of individual components varies through time and also in response to relative intake. This is illustrated in Fig. 6.5 for both cattle and sheep, corresponding to the growth dynamics in Fig. 6.4 where the general pattern of the growth rate is consistent with sigmoidal growth. It can be seen that

growth rates of all components are reduced as intake declines, and that the time for peak growth rate is delayed, most noticeably for the fat component.

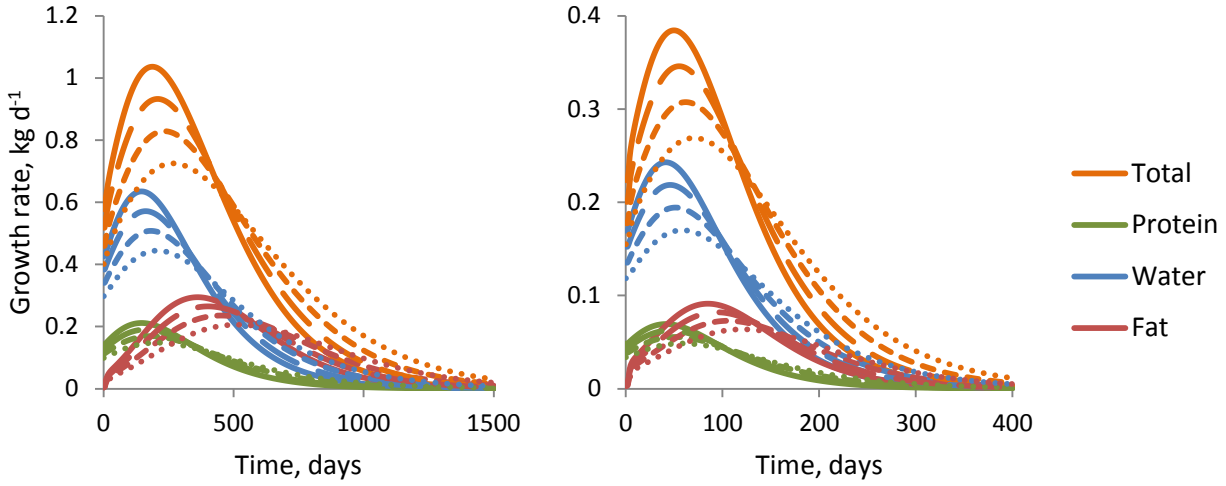

Figure 6.5: Total animal growth rate and that of the protein, water, and fat components of body weight, as indicated, during growth for cattle (left) and sheep (right), corresponding to Fig. 6.4. The solid lines are maintenance plus 100% growth requirement, large dashes 90%, small dashes 80%, and dots 70%. Note the different scales.

The simulations in Figs 6.4 and 6.5 are for animals under feeding regimes that provide full maintenance plus a fixed proportion of growth requirements. These illustrations are important as a means of examining the model's performance but, in practice, the intake is likely to vary in response to both pasture quality and availability, as well as management. The model can be applied directly to any feeding regime and can respond to varying pasture availability. As a simple example, the above simulations are repeated but with intake taken to be full maintenance plus a proportion of growth requirement that varies randomly between 70% and 100% of normal growth requirement, so that it fits somewhere between the illustrations shown in Figs 6.4 and 6.5. This could apply, for example, to situations where supplementary feeding is provided to ensure intake meets a required minimum. The results for empty BW, W, and energy requirements are shown in Fig. 6.6 where it can be seen that, as expected, W lies between the two fixed regimes. Also, although there are fluctuations in energy supply, the actual growth curves for W are quite smooth, demonstrating that BW growth is buffered in relation to moderate fluctuations in intake.

One characteristic of the simulations illustrated in Figs 6.4, 6.5, and 6.6 for growing animals is that there was no fat catabolism because, according to these feeding strategies, maintenance costs are always met. In practice intake will vary and, particularly when animals are close to maturity, there may be some fat loss to satisfy energy requirements. To explore this, the final set of illustrations considers mature animals with intake reduced from mature maintenance requirement. The above analysis applies without modification, although for animals at their mature optimum weight there will be no energy requirements for growth. Consequently, for a mature animal that has less than its optimum protein or fat composition, intake requirement may be greater than for the equivalent animal at optimum weight because there is a growth energy requirement, notwithstanding the fact that activity costs will fall slightly as an animal loses BW. In the following illustrations, that consider the effect of restricted intake on mature animals, intake is prescribed as fractions of the mature maintenance requirement at optimum fat composition.

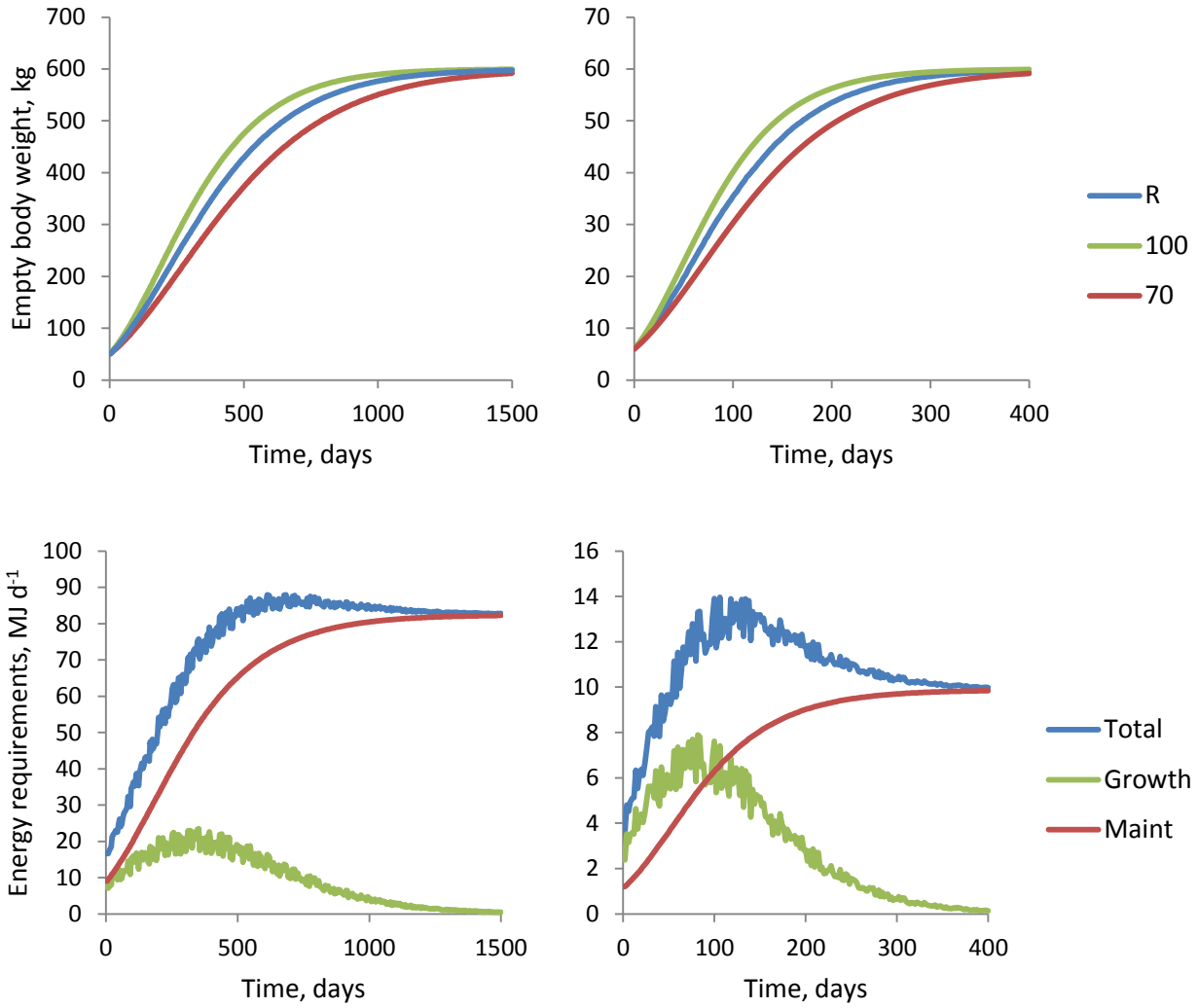

Figure 6.6: Top: growth dynamics for growing cattle (left) and sheep (right), for intake either at full requirement (100%) or maintenance requirement plus 70% growth requirement, as well as switching randomly between these two regimes, indicated by 'R'. Bottom: the corresponding total, growth, and maintenance energy requirements, as indicated for the 'R' simulations. Note the different scales.

The total empty BW, as well as the protein, water, and fat components, are shown in Fig. 6.7 for animals receiving 90%, 80%, and 70% of mature maintenance requirement. It can be seen that in all cases the weight components fall as expected. However, note that fat decline is virtually identical for the 80% and 70% regimes, which is due to fat catabolism occurring at the maximum rate, eqn (6.54). Consequently, the protein weight decline is more rapid for the 70% regime. (The changes in protein weight may be difficult to detect in this figure due to the relative size of this pool, although it should be noted that the fractional decline in protein is identical to that for water since these components are in direct proportion, eqn (6.2).

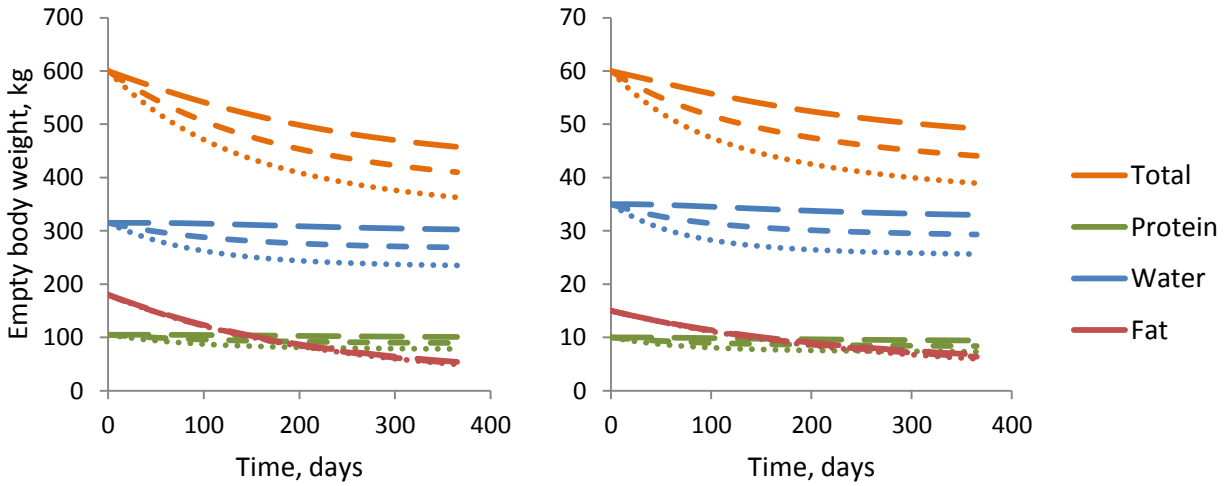

Figure 6.7: Growth dynamics for mature cattle (left) and sheep (right) under a range of feed intakes. Left: empty BW and components as indicated, with intake either at 90% (large dashes), 80% (small dashes), or 70% (dots) of mature maintenance requirement as indicated. (The colours and line styles are consistent with Fig. 6.5.)

The illustrations presented here demonstrate that the model gives realistic behaviour of cattle and sheep growth under a range of energy intake levels.

6.6 Pregnancy and lactation

The analysis so far is for growing animals and pregnancy and lactation are now considered. The approach is a natural extension of the growth model.

6.6.1 Pregnancy

Foetal growth is assumed to be exponential so that the growth rate is

$$\frac{\mathrm{d}W_f}{\mathrm{dt}} = k_f W_f \tag{6.57}$$

where W_f, kg, is the foetus weight and k_f, d^{-1}, is a growth coefficient. For normal growth, this equation is solved to give

$$W_f = W_{f,0} e^{k_f t} \tag{6.58}$$

If the pregnancy duration is denoted by t_{preg} then the foetus weight at $t = t_{preg}$ is the birth weight, $W_{f,b}$, and it follows that

$$W_{f,0} = W_{f,b} e^{-k_f t_{preg}} \tag{6.59}$$

Rather than prescribing the growth coefficient k_f, the parameter λ_f is defined as the fraction of the pregnancy duration to 50% birth weight, so that

$$W_f\left(t = \lambda_f t_{preg}\right) = W_{f,b}/2 \tag{6.60}$$

which, with eqn (6.58), gives

$$k_f = \frac{\ln(2)}{t_{preg}\left(1-\lambda_f\right)} = \frac{0.69}{t_{preg}\left(1-\lambda_f\right)} \tag{6.61}$$

so that the foetal growth parameters to be defined are t_{preg} and λ_f. Defaults are:

$$\begin{aligned} &\text{cattle:} \quad t_{preg} = 280 \text{ d}, \quad \lambda_f = 0.8 \\ &\text{sheep:} \quad t_{preg} = 150 \text{ d}, \quad \lambda_f = 0.8 \end{aligned} \tag{6.62}$$

Equation (6.58) with (6.59) and (6.61) defines foetal growth in terms of birth weight, pregnancy duration and the time to 50% birth weight. W_f is illustrated in Fig. 6.8 for a dairy cow – the response for sheep has the same characteristic shape but with different scale. It can be seen that, at conception, foetal weight does not increase smoothly from zero – the model could be refined to make this the case but the effect on the simulations would be negligible and would not justify the extra complexity.

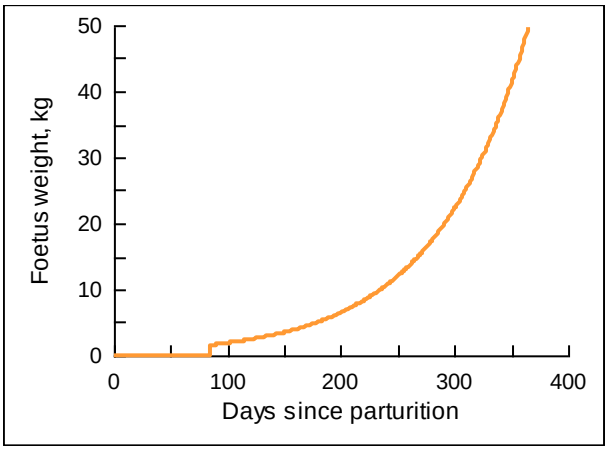

Figure 6.8: Foetal growth in dairy cows with default parameters.

If there are multiple foetuses, the birth weight is generally reduced so that, if the number of foetuses if n_f, it is assumed that

$$W_{f,b} = \left(\frac{2}{1+n_f}\right) W_b \tag{6.63}$$

where W_b is the normal birth weight discussed in Section 6.2 above.

It can be seen that total foetal weight has been considered and not the individual protein, fat and water components. This has been done to avoid unnecessary complexity. The energy requirement during pregnancy is calculated in a similar manner to growth requirements, with the assumption that the fat and protein composition during foetal growth is constant and the same as at birth. Thus, the energy density of the foetus is

$$E_f = \left(f_{F,\mathrm{b}} \frac{\varepsilon_F}{Y_{F,g}} + \frac{W_{P,b}}{W_b} \frac{\varepsilon_P}{Y_{P,g}} \right) \left(1+\gamma_{preg}\right) n_f \tag{6.64}$$

where all terms have been defined previously with the exception of γ_{preg} which is a scale factor to allow for the fact that the energy required during pregnancy is greater than the energy density in the foetus. The default value is

$$\gamma_{preg} = 1 \tag{6.65}$$

which means that the energy requirement to grow 1 kg of foetus is double that of animal growth with the same body composition.

6.6.2 Lactation

The primary focus for the treatment of lactation is for dairy systems, although it is obviously important in livestock systems with calves or lambs. Milk production can be defined either as L d^{-1} or milk solids d^{-1}, although milk solids are probably only relevant to dairy systems. Denoting the fat, protein and lactose fractions of milk as $f_{F,milk}$, $f_{P,milk}$, $f_{L,milk}$ respectively, and the density of milk as ρ_{milk}, the fraction of milk solids, $f_{milk,solids}$ kg solids L^{-1} is

$$f_{milk,solids} = \rho_{milk}\left(f_{F,milk} + f_{P,milk}\right) \tag{6.66}$$

and energy density of milk, ε_{milk} MJ L^{-1} is

$$\varepsilon_{milk} = \rho_{milk}\left(\varepsilon_F f_{F,milk} + \varepsilon_P f_{P,milk} + \varepsilon_L f_{L,milk}\right) \tag{6.67}$$

where the energy densities for fat and protein were defined earlier, with values in (6.24), and the energy density of lactose has default value

$$\varepsilon_L = 16.5 \text{ MJ kg}^{-1} \tag{6.68}$$

The efficiency of milk production, Y_L, has default value

$$Y_L = 0.5 \tag{6.69}$$

so that the energy required for milk production, again applying eqn (6.22), is

$$E_L = \frac{\varepsilon_L}{Y_L} \text{ MJ L}^{-1} \tag{6.70}$$

Default values are

$$\begin{aligned} &\text{cattle:} \quad \rho_{milk} = 1.03 \text{ kg L}^{-1}, \quad f_{F,milk} = 0.04, \quad f_{P,milk} = 0.033, \quad f_{L,milk} = 0.046 \\ &\text{sheep:} \quad \rho_{milk} = 1.03 \text{ kg L}^{-1}, \quad f_{F,milk} = 0.06, \quad f_{P,milk} = 0.055, \quad f_{L,milk} = 0.06 \end{aligned} \tag{6.71}$$

With these parameters, the net energy content of milk is 3.2 MJ L^{-1} and 4.8 MJ L^{-1} for cattle and ewes respectively.

Actual milk production is defined in terms of available energy from intake and is discussed later.

Fat catabolism during lactation

The potential for fat catabolism to provide energy for other metabolic processes was discussed earlier. During lactation, additional fat catabolism occurs to provide the extra energy requirements associated with the production of milk. As time progresses, there is a shift from priority for milk production which incurs fat catabolism, to replacing body fat through fat growth. This is defined in the model through the scale function

$$f_{F,lact}\left(\tau_{lact}\right)=\frac{\tau_{lact}-\tau_{lact,F_0}}{\tau_{lact}+\tau_{lact,F_0}} \tag{6.72}$$

where $f_{F,lact}$ lies between -1 and 1 as τ_{lact} increases from zero, taking the value 0 when $\tau_{lact} = \tau_{lact,F0}$. The parameters are:

$$\begin{aligned} &\text{cattle:} \quad \tau_{lact,F0} = 80 \text{ d} \\ &\text{sheep:} \quad \tau_{lact,F0} = 50 \text{ d} \end{aligned} \tag{6.73}$$

Equation (6.72) is illustrated in Fig. 6.9 for the defaults for sheep and cattle.

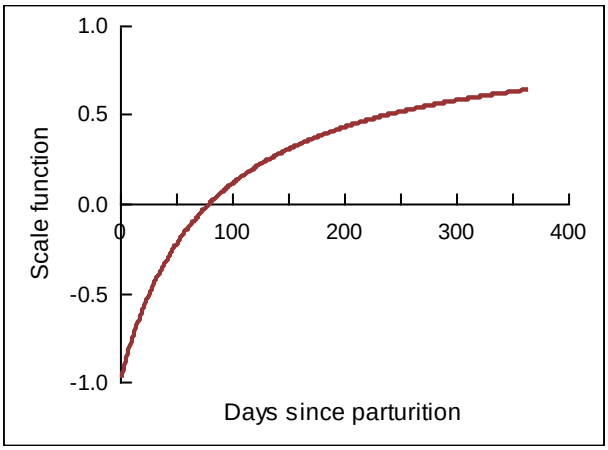

Figure 6.9: Scale function, eqn (6.72), for fat catabolism and partitioning between fat growth and milk production for a dairy cow.

When this function is negative, there is compulsory fat catabolism, whereas when it is positive it defines the relative priority for fat growth and milk production. The overall growth dynamics are discussed later.

6.7 Animal intake

Animal intake is defined in relation to feed composition, animal weight and, and pasture availability in the case of grazed pasture. In the following analysis, all pasture mass and intake units are expressed in carbon units with the corresponding nitrogen units. In some cases, these will be converted to dry weight or protein fractions for illustration. However, retaining C and N units in the analysis avoids problems with conversion factors.

6.7.1 Potential intake

It is common for models to relate potential intake to animal BW in some way. The approach here is to assume that, for a reference digestibility, normal growth can be satisfied with non-limiting feed availability. Potential intake at this digestibility is then related to animal body protein, rather than total weight, since, as discussed in detail above, body protein is taken as an indicator of metabolic state. Thus, for example, if a mature animal loses body fat but not protein, the potential intake is unchanged.

The approach in the model code is to grow an animal under normal conditions, as discussed above, and calculate the ME required which is then stored in an array as a function of body protein, W_P, so that intake at reference digestibility is defined by

$$I_{pot,ref}\left(W_P\right) \tag{6.74}$$

This is then applied at all stages of growth.

During lactation or pregnancy, it is assumed that potential intake increases due to physiological changes in the rumen. These are considered in turn.

Intake during pregnancy

Potential intake is assumed to increase during pregnancy to provide the extra energy required. The simple scale function is defined as

$$f_{I,preg}\left(\tau_{preg}\right)=1+\frac{E_{preg,req}}{E_{mat,req}} \tag{6.75}$$

where τ_{preg}, d, is the time since conception, $E_{preg,req}$ MJ d^{-1}, is the energy required for pregnancy, and $E_{mat,req}$ MJ d^{-1}, is the energy required at normal mature weight for a non-pregnant and non-lactating animal. The potential intake during pregnancy is then defined by combining eqns (6.74) and (6.75) as

$$I_{pot,ref,preg}=I_{pot,ref}\left(W_P\right)f_{I,preg}\left(\tau_{preg}\right) \tag{6.76}$$

Intake during lactation

Potential intake is assumed to increase to a peak following parturition and subsequently decline, according to the function

$$f_{I,lact}\left(\tau_{lact}\right)=1+\left(f_{I,lact,mx}-1\right)\Gamma\left(\tau_{lact}\right) \tag{6.77}$$

Where $\Gamma(\tau_{lact})$ is defined as a normalized gamma function in terms of the time since parturition, τ_{lact} d, the time to maximum intake, $\tau_{lact,mx}$ d, and the curvature coefficient α, as given by

$$\Gamma\left(\tau_{lact}\right)=\left(\frac{\tau_{lact}}{\tau_{lact,mx}}\right)^{\alpha}\exp\left[-\alpha\left(\frac{\tau_{lact}}{\tau_{lact,mx}}-1\right)\right] \tag{6.78}$$

where

$$\begin{aligned}&\Gamma\left(\tau_{lact}=0\right)=0\\&\Gamma\left(\tau_{lact}=\tau_{lact,mx}\right)=1\end{aligned} \tag{6.79}$$

so that

$$\begin{aligned}&f_{I,lact}\left(\tau_{lact}=0\right)=1\\&f_{I,lact}\left(\tau_{lact}=\tau_{lact,mx}\right)=f_{I,lact,mx}\end{aligned} \tag{6.80}$$

Note that, in the model, different curvature parameter values for α are used for pre- and post-peak lactation.

During lactation the potential intake function in eqn (6.74) is scaled according to

$$I_{pot,ref,lact}=I_{pot,ref}\left(W_P\right)\Gamma\left(\tau_{lact}\right) \tag{6.81}$$

Default parameter values are

$$\begin{aligned}&\text{dairy:}\quad \tau_{lact,mx}=80\text{ d},\quad \alpha=0.8,\ \tau<\tau_{lact,mx},\quad \alpha=0.5,\ \tau>=\tau_{lact,mx},\quad f_{I,lact,mx}=2.2\\&\text{cattle:}\quad \tau_{lact,mx}=80\text{ d},\quad \alpha=0.8,\ \tau<\tau_{lact,mx},\quad \alpha=0.5,\ \tau>=\tau_{lact,mx},\quad f_{I,lact,mx}=1.8\\&\text{sheep:}\quad \tau_{lact,mx}=50\text{ d},\quad \alpha=0.8,\ \tau<\tau_{lact,mx},\quad \alpha=1.0,\ \tau>=\tau_{lact,mx},\quad f_{I,lact,mx}=2.0\end{aligned} \tag{6.82}$$

where it can be seen that, in this case, different defaults apply to dairy cows and cattle.

If the animal is also pregnant, then the scale function $f_{I,preg}$ in eqn (6.75) is also applied.

Equation (6.78) is illustrated in Fig. 6.10 for the dairy cow default values.

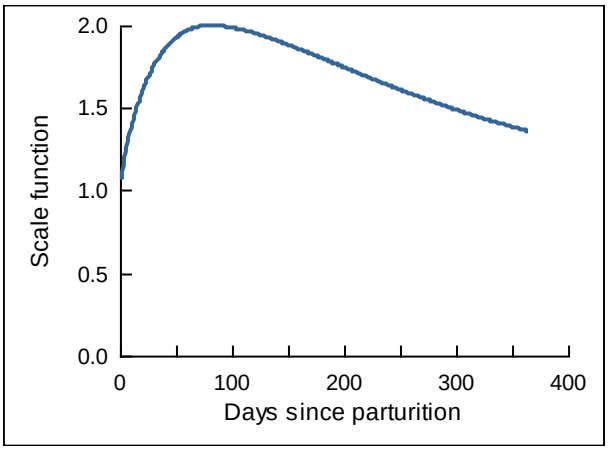

Figure 6.10: Intake scale function during lactation, eqn (6.78)

6.7.2 Intake in relation to feed composition

Animal feed, whether from pasture or supplement, is assumed to comprise three basic components: *neutral detergent fibre* (NDF) which is primarily cellulose, hemicellulose and lignin in cell wall material; protein; and the remainder which is the *neutral detergent solubles* (NDS) and is mainly sugars for pasture but may include compounds such as starch and fat for other feeds. The fractions of these are denoted by f_F, f_P, f_S respectively so that

$$f_F + f_P + f_S = 1 \tag{6.83}$$

where subscripts refer to 'fibre', 'protein' and 'solubles'. If these components have digestibilities by δ_F, δ_P, δ_S, then the total digestibility is

$$\delta = \delta_F f_F + \delta_P f_P + \delta_S f_S \tag{6.84}$$

It is assumed that, for all feed types, the protein and NDS digestibilities are fixed for all feed types, and are:

$$\delta_P = \delta_S = 0.85 \tag{6.85}$$

Thus, total digestibility δ is influenced primarily by feed composition and the digestibility of the NDF component.

A digestibility intake scale factor ϕ_δ is defined as

$$\phi_\delta = \frac{\xi_\delta}{\xi_{\delta,ref}} + \phi_{\delta,mn}\left(1 - \frac{\xi_\delta}{\xi_{\delta,ref}}\right) \tag{6.86}$$

where ξ_δ is a generic function based on the mathematical structure of the temperature response function, eqn (1.39) in Chapter 1, Section 1.3.5, as given by

$$\xi_\delta(\delta)=\begin{cases}0, & \delta\le\delta_{opt}\\ \left(\dfrac{\delta-\delta_{mn}}{\delta_{opt}-\delta_{mn}}\right)^q\left(\dfrac{(1+q_\delta)\delta_{opt}-\delta_{mn}-q_\delta\delta}{(1+q_\delta)\delta_{opt}-\delta_{mn}-q_\delta\delta_{opt}}\right), & \delta_{mn}<\delta<\delta_{opt}\\ 1, & \delta\ge\delta_{opt}\end{cases} \tag{6.87}$$

According to this formulation, the function ϕ_δ is constrained by

$$\begin{aligned}&\phi_\delta(\delta=\delta_{mn})=\phi_{\delta,mn}\\ &\phi_\delta(\delta=\delta_{ref})=1\end{aligned} \tag{6.88}$$

and increases sigmoidally between these two values as digestibility δ increases from δ_{mn} to δ_{opt}. Equation (6.86) is illustrated in Fig. 6.11 for the default values

$$\begin{aligned}&\delta_{mn}=0.3;\ \delta_{opt}=0.8;\ \delta_{ref}=0.7\\ &\phi_{\delta,mn}=0.5;\ q_\delta=2\end{aligned} \tag{6.89}$$

Note that δ_{mn} and δ_{opt} are fixed in the model and cannot be changed by the user. These are taken to define the realistic range of digestibilities of feed supply.

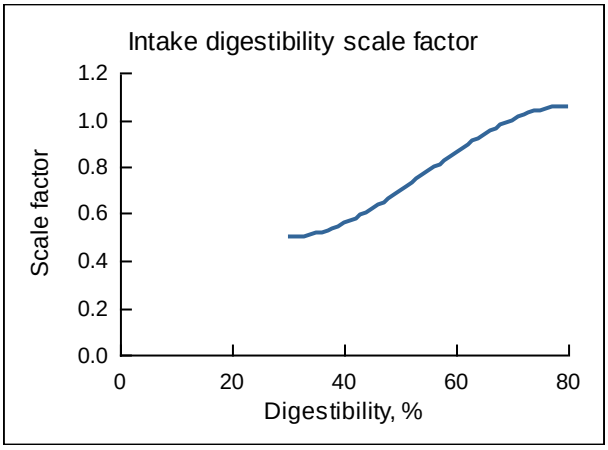

Figure 6.11: Intake digestibility scale factor, eqn (6.86), with parameter values eqn (6.89)

This approach to defining the relative effect of digestibility on intake is applied to any source of intake – that is, pasture, concentrate, forage (silage or hay) and mixed ration. NDF is sometimes used directly as an indicator of the effect of feed quality on intake but I have found that digestibility offers more flexibility and is simpler to work with mathematically.

6.7.3 Pasture intake

Pasture intake depends on availability as well as pasture quality. A scale factor to define intake in relation to available pasture is defined as

$$\phi_{pas}=\frac{\xi_{pas}}{\xi_{pas,ref}} \tag{6.90}$$

with the function $\xi_{pas}(W_{pas})$ given by

$$\xi_{pas}\left(W_{pas}\right)=\frac{\left(W_{pas}/W_{pas,h}\right)^{q_{pas}}}{1+\left(W_{pas}/W_{pas,h}\right)^{q_{pas}}} \tag{6.91}$$

where W_{pas}, kg C m^{-2} is available pasture, q_{pas} is a curvature coefficient, $W_{pas,h}$ is the available pasture at which $\xi_{pas}=0.5$, and $\xi_{pas,ref}$ is the value of ξ_{pas} at reference pasture $W_{pas,ref}$ so that

$$\phi_{pas}\left(W_{pas}=W_{pas,ref}\right)=1 \tag{6.92}$$

When pasture is unlimited, ϕ_{pas} approaches the limit

$$\phi_{pas,mx}=\frac{1}{\xi_{pas}\left(W_{pas,ref}\right)} \tag{6.93}$$

so that

$$\phi_{pas}\left(W_{pas}=W_{pas,h}\right)=\frac{\phi_{pas,mx}}{2} \tag{6.94}$$

Thus, ϕ_{pas} is readily parameterized in terms of the available pasture at which intake is restricted to 50% of potential and a reference pasture availability at which the ϕ_{pas} is unity. Default values for cattle and sheep, expressed in t d.wt ha^{-1} (although the model internal units are kg C m^{-2}), are

$$\begin{aligned}&\text{cattle:}\quad W_{pas,h}=0.7\text{ t d.wt ha}^{-1},\quad q_{pas}=1.5\\&\text{sheep:}\quad W_{pas,h}=0.5\text{ t d.wt ha}^{-1},\quad q_{pas}=1.5\end{aligned} \tag{6.95}$$

and the reference value is

$$W_{pas,ref}=2\text{ t d.wt ha}^{-1} \tag{6.96}$$

Thus, pasture intake is

$$I_{pas}=I_{pot,ref}\left(W_P\right)\phi_{\delta}\left(\delta_{pas}\right)\phi_{pas}\left(W_{pas}\right) \tag{6.97}$$

where δ_{pas} is pasture digestibility and W_{pas} is pasture availability. Note that if the animal is pregnant and/or lactating then the scale factors given by eqns (6.76) and (6.78) are implemented.

6.7.4 Supplement intake

Supplement intake is related to supplement composition and digestibility, as well as any management restrictions in supply. The potential intake is given by the above analysis. However, the intake function in relation to pasture availability is also applied at its asymptote, eqn (6.93). Thus, the maximum potential supplement intake is

$$I_{supp,mx}=\phi_{pas,mx}\phi_{\delta}\left(\delta_{supp}\right)I_{pot,ref}\left(W_P\right) \tag{6.98}$$

where δ_{supp} is the digestibility of the supplement. Again, if the animal is pregnant and/or lactating then the scale factors given by eqns (6.76) and (6.78) are implemented.

6.7.5 Substitution

Substitution is the phenomenon where intake of supplement can cause reductions in pasture intake. Substitution will only occur in response to supplement that is fed prior to pasture. Thus, for example, if a

minimum concentrate is fed followed by pasture, and then more concentrate, substitution is calculated in relation to the minimum concentrate only. Obviously, total intake is constrained by animal intake capacity. There is a single substitution coefficient prescribed for the animal on the 'Stock' module under the 'Biophysics' page. This is the substitution that occurs when pasture availability is non-limiting, and the default is 0.8.

Once supplement intake has been calculated, the potential pasture intake is then scaled by the function

$$f_{supp} = 1 - \frac{\gamma_{supp} I_{supp}}{\phi_{pas,mx} \phi_{\delta}\left(\delta_{pas}\right) I_{pot,ref}\left(W_P\right)} \tag{6.99}$$

and, again, eqns (6.76) and (6.78) are implemented if necessary.

6.8 Metabolisable energy and nitrogen dynamics

The theory so far describes the diet composition and digestibility which determine potential animal intake and I shall now consider calculations for metabolisable energy in relation to feed composition and nitrogen dynamics, which are central to overall nutrient dynamics in the model. Nitrogen dynamics are considered first since there are energy costs associated with urine excretion and these affect overall available metabolisable energy. The net nitrogen balance through the animal is simple in that the input is equal to the sum of nitrogen retained (body tissue or milk) and that excreted in dung and urine. In the case of a non-lactating cow maintaining a fixed body weight, excreted N will exactly balance input. However, the animal requires dietary N to balance turnover of rumen microbes. It is beyond the scope of the present model to include full rumen functionality, although such models provide valuable insight into rumen dynamics. A simpler approach will be adopted.

Before proceeding, note that in the following analysis, intake is expressed in d.wt units. Since the model works with carbon units, care must be taken to ensure that appropriate conversions are made when implementing the model in code.

Denoting the total intake by I, kg d.wt d^{-1}, the corresponding N intake is

$$I_N = \alpha_N f_P I_C \tag{6.100}$$

where, as discussed above, f_P is the protein fraction, and α_N is the N fraction of protein taken to be

$$\alpha_N = 0.16 \text{ kg N } \left(\text{kg protein}\right)^{-1} \tag{6.101}$$

which is equivalent to the usual factor of 6.25 for converting N to protein.

It is assumed that senescence and excretion of rumen microbes is exactly balanced by new growth. It is further assumed that rumen microbial senescence, B_{sen} kg d.wt d^{-1}, is proportional to intake which implies that as microbial activity increases through a greater intake, so does the turnover of microbes. Thus

$$B_{sen} = \mu_B I \tag{6.102}$$

The corresponding N excretion from rumen microbes is then

$$B_{sen,N} = f_{B,N} B_{sen} \tag{6.103}$$

where $f_{B,N}$ kg N (kg d.wt)$^{-1}$ is the N fraction of the rumen microbes with default value

$$f_{B,N} = 0.1 \tag{6.104}$$

Now consider dung, D kg d.wt d^{-1}, which is given by

$$D = (1-\delta)I + B_{sen} = (1-\delta)I + \mu_B I \quad (6.105)$$

and the corresponding dung N, D_N kg N d^{-1} is

$$D_N = \alpha_N f_P I(1-\delta_P) + B_{sen,N} = \alpha_N f_P I(1-\delta_P) + \mu_B f_{B,N} I \quad (6.106)$$

The N fraction of dung can now be written

$$f_{N,dung} = \frac{\alpha_N f_P (1-\delta_P) + \mu_B f_{B,N}}{(1-\delta+\mu_B)} \quad (6.107)$$

The default value of μ_B is

$$\mu_B = 0.04 \quad (6.108)$$

so that microbial decay is equivalent to 4% of intake.

Thus, for example, for a good quality pasture with digestibility 75%, and 25% protein, the dung N concentration is 3.4% which is realistic.

Now consider urine N, which is taken to be the excess intake N that is not utilized by the animal or excreted as dung. The total daily N input balance between intake, retained and losses to dung and urine is

$$I_N = \Delta W_N + L_N + D_N + U_N \quad (6.109)$$

where ΔW_N is the body weight N balance, which will be negative for protein weight loss, L_N is the N content of milk (where appropriate), and U_N is the N loss as urine. Thus, U_N becomes

$$U_N = I(\alpha_N f_P \delta_P - \mu_B f_{B,N}) - L_N - \Delta W_N \quad (6.110)$$

This gives the urine N balance in terms of intake, N retained by microbial biomass, milk and body weight change. For example, if the animal is not lactating and has no weight change, then all digested N that is not retained by the microbes is excreted as N. The N retained by the microbes is balanced by the corresponding losses to dung through microbial senescence.

The metabolisable energy available to the animal, E_{ME} MJ d^{-1}, is the difference between the gross energy of feed intake and energy costs associated with the production of methane, urine and dung, and can be written

$$E_{ME} = \varepsilon_g \delta I - E_{CH4} - E_D - E_U \quad (6.111)$$

where ε_g, MJ kg^{-1}, is the energy density of the feed and the last three terms are energy costs associated with the production of CH_4, dung and urine respectively, and are considered in turn.

Energy costs associated with CH_4 production are assumed to be given by

$$E_{CH_4} = \lambda_{CH_4} \varepsilon_g \delta I \quad (6.112)$$

where

$$\lambda_{CH_4} = \lambda_{CH_4,ref} \left(\frac{f_F}{f_{F,\mathrm{CH_4},ref}} \right)^{1/2} \quad (6.113)$$

and $\lambda_{CH4,ref}$ is the energy associated with CH_4 production as a proportion of digestible energy intake at reference NDF content, $f_{F,CH4,ref}$, of the feed. In the model,

$$\lambda_{CH_4,ref} = 0.09 \tag{6.114}$$

where

$$f_{F,CH_4,ref} = 0.65 \tag{6.115}$$

Thus, for example, if δ_F = 0.6, $\delta_P = \delta_S = 0.85$ then for composition $f_F = 0.55$, $f_P = 0.2$, $f_S = 0.25$, which is representative of pasture, the fraction of energy lost through methane fermentation is 6.1%, whereas if the composition is $f_F = 0.2$, $f_P = 0.1$, $f_S = 0.7$, which is representative of a concentrate supplement, the energy fraction is now 4.2%. These values are consistent with lower energy costs through methane fermentation for low fibre diets.

The energy costs associated with dung production are taken to be proportional to dung, so that

$$E_D = \varepsilon_D D \tag{6.116}$$

where the dung output, D, is given by eqn (6.105) and ε_D, MJ kg^{-1} is the energy cost of producing dung with default value

$$\varepsilon_D = 4 \text{ MJ kg}^{-1} \tag{6.117}$$

For urine, it is assumed that the energy costs are related to the urine N, so that

$$E_U = \varepsilon_{U,N} U_N \tag{6.118}$$

where the urine output, U_N, is given by eqn (6.110) and $\varepsilon_{U,N}$, MJ (kg N)$^{-1}$ is the energy cost of producing N, with default value

$$\varepsilon_{U,N} = 30 \text{ MJ } (\text{kg N})^{-1} \tag{6.119}$$

It is convenient to separate the urine N into the component corresponding to no N retention by the animal and then allow for any retention as milk or body weight change. Write eqn (6.110) as

$$U_N = U_{N,0} - \Delta N_{ret} \tag{6.120}$$

where

$$U_{N,0} = I\left(\alpha_N f_P \delta_P - \mu_B f_{B,N}\right) \tag{6.121}$$

and

$$\Delta N_{ret} = L_N + \Delta W_N \tag{6.122}$$

The metabolisable energy, eqn (6.111), can now be written

$$E_{ME} = \phi I + \varepsilon_{U,N} \Delta N_{ret} \tag{6.123}$$

where

$$\phi = \varepsilon_g \delta\left(1 - \lambda_{CH_4}\right) - \varepsilon_D\left(1 - \delta + \mu\right) - \varepsilon_{U,N}\left(\alpha_N f_P \delta_P - f_{B,N}\mu_B\right) \tag{6.124}$$

This coefficient, with units MJ kg^{-1}, is termed the *apparent metabolisable energy coefficient* and is the metabolisable energy content of the feed in the absence of any N retention by the animal.

6.9 Growth dynamics in response to metabolisable energy

The analysis so far defines the metabolisable energy available to the animal in terms of available pasture and quality, supplement supplied, and animal metabolic state. It now remains to calculate the overall growth dynamics including foetal growth and milk production where appropriate. The sequence of calculations using the theory described above is as follows:

- Calculate potential intake from pasture and supplement, including any substitution effects.
- Calculate ME required for growth, maintenance and, if relevant, pregnancy.
- If the animal is lactating and $\tau_{lact} < \tau_{lact,F0}$ in eqn (6.72), so that fat catabolism occurs, calculate the energy released.

It then remains to calculate growth. First consider a non-lactating animal in which case, three conditions are considered.

- ME available exceeds requirements for growth, maintenance and pregnancy (if appropriate). In this case, intake is reduced to maximum requirement and growth is calculated accordingly.
- ME available is less than requirements for growth, but there is sufficient fat catabolism to meet maintenance requirements. In this case there is no growth and the necessary fat catabolism occurs to provide energy, along with intake, to meet maintenance requirements.
- ME available through intake and fat catabolism is insufficient to meet maintenance requirements. This is an animal that is going to lose weight and does so first through maximum fat catabolism. Body protein will then be lost as a result of insufficient energy to resynthesis degraded protein through protein maintenance requirements.

For a lactating animal, lactation will only occur if the energy available exceeds maintenance requirements. If this is the case and the available energy after meeting other costs is E_{avail} and daily milk production is L, L d^{-1}, then the energy balance is

$$L\left(\frac{\varepsilon_L}{Y_L} - f_{N,L}\varepsilon_{U,N}\right) = E_{avail} \tag{6.125}$$

where $f_{L,N}$, kg N L^{-1}, is the milk N fraction. This equation accounts for the energy that is available through N retention in the milk that would otherwise have incurred a cost to be excreted as urine. Thus, the milk production is

$$L = \frac{E_{avail}}{\left(\frac{\varepsilon_L}{Y_L} - f_{N,L}\varepsilon_{U,N}\right)} \tag{6.126}$$

In practice in the model, milk production will respond to pasture availability and quality as well as feed management. As a simple example, consider a dairy cow being fed two contrasting feeds:

- a fixed good quality pasture based feed with 50% NDF at 60% digestibility, 20% protein so that it is 20% NDS;
- a mixed ration feed with 25% NDF at 70% digestibility, 20% protein so that it is 60% NDS.

In both cases protein and NDS have digestibility 85%. The corresponding lactation over 300 days is shown in Fig. 6.12 where it can be seen that, as expected, substantially greater milk production occurs with the mixed ration, with total milk production being 5,028 L and 7,271 L respectively. The feed conversion efficiencies, FCE L (kg feed)$^{-1}$, are also shown and, as expected these are greatest during early lactation, due to fat catabolism, and also for the mixed ration. The overall average FCEs are 0.85 and 1.22 for the pasture

and mixed ration fed cows respectively. These examples show two extremes and, in practice, cows are likely to receive a balance between pasture, concentrate, forage and mixed ration. However, this example demonstrates the model gives the appropriate response to differing feed supply. It should be noted that the absolute values for milk production will depend on the size and genetic merit of the cow.

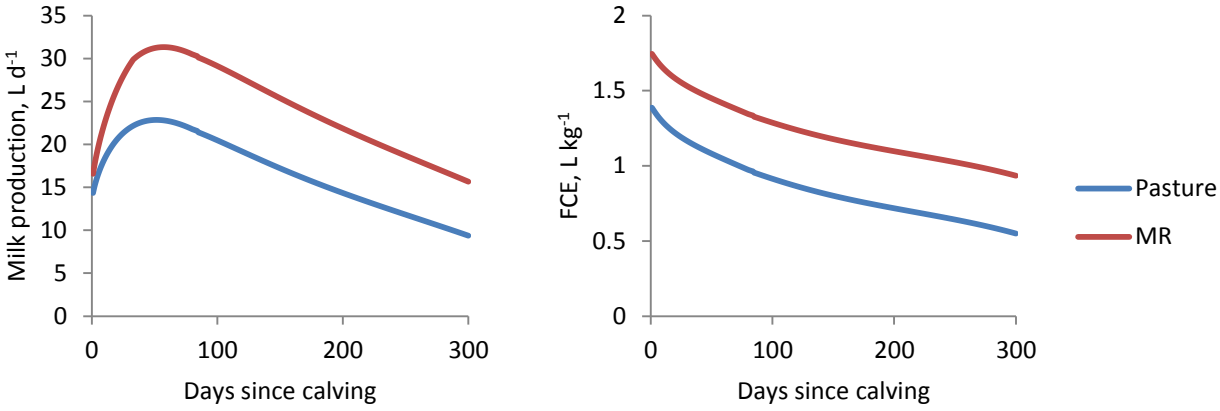

Figure 6.12: Milk production over 300 day lactation (left) and corresponding feed conversion efficiency (right) for a cow being fed good quality pasture or mixed ration feed as indicated. See text for details.

Figure 6.13 shows the body weight and energy dynamics corresponding to the pasture fed cow in Fig. 6.12: The characteristics of the dynamics are similar for the mixed ration feed supply. The negative growth energy corresponds to fat catabolism.

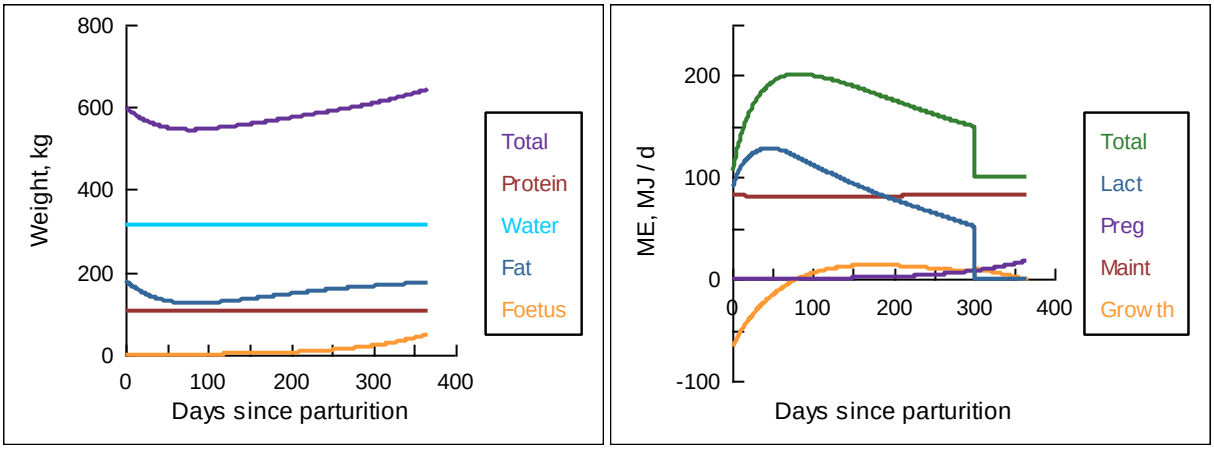

Figure 6.13: Body weight (left) and energy dynamics (right) for the pasture fed dairy cow as illustrated in Fig. 6.12. See text for details.

6.10 Final comments

The animal growth and metabolism model has been described. It is a generic animal based on Johnson *et al.* (2012) and can be applied to sheep, cattle or dairy cows. It includes growth, pregnancy and lactation, and the full energy dynamics including costs associated with growth of body protein and fat, resynthesis of degraded protein, termed protein maintenance, maintenance costs associated with travel, and fat catabolism. Costs of N production through urine excretion and dung are included. It also includes methane emissions from rumen fermentation and partitioning of N between dung and urine and so is ideally suited for greenhouse gas dynamics studies. The model is versatile and can simulate a wide range of pasture and feed management systems.

6.11 References

Agricultural Research Council. (1981). The nutrient requirements of farm livestock, no. 2 ruminants (2nd ed.) Agricultural Research Council, London.

Baldwin RL, France J, Beever DE, Gill M, Thornley JHM (1987). Metabolism of the lactating dairy cow. III. Properties of mechanistic models suitable for evaluation of energetic relationships and factors involved in the partition of nutrients. *Journal of Dairy Research*. **54**, 133-145.

Baldwin R L (1995). *Modeling Ruminant Digestion and Metabolism*. Chapman & Hall, London.

Bergen WG (2008). Measuring in vivo intracellular protein degradation rates in animal systems. *Journal of Animal Science*, **86,** E3-E12.

Dijkstra J (1994). Simulation of the dynamics of protozoa in the rumen. *British Journal of Nutrition*, **72**, 679-699.

Dijkstra J, Neal HD St. C, Beever DE, France J (1992). Simulation of nutrient digestion, absorption and outflow in the rumen: model description. *Journal of Nutrition,* **122**, 2239-2256.

Emmans GC (1997). A method to predict the food intake of domestic animals from birth to maturity as a function of time. *Journal of Theoretical Biology,* **186,** 189-199.

Finlayson JD, Cacho OJ, Bywater AC (1995). A simulation model of grazing sheep: I. Animal growth and intake. *Agricultural Systems,* **48**, 1-25.

Fox DG, Black JR (1984). A system for predicting body composition and performance of growing cattle. *Journal of Animal Science,* **58,** 725-739.

Gerrits WJ, Dijkstra J, France J (1997). Description of a model integrating protein and energy metabolism in pre-ruminant calves. *Journal of Nutrition,* **127**, 1229-1242.

Johnson IR, France J, Thornley JHM, Bell MJ, Eckard RJ (2012). A generic model of growth, energy metabolism, and body composition for cattle and sheep. *Journal of Animal Science,* **90,** 4741-4751.

Lewis RM, Emmans GC (2007). Genetic selection, sex and feeding treatment affect the whole-body chemical composition of sheep. *Animal,* **10,** 1427-1434.

National Research Council. 2001. *Nutrient requirements of dairy cattle*, 7th rev. ed.: National Academies Press, Washington.

Thornley JHM, France J (2007). *Mathematical Models in Agriculture*. CAB International. Wallingford, UK.

Williams CB (2005). Technical Note: A dynamic model to predict the composition of fat-free matter gains in cattle. *Journal of Animal Science,* **83**, 1262-1266.

Wright IA, Russell AJF (1984). Partition of fat, body composition and body condition score in mature cows. *Animal Production*, **38**, 23-32.